Dipartimento di Fisica "E. Amaldi"

Università Degli Studi Roma Tre

Dottorato in Fisica XIX ciclo

Anomalous Dimension Matrix and Wilson Coefficients relevant to dipole transitions in the Minimal Supersymmetric Standard Model

Schedar Marchetti

Chairperson of the Ph.D. School

Prof. Orlando Ragnisco

Supervisor

Prof. Giuseppe Degrassi

A.A. 2004-2005

Contents

1. Introduction

This chapter aims at defining and motivating the subject of the present Thesis work, namely the analysis of the Electric Dipole Moment (EDM) of the Neutron and the radiative B decays in the Minimal Supersymmetric Standard Model (MSSM).

Given the New Physics (NP) nature of the work itself, a short presentation of the phenomenological status of the Standard Model (SM) and its extension will be mandatory as well. The picture emerging when constraining with experimental data is that of a Model - the SM, in fact - performing very well. Unexpectedly well, according to a number of theoretical motivations hinting at a close-by scale of NP. As for the specific realization of the latter, with the important preliminary remark that the mentioned clash between the observed health of the SM and its expected breakdown makes the situation not quite clear ("The train is already late", G. Altarelli), the message to convey is that supersymmetry remains the most promising candidate. Consequently the quest for its low-energy realization, both directly via experimental detection - whenever possible - and indirectly via loop effects in already measured processes, constitutes a high-priority task in the agenda of particle physics.

1.1. The LEP-2 lesson

The SM is today a widely and accurately tested theory: a huge amount of data has been accumulated over the years for quite a number of observables and the knowledge of some of them has been pushed to below the per-mil precision. This statement synthesizes the result of the joint effort of several accelerator-based experiments carried out around the world. These include first of all the four LEP Collaborations, namely ALEPH, DELPHI, L3 and OPAL (see [LEP] for updated results), then notably CDF, DØ and NuTeV at Fermilab [FNA] and the SLD Collaboration at SLAC [SLC]. The theoretical interpretation of the full host of observables accessed by the abovementioned experiments can be summarized, following a recent paper by Altarelli [Alt], in a sort of scorecard on the performance of the SM as follows. Couplings among W, Z, γ gauge bosons and those between bosons and fermions have been measured with great accuracy. In particular the error reached for the latter is of a few per-mil. Comparison with the SM predictions leads to the conclusion that the gauge currents are indeed conserved: the gauge symmetry is unbroken in the vertices and precisely of the $SU(2)_L \times U(1)_Y$ form. On the other hand, this symmetry is broken by the unquestionable presence of mass terms for fermions and W, Z bosons, so that the symmetry exhibited by the SM Lagrangian must be broken spontaneously by

the vacuum, via a Higgs mechanism. The question is how this mechanism is practically realized. According to the SM, spontaneous symmetry braking (SSB) is carried out via a weak doublet of complex scalar fields, 4 degrees of freedom. Three of them provide the longitudinal degree of freedom for the massive gauge bosons $W^{\pm}, Z$. One is left over and should give rise to a scalar Higgs particle - the only one in the SM-, which is the sole SM building block still not directly detected. However LEP-2 data allow to gather some information, albeit indirect, on it. First of all, a lower bound on its mass m_H of 114.4 GeV (95 % CL,[LEP]) was established by direct scanning. In addition, the authors of ref. [ABC98] showed that, by manipulating four appropriate experimental quantities, it is possible to define the so-called epsilon variables $\epsilon_{1,2,3}$ and ϵ_b as objects that are non-zero only from the one-loop level in weak couplings. By definition such epsilons are golden variables to test purely weak radiative corrections: in particular ϵ_1 and ϵ_3 are sensitive to the Higgs sector. By accurate analyses of the latter quantities (see [ABC98, BS00, LEP]) it was possible to test such relations as $m_W^2 = m_Z^2 \cos^2\theta_W$, that indeed comply with a weak isospin doublet structure for the Higgs field. Electro Weak Precision Tests (EWPT) show as well indirect (yet clear) evidence for a light Higgs, not far from the LEP-2 lower mass bound: in fact the SM accommodates all data with a $m_H = 91\,^{+45}_{-32}$ GeV, see [LEP].

On top of the above discussion, it is fair to say that there is no evidence for the presence of new, unaccounted for, degrees of freedom beyond those of the SM, at least within the present accuracy. In addition, the SM Higgs, or variations thereof, is very likely to be there and this will be verdict by the LHC in the forthcoming years.

So we could simply conclude: the SM works. We have just to complete the picture with the Higgs. Actually, what said above is only one side of the story, the "experimental" one. On the theoretical side, the SM as it is cannot be regarded as the final theory of fundamental interactions, but only as an "effective" version of it, valid below some energy scale $\Lambda_{\rm NP}$ above with new physical degrees of freedom cannot be integrated out anymore. This conclusion holds for the SM independently of the specific mechanism realizing the spontaneous breaking of the $SU(2)_L \times U(1)_Y$ symmetry (the SM Higgs leads even to a paradox, as we will see in the next section), and is due to a number of well known reasons. To start with, the SM, and particularly its Higgs sector, generates a lot of free/unexplained parameters, in particular, the origin of fermion masses (including neutrinos) and the pattern of CP violation. Moreover, it does not address "grand-unification" problems like the unification of the gauge couplings at some high energy scale and a quantum description of gravity. In addition, while the SM is no doubt successful in reproducing data at the energies explored by accelerators, it badly fails to explain fundamental phenomena of astrophysical-cosmological interest. In particular: the amount of CP violation pertaining to the SM cannot explain the observed matter/antimatter asymmetry in the Universe and the SM has no candidate whatsoever for Dark Energy and Dark Matter, that together amount to $\sim 96\%$ of the total energy budget of the Universe. We could actually say that the SM is unable to explain almost the totality of the Universe composition, since the remaining $\sim 4\%$ of matter composition (and $\sim 0\%$ of antimatter) clashes with the abovementioned "shortage" of CP violation.

So the SM must be an effective theory that breaks down at the scale $\Lambda_{\rm NP}$. The big issue is where this energy threshold is, whether "behind the corner" (within the reach of the LHC), or far away, somewhere below $M_{\rm Pl} \simeq 10^{19}$ GeV. We will dwell on this point in the next section, and it will be apparent that while it is far from being a settled issue for the moment being, it is very likely to receive light from a seemingly related problem, namely a deeper understanding of the SSB in the SM - what the LHC will certainly provide.

1.2. On the scale of new physics

Given the above discussion a relevant question, in the absence of direct evidence for new physics, is a trustworthy guess for the scale at which it should emerge. At least partial answers can in turn be found following two main roads [Isi], namely by: (i) studying the SM Higgs potential beyond the tree level, in order to determine its sensitivity to the cutoff and the conditions for stability of the vacuum; (ii) using EW precision tests or rare decays to derive bounds on operators of dimension > 4, that appear in the phenomenological expansion in inverse power of $\Lambda_{\rm NP}$ of the "full" Lagrangian containing the SM one as the leading part.

Let us start off from the information that can be drawn by studying the quantum corrections to the SM Higgs potential. It is well known that such potential is of the form

$$V(\Phi) = V_0 - \mu^2 \Phi^\dagger \Phi + \lambda \left(\Phi^\dagger \Phi\right)^2 \ , \tag{1.1}$$

where Φ is a complex doublet of scalar fields. The two constants μ^2 and λ raise consistency or stability problems when studied beyond the tree level. The latter problems can in turn be controlled - at least partially - by imposing certain constraints, which translate into hints on $\Lambda_{\rm NP}$. We did not include the vacuum constant V_0 in the list, since it is related to the well known cosmological constant problem. On the basis of the latest estimates, one should set $V_0 \sim (10^{-2} eV)^4$, whereas a naive field theoretical guess would suggest for the vacuum energy the estimate $(\text{cutoff})^4$. Considering that the latter cutoff is typically identified with the Planck scale $M_{\rm Pl}$, the value of V_0 is by far the worst prediction of quantum field theory and today a huge, unsolved, problem.

Turning to λ, it can be studied beyond the tree level in order to determine the conditions required for the potential to be stable (or at least metastable) [Isi]. A pioneering study of the $\beta-$function for λ was performed by the authors of ref. [CMPP79]. They showed that if the value of λ at the EW scale is too low, RGE evolution to higher energy makes $\lambda(\mu)$ eventually zero (implying a free or "trivial" theory) and then negative. On the other hand if the initial condition on λ is too high, when increasing μ the theory quickly enters the non-perturbative regime in λ itself, displayed by the appearance of a Landau pole. Recalling that λ is proportional to the square of the Higgs mass m_H, the above pieces of information on the behavior of the Higgs potential can be turned into bounds on m_H itself.

In particular, the requirement of non-triviality sets the lower limit $m_H \geq 136$ GeV, whereas the absence of the Landau pole up to the Planck scale determines the upper limit

$m_H \leq 174$ [Isi]. So this argument - albeit of one-loop "nature" and restricted to the SM realization of the Higgs potential - allows only a very narrow window for the Higgs mass. Comparing with the experimental hint of a light m_H coming from the EWPT's, this in turn seems to point towards a quite close scale of NP [Isi]. However this conclusion is very strongly dependent on the value of the top quark mass m_t, lower values of m_t moving the zero in $\lambda(\mu)$ to higher energies [AI94, IRS01]. As a consequence, it is hard to attain more than vague indications from this argument.

We now address the case of the mass term in the Higgs potential. Since dimension 4 terms in the Higgs Lagrangian are not protected by any symmetry playing the role of the chiral one in the fermion case, nothing prevents the occurrence of power-like divergences when computing loop corrections to the Higgs mass, that in fact are well known to appear. Restricting to the top quark contribution, one has [BS00]

$$\delta m_H^2 = \frac{3}{\sqrt{2}\pi^2} G_F m_t^2 \Lambda^2 = (0.3\ \Lambda)^2\ , \tag{1.2}$$

where Λ is the hard cutoff employed as ultraviolet regulator. Is is immediate to see that, if the correction δm_H^2 is allowed a value in the range of the hundreds GeV, namely comparable with the expected experimental value for the Higgs mass, then quite a stringent upper bound on $\Lambda_{\rm NP}$ is implied, $\Lambda_{\rm NP} \leq 1$ TeV. We note that from the strictly technical point of view of renormalization, the power-like divergence in eq. (1.2) is just like any other one and it can simply be removed in the usual way, by redefining constants and fields in the bare Lagrangian. The problem arises when one takes it "seriously" and gives the cutoff the meaning of a threshold for NP. Notice that this is the only known way to append to the renormalization process a physical interpretation and not simply the status of a technical working procedure for removing unwanted infinities. Now, when divergences are severe as in eq. (1.2), it is hard to keep δm_H^2, hence m_H, separated from the NP scale $\Lambda_{\rm NP}$, unless either $\Lambda_{\rm NP}$ is taken to be low enough or unappealing fine-tunings are invoked.

The constraint on $\Lambda_{\rm NP}$ coming from the above argument is thus seemingly under control, albeit obtained with a model-dependent estimate. Actually the situation gets considerably complicated when comparing with the estimate coming from bounds on dimension > 4 operators imposed by EW precision tests, as mentioned at the beginning of this section. The procedure [BS00] is to first list, in a model-independent way, all the structures up to dimension 6, suppressed by inverse powers of $\Lambda_{\rm NP}$ and restricted to comply with some "reasonable" (yet minimal) symmetries. Then the maximum contribution allowed to each operator by the analysis of precisely measured quantities in the SM, translates into a lower bound on $\Lambda_{\rm NP}$. The point is that most fits favor in this case a NP scale (well) beyond about 5 TeV [BS00], a bound that however clashes with the one derived from eq. (1.2): this is the "LEP paradox", the contradiction between eq. (1.2), that pulls NP down, and the remarkable performance of the SM when contrasted with data, that leaves small room for new effects, pushing $\Lambda_{\rm NP}$ up. It should be stressed however that the [BS00] analysis is carried out supposing the higher-dimensional operators as "strongly coupled", namely multiplied by an overall "coupling" factor taken to be 1 (or -1). The LEP paradox would of course be alleviated or removed altogether, were

the higher-dimensional structures weakly coupled, as is the case for the supersymmetric contributions to the observables considered in EW precision tests.

Another possibility to get information on $\Lambda_{\rm NP}$ is to analyze rare processes. In this case, rather than the extreme precision of experimental data, the guiding strategy is the observation that the considered processes are suppressed within the SM, hence represent a likely window for NP contributions to be competitive. The emphasis is on the so-called Flavour Changing Neutral Currents (FCNC), that in the SM are suppressed by being loop processes and by other conspiring effects, in particular the approximate flavour symmetry of the theory and the hierarchy of the CKM matrix entries. Among the full host of FCNC processes, the best measured are K, B_d meson-antimeson mixings and the $B \to X_s\gamma$ decay. They are as well very precisely known in the framework of the SM *and* of its most popular extensions, like low-energy SUSY. In these cases, bounds on NP indicate $\Lambda_{\rm NP} \geq 100$ TeV or higher, unless additional symmetries are called for to constraint NP contributions. This is presently an active field of investigation [Isi].

To conclude our short inventory on the most popular arguments for getting hints on $\Lambda_{\rm NP}$, we should mention also the case of operators explicitly violating lepton (L) or baryon (B) number symmetries. They give rise to such phenomena as proton and neutrinoless double beta decay, for which very stringent bounds exist, thus pointing to high values for $\Lambda_{\rm NP}$. Quite a clear indication on the occurrence of L-violating operators comes notably from neutrino masses as well. Different approaches (with or without right-handed neutrinos) lead in this case to the remarkably common conclusion of $\Lambda_{\rm NP} \sim 10^{15}$ GeV [Isi].

The bottom line of the above discussion is that the question where one should reliably expect the SM to break down does not admit a clear answer, at least for the time being. Different approaches lead to even vastly different limits on $\Lambda_{\rm NP}$, strongly depending on the symmetries required to (or assumed to be broken by) the new operators. Sometimes contradictions appear as well.

In the absence of unquestionable indications, one can only form a "personal" point of view on the chances of having "surprises" behind the corner, at the TeV scale. A pessimistic approach would be to extend the unexpected success of the SM recorded at LEP-2 to the LHC case: if NP is for some reason much above the TeV scale, it will be very hard to detect it at the LHC as well. All the inconsistencies pointed out above would in this case remain perhaps unexplained.

On the other hand, the experimental exploration of the TeV scale will for sure provide us with the capital opportunity to penetrate from the data the mechanism of EW symmetry breaking. As stressed before, the latter is still an unsolved conundrum, mainly because of the already mentioned LEP paradox raised by the quadratic divergence in eq. (1.2). If such divergence has a physical meaning, as analogy with similar situations in the past as well as a purely "prejudice" would suggest, then there must be a mechanism taking care of it.

1.3. New physics from SUSY

The problem of finding a consistent and phenomenologically acceptable extension of the SM has been a central issue in theoretical physics since the last decades. Many ideas have been introduced and developed to cope in particular with the "hierarchy" problem apparent from eq. (1.2), namely the problem of having a close connection between vastly different scales like $M_{\rm Pl}$ and the EW breaking scale.

A very elegant route is that of invoking a new symmetry, SUperSYmmetry (SUSY). SUSY is the symmetry that turns fermions into bosons and vice-versa [CM67, HLS75]. As such it roughly doubles the degrees of freedom normally present in the SM, since for every fermion (boson) present, it requires the introduction of a corresponding boson (fermion). Of course since superpartners are not part of the observed spectrum, a mechanism for breaking SUSY must also be provided to construct a realistic model. All these issues will be the subject of the next chapter, where we will present a well-known supersymmetric model consistently extending the SM and able to provide a beautiful solution to the hierarchy problem. This is the Minimal Supersymmetric Standard Model (MSSM).

What is relevant to the present discussion is that SUSY - and its phenomenological realization via the MSSM - entails the cancellation of the quadratic divergence in eq. (1.2), caused by the top-quark loop, with a similar divergence brought by another loop diagram with the scalar partner of the top itself, namely the s-top. By this mechanism, eq. (1.2) goes into

$$\delta m_H^2 = \frac{3}{\sqrt{2}\pi^2} G_F m_t^2 \Lambda^2 \stackrel{\rm MSSM}{\longrightarrow} \frac{3}{\sqrt{2}\pi^2} G_F m_t^2 m_{\tilde{t}}^2 \ln \frac{\Lambda^2}{m_{\tilde{t}}^2} \,, \tag{1.3}$$

where $m_{\tilde{t}}$ is the mass of the stop. So the quadratic divergence is replaced by the "usual" log-like one, allowing m_H to remain in the hundreds GeV range even with Λ at the Plank scale. The cancellation of quadratic divergences is guaranteed to all orders in perturbation theory by non-renormalization theorems [SS75].

A couple of observation are in order here. First, the solution to the hierarchy problem provided by eq. (1.3) is a "technical" one: within the MSSM it is possible to keep m_H and $M_{\rm Pl}$ separated, but on the other hand the question why they are so different is not addressed. It is also true however that the latter, ambitious question is likely to have an answer (if any) only when the quantum regime of gravity will be fully understood.

A second observation follows from noting the proportionality of eq. (1.3) to the $\tilde{t}$ squark mass. Even not considering the full one loop correction formula to the Higgs mass in the MSSM, from eq. (1.3) it is clear that $m_{\tilde{t}}$ cannot be too big, since otherwise m_H would blow up in turn. A careful analysis (see in particular [BS00, MPR98]) including also MSSM corrections to the Z boson mass, indicates in fact that the lightest SUSY partners must be found about 1 TeV in order not to cope with heavy fine-tuning problems again.

A clear solution to the hierarchy problem is not the only virtue of SUSY. Another attractive option is the proposal of a candidate for Dark Matter (DM), provided by the so-called Lightest Supersymmetric Particle (LSP), usually identified with the neutralino. It should be stressed that there are cosmological arguments pointing to the TeV range for

the mass of DM particles [Mu, St]. In addition the MSSM would require the LSP to be stable, as a consequence of R-parity conservation. The latter symmetry is an elegant way for removing from the MSSM superpotential operators that would violate Baryon (B) and Lepton (L) number conservations. Proton decay, the most sensitive probe for this kind of effects, violates both B and L so that the absence in the Lagrangian of these terms could be enough to suppress proton decay within the experimental bounds. Now, SM particles and their SUSY partners are required to have opposite quantum number under R-parity, so that the conservation of the latter automatically entails LSP not to decay.

An additional striking feature of SUSY emerges when including it as an ingredient of Grand Unified Theories (GUT). The latter are gauge theories in which the SM group $SU(3)_c \times SU(2)_L \times U(1)_Y$ is embedded in a larger simple group, for example $SU(5)$ or $SO(10)$. If SUSY is assumed to compute the evolution to high energies of the three SM couplings, namely α_s, α_W and $\alpha_{\rm em}$, it notably turns out [EKN91] that their values almost coincide at a scale of around 10^{16} GeV, hinting at a "grand" unification. This is a non trivial test [St] , since it requires three lines to cross in a single "point": as a matter of fact the same test fails when computing the runnings without SUSY.

We underline that the issue of a suitable extension of the SM able to address, at least partly, the open problems abovementionated, has been dealt with following other non-SUSY approaches as well. The latter led to models that can be roughly classified into three big groups, namely (i) technicolor theories, in which the Higgs is a condensate of new fermions; (ii) theories with large compactified extra dimensions, with a corresponding explanation of the weakness of gravity as a "geometrical" effect (in this general context other interesting directions of development are represented by "Higgsless" models and models with "gauge-Higgs" unification); (iii) "little Higgs" models, in which group theory work allows to make corrections to the Higgs mass appear only at the two-loop level.

It must be stressed that none of the above approaches is free of criticisms and problems: for a quite complete coverage in this respect, the reader is referred to [Alt]. The message we would like to convey here, also stressed in [Alt], is that such alternative models are actually not as maturely formulated and studied as SUSY, so that they (still) lack a well defined and phenomenologically viable baseline.

On the other hand, with the MSSM − or variations thereof −, SUSY offers a class of models that share the unique feature of being consistently and completely formulated, hence calculable, exactly like the SM. This non negligible virtue, together with those sketched before, leave supersymmetry as the "standard" way beyond the SM [Alt].

1.4. Rare processes

Models of NP can not only be verdict by the experimental detection of the new particles, but also undergo indirect test by calculating their contributions to very well measured processes and/or rare ones. The option of indirect searches of NP is obviously based on a given model being calculable and well defined. This is a special virtue of the MSSM, as we have already stressed.

Putting rigorous constraints is also important in the particular case of the MSSM, given the big number of basically free parameters characterizing this model. Taking into account the (more than) doubling of the particle content, and the presence of SUSY-breaking terms, the MSSM entails some 100 parameters in addition to those pertaining to the SM.

In order to allow to reliably explore such large space of parameters, it is important to choose a suitable set of observables able to put the most restrictive limits on them. The latter limits are in turn useful handles on possible symmetries that are still missed in the construction of the model, and that could considerably simplify the pattern of parameters. In this respect, many elaborating hypotheses like Minimal Flavor Violation (MFV) [DGIS02, HR90] have been proposed.

In the present work we analyze in turn two observables which allow us to investigate rather different scenarios for the MSSM parameter space. They both belong to the category of rare processes, physical transitions that are strongly suppressed already within the SM, so that NP contributions have a better chance of being competitive. The first one is the Electric Dipole Moment (EDM) of the Neutron, whose experimental bounds is [Har99]

$$|d_n| < 6.3 \cdot 10^{-26}\,\mathrm{e}\cdot\mathrm{cm}\ . \tag{1.4}$$

The latter, together with other particles' EDM, is strictly connected with the new sources of CP violation present in the MSSM. We have specialized our analysis to the minimal supergravity (mSUGRA) models, a class of NP models that allow us a numerical prediction of the magnitude of the new CP-violating phases. We underline that a careful analysis of EDM processes is mandatory in order to assess the allowed size of these NP contributions to CP violation and their possible effects in electroweak baryogenesis and in other CP violating processes.

However, the MSSM in turn can be formulated as the low energy description of an high energy theory less rigid than the mSUGRA models. Without assuming any special scenario for the ultimate theory, the choice of appropriate experimental quantities to compare to the experimental predictions becomes of particular concern. In this context, the dynamics of flavour physics in the quark sector provides a promising way to explore the structure of the SUSY theories. We are thinking, in particular, to the already mentioned FCNC processes. The theoretical predictions for these observables, receiving loop-induced contributions from the new SUSY particles, must be as general as possible. The philosophy under this statement is clear: whatever the ultimate theory, once the SUSY parameter space is provided at a scale around the EW one, it is possible to directly compute the theoretical prediction for these processes, compare with the experimental number and decide if the model is phenomenologically aviable.

In this Thesis we have applied such approach to the $B \to X_s\gamma$ inclusive decay. For this long-time observable, the Heavy Flavor Averaging Group [HFAG] quotes for the measured branching ratio the following world average (see ref. [B$^+$06] for the explanation of the various errors in (1.5)), obtained with $E_\gamma > 1.6$ GeV:

$$\mathrm{BR}(\mathrm{B}\to\mathrm{X_s}\gamma) = (355 \pm 24^{+9}_{-10} \pm 3)\times 10^{-6}\ . \tag{1.5}$$

Notably, this quantity is well suited to be part of a "precision" program, thanks to its low sensitivity to non-perturbative effects. This is because the mass of the b-quark is much larger than the QCD scale $\Lambda_{\rm QCD}$.

We performed the calculation of the effective Hamiltonian responsible in the MSSM for the flavor-changing $\Delta B = 1$ ($\Delta S = 1$) transition at Leading Order (LO), and provides some basic ingredient to push the theoretical prediction to Next-to-Leading Order (NLO). The main difference of this computation with respect to the choice of some restrictive hypothesis as MFV, lies in the fact that the strong interacting sector of the MSSM enters in the prediction for the branching ratio in (1.5) already at the LO, through the exchange of virtual gluinos. The tree level interaction responsible for the magnetic, penguin and box diagrams calculated in chapter 6, called flavour changing gluino (FCG), is introduced in sec. 2.3.

We underline that a complete NLO calculation for the branching ratio of the radiative B decays in a model-independent scenario for the MSSM is a very involved task and, as for the SM predictions for the same quantity, will require a certain number of years and "human resources" to be completed.

However, the LO formulae presented here are the first step to perform a phenomenological analysis of the mass matrices of the up- and down- type squark, the supersymmetric scalar partners of the SM quarks. Given the strong suppression of the flavour changing effects already inside the SM, dictated by the almost diagonal pattern of the CKM matrix, it is possible to derive severe bounds also for the off-diagonal terms of the corresponding squark mass matrix. We adopted the Mass Insertion Approximation (MIA) as a useful tool which permits a simple quantification of such a non-diagonal entries.

1.5. Outline of this work

The Thesis is organized in the following way.

Chapter 2 starts with a short summary of the main features of the low-energy SUSY in sec. 2.1-2.2, with particular emphasis on the particle content of the MSSM. Sec. 2.3 focus on the flavour and CP content of the MSSM in the quark sector, as the common framework for the calculations presented in this work. We also describe the pattern of the supersymmetric parameters, once we assumed the MSSM as a low energy remnant of a mSUGRA model. In fact, this is the model we have used in our analysis of the EDM of the Neutron.

In chapter 3 we then enter into the technical details at the basis of the calculation we want to present. In particular, sec. 3.1 is an introduction to the OPE while sec. 3.2 explain how to use the RGE in order to relate the supersymmetric high energy interactions to the hadronic low energy dynamics.

Chapter 2 and 3 represent somewhat an introductory part on the main field theoretical tools, to the aim of making the treatment as self contained as possible and to define a common notation. The original part of the work follows.

In particular, chapters 4-5 deal with a deepened study of the EDM of the Neutron

within the mSUGRA models. After a brief introduction to the EDM interaction in sec. 4.1, we briefly summarize the SM predictions for the EDM of the Neutron in sec. 4.2. In order to obtain the physical amplitude, calculated at the high energy scale given by the masses of supersymmetric particles, in sec. 4.3 we give the relevant formulae to evolve the Wilson coefficients down to a few GeV, where the matrix elements of the operators are estimated with non-perturbative methods (sec. 4.4). In sec. 4.5 we will derive all the possible SUSY contributions at LO. Sec. 4.6 is dedicated to the phenomenological implications of the LO results. We suggests that cancellations between the various supersymmetric contributions to the EDM of the Neutron can be active only in special regions of the parameter space, but cannot be invoked as a general argument in order to pass the severe experimental constraint given in eq. 1.4. We discuss all the uncertainties hidden inside the LO approximation, and stress in particular that the dependence on the matching scale for the gluino contribution is considerably pronounced. This naturally explain our efforts to compute the NLO corrections to the EDM of the Neutron, specializing to the strong sector of the MSSM.

These are included in chapter 5 by considering the relevant anomalous dimension matrix (ADM) and Wilson coefficients at the two loop level. In sec. 5.1 we present the NLO implementation of the "magic numbers", obtained as a solution of the RGE dictated by the ADM generated by the mixing of the dipole operators with the Weinberg operator. The Wilson coefficients is the second ingredient in order to complete the NLO calculation. In 5.2 we describe, in detail, the full theory computation. The list of the two-loop diagrams computed is given in figs. 5.1-5.6. The effective theory calculation and the matching procedure are given in sec. 5.3. At the NLO, the result in the full theory depends on the choice of the regularization scheme. We obtained the final result for the Wilson coefficients in the $\overline{\text{MS}}$-NDR scheme. In sec. 5.4, we describe the procedure followed to translate the result in the $\overline{\text{MS}}$-DRED scheme. This is always required when dealing with supersymmetric calculation, since NDR breaks supersymmetry. The Wilson coefficients satisfy the proper Callan-Symanzik equation (sec. 5.6), and, as expected, the dependence of the result for the gluino contribution from the matching scale is considerably reduced with respect to the LO (sec. 5.7).

Chapter 6 turn to radiative B decays, analyzed in the presence of supersymmetric FCG interactions. We give all the ingredients needed to an evaluation of the Branching Ratio at LO. Some specific tools for the calculation, namely the MIA and the Fierz relations, are collected in appendices A and B, respectively. We stress again that the part of the Thesis embedded in this chapter is only an exploratory study. Our first aim is to confirm the already known results present in the literature for the gluino contribution to radiative B decays in SUSY. In particular, we find agree with the results of [BGHW00], once the latter are translated to the MIA formalism used here.

The last chapter of the Thesis is devoted to our conclusions and outlook.

2. Theoretical framework I: Supersymmetry

In this chapter we briefly review the construction of "low-energy" Supersymmetric models, focusing in particular to the MSSM in sec 2.2. We will present only the aspects more closely related to the original part of the Thesis. For a more formal analysis in the framework of the superfield formalism, the reader is referred for example to [Der].

In particular, we will focus on the new flavour- and CP- violating interactions which naturally arise if the New Physics proposed to solve the hierarchy problem is SUSY. As explained in sec. 2.3, all these new effects are embedded into the mass matrices of the new particles present in the physical spectrum at the electroweak scale (squark, charginos and neutralinos).

2.1. Low-energy Supersymmetry

The presence of elementary scalar fields, namely the Higgs fields, can be allowed without a rising of the hierarchy problem, as previously mentioned, if the SM is extended in a supersymmetric way. For phenomenological reasons, supersymmetry cannot be exact, otherwise supersymmetric partners degenerate in mass with the known particles would have been already observed. It is possible, however, for this boson-fermion symmetry to be broken and in turn for the theory not to develop any further quadratic (and in general power-like) divergences beyond the usual logarithmic ones. This can be managed either via a spontaneous or via an explicit breaking of the supersymmetry. Obviously, the supersymmetric breaking scale, linked for example to the splitting δm^2 inside of the supermultiplets, must be close to the electroweak one: in fact, in the limit $\delta m^2 \gg M_W^2$, the hierarchy problem would arise again, since the radiative corrections to the scalar masses are proportional to such splitting.

In explicit realizations of models with global supersymmetry spontaneously broken, it turns out that realistic mass splittings between SM particles and SUSY partners do not arise in a natural way [O'R75, BFNS82]. Such difficulties do not support to the belief that breaking of global supersymmetry be of spontaneous nature.

Consequently, most of the supersymmetric models used in phenomenology, in particular the MSSM, feature explicit soft breaking of supersymmetry, through the addition of suitable non-supersymmetric terms to the Lagrangian. This solution, not really esthetic at first sight, find a justification in a more wide context, in which also gravity is considered. The connection with the latter is intuitive: in fact the generators of supersymmetry are part of a larger algebra, comprising also the Poincaré Group generators (superalgebra

or graded Lie algebra), and the gravitational field is connected to the local transformation generated from the latter. One is therefore induced to consider also the local version of the supersymmetric transformations and to build the so-called supergravity theories. The latter should in turn be an effective version of SuperStrings, that are presently the only known candidate for a one-parameter, finite theory eligible to describe gravity at the quantum level together with the SM forces. Note that this connection with the gravity is another important motivation for supersymmetry.

In order to obtain models in which supersymmetry, not broken at the Planck scale, survives, one assume that the local supersymmetry be spontaneously broken in an "hidden" sector that have no (or only very small) direct couplings to the "visible" sector. The ultimate supersymmetry-breaking order parameter do not belong to any of the SUSY super-multiplets and is provided by a nonvanishing vacuum expectation value (v.e.v.) for some auxiliary field F embedded in the hidden sector. The latter must be introduced, and indicated as F and D for matter and gauge super-multiplets, respectively, in order to preserve SUSY also off-shell.

In an effective theory approach, it is possible to infer the scale of the breaking of the supersymmetry considering gauge-mediated interactions with the hidden sector dictated by a group G

$$\delta m \sim \frac{\alpha_G}{4\pi} \frac{\langle F \rangle}{M_{mess}} \ , \tag{2.1}$$

where $\alpha_G/4\pi$ is a loop factor and the index G labels the gauge group which mediates the breaking. SUSY breaking can be communicated to the observables sector also by means of gaugino condensates [Nil82] or by anomalies in extra dimensional models.

All the abovementioned options can be used to explore the dynamics until a certain energy, since we expect gravity mediation to become the dominant mechanism near the Planck scale. In supergravity, one important consequence of the spontaneous symmetry breaking is the generation of a mass term $m_{3/2}$ for the gravitino to expenses of a massless fermion called Goldstino, like in the ordinary Higgs mechanism.

Lacking a renormalizable description of quantum gravity, in an effective theory format supergravity enters the MSSM Lagrangian through interactions of negative mass dimension, scaled by inverse powers of the Plank scale M_P. With the addition of these non-renormalizable terms, beyond the superpotential invariant under global SUSY transformations, two other independent terms must be specified in the most general Lagrangian: the Kahler potential with dimensions of the squared mass and the dimensionless gauge kinetic function. The general construction of the model is more involved than in global SUSY. For phenomenogical applications, however, the key point is the existence of a special configuration, dictated by a choice of minimal kinetic terms and a "flat limit" ($M_P \to \infty$ with $m_{3/2}$ fixed). In this minimal model, spontaneously broken supergravity at high energy is equivalent to a low energy global supersymmetric theory explicitely broken by soft terms. The scale of this terms is connected to the gravitino mass:

$$\delta m \sim m_{3/2} \sim \frac{\langle F \rangle}{M_P} \ . \tag{2.2}$$

In particular, this is the order of magnitude of the masses contained in the scalar potential, and consequently also the order of magnitude of the electroweak symmetry breaking. In this way, is is possible to establish a natural link between the latter and the "effective" scale of the supersymmetry breaking.

2.2. Minimal Supersymmetric Standard Model

The simpler realization of the abovementioned scenario is embedded in the Minimal Supersymmetric Standard Model, which will now briefly introduced. For a systematic presentation of the MSSM the reader is referred for example to [Mar97].

The particle content of the MSSM is given by the Standard Model fields, with a second Higgs doublet, in a one-by-one correspondence to supersymmetric partners with the same quantum numbers. The supersymmetric multiplets are described by *chiral* or *matter* and *gauge* or *vector* superfields: the chiral superfields are collected in table 2.1, according to the transformation properties under the $SU(3)_c \times SU(2)_L \times U(1)_Y$ gauge group, and have component of spin 1/2 (three generations of lepton and quarks, beyond the Higgsinos) and of spin 0 (three generations of sleptons and squarks, beyond the Higgs fields). The vector superfields, given in table 2.2, have physical component of spin 1 (standard gauge fields) and spin 1/2 (gauginos).

The electric charge of each particle satisfies the relation $Q_{\rm em} = Y + T_3$, where T_3 is the $SU(2)_L$ eigenvalue, which equals $\pm 1/2$ for doublets, zero for singlets. Gauge invariance specify completely the gauge-mediated interactions between the chiral and the vectorial superfields [1]

$$\mathcal{L}_{gauge} = (D_\mu \phi)^\dagger (D^\mu \phi) + i\psi\sigma^\mu (D_\mu \overline{\psi}) + \sum_{P=B,W,G} \left\{ i\lambda_P^p \sigma^\mu (D_\mu \overline{\lambda}_P^p) - \frac{1}{4} F_P^{p\ \mu\nu} F_{P\ \mu\nu}^p \right.$$
$$\left. - \frac{1}{2} g_P^2 \sum_{p=1}^{n_p} \left(\phi_i^\dagger T_{Pij}^p \phi_j \right)^2 - i\sqrt{2} g_P \left(\overline{\psi}_i \overline{\lambda}_{Pij}^p \right) \phi_j + i\sqrt{2} g_P \phi_i^\dagger \left(\lambda_{Pij}^p \psi_j \right) \right\} , \quad (2.3)$$

where ϕ represent a general scalar superpartner of the matter field ψ, $\lambda_{Pij}^p \equiv \lambda_P^p T_{Pij}^p$ and indices i, j and p span the fundamental and the adjoint representation of the gauge group P, respectively.

Now we turn to the mass and auto-interaction terms between components of the chiral superfields. In this sector both the Yukawa Lagrangian $\mathcal{L}_Y = \mathcal{L}_Y(\phi, \psi)$ and the scalar

[1] Some warning about the notation: in this section all the fermionic components are left-handed Weyl spinors, more suitable for the theoretical building of the SUSY Lagrangian. In the following section we will pass to the Dirac and Majorana representations, more useful when dealing with perturbative calculations.

superfield	**spin 0**	**spin $\frac{1}{2}$**	$\mathbf{SU(3)_c}$	$\mathbf{SU(2)_L}$	$\mathbf{U(1)_Y}$
L^I	$\begin{pmatrix}\tilde{\nu}\\ \tilde{e}\end{pmatrix}_L$	$\begin{pmatrix}\nu\\ e\end{pmatrix}_L$	**1**	**2**	$-\frac{1}{2}$
E_c^I	$(\tilde{e}_R^I)^*$	$(e_L^I)^c$	**1**	**1**	$+1$
Q^I	$\begin{pmatrix}\tilde{u}^I\\ \tilde{d}^I\end{pmatrix}_L$	$\begin{pmatrix}u^I\\ d^I\end{pmatrix}_L$	**3**	**2**	$+\frac{1}{6}$
U_c^I	$(\tilde{u}_R^I)^*$	$(u_L^I)^c$	$\overline{\mathbf{3}}$	**1**	$-\frac{2}{3}$
D_c^I	$(\tilde{d}_R^I)^*$	$(d_L^I)^c$	$\overline{\mathbf{3}}$	**1**	$+\frac{1}{3}$
H_u	$\begin{pmatrix}h_u^1\\ h_u^2\end{pmatrix}$	$\begin{pmatrix}\tilde{h}_u^1\\ \tilde{h}_u^2\end{pmatrix}$	**1**	**2**	$+\frac{1}{2}$
H_d	$\begin{pmatrix}h_d^1\\ h_d^2\end{pmatrix}$	$\begin{pmatrix}\tilde{h}_d^1\\ \tilde{h}_d^2\end{pmatrix}$	**1**	**2**	$-\frac{1}{2}$

Table 2.1: Left-handed matter multiplets of the MSSM. Index I run over the three generations of quarks and leptons.

potential $V = V(\phi)$ are determined by the superpotential $W = W(\phi)$ of the theory:

$$\mathcal{L}_Y = -\frac{1}{2}\sum_{ij}\left[\frac{\partial^2 W}{\partial\phi_i\partial\phi_j}\psi_i\psi_j + h.c.\right] , \tag{2.4}$$

$$V = \sum_i \left|\frac{\partial W}{\partial\phi_i}\right|^2 . \tag{2.5}$$

Specializing to the MSSM, we give here the explicit form of the superpotential as a function of the superfields in table 2.1, even if they can be just thought of as the correspondence scalar fields, when applying the rule in eqs. (2.4-2.5) [Mar97]:

$$W = \quad \epsilon_{ij}Y_U^{IJ}U_c^I Q^{Ji}H_u^j - \epsilon_{ij}Y_D^{IJ}D_c^I Q^{Ji}H_d^j - \epsilon_{ij}Y_E^{IJ}E_c^I L^{Ji}H_d^j + \mu\epsilon_{ij}H_u^i H_d^j + h.c. , \tag{2.6}$$

In eq. (2.6) $SU(2)_L$ singlets are obtained contracting with the antisymmetric tensor ϵ_{ij}. Moreover, a sum run over the repeated indices of generation I, J is understood throughout this chapter.

This is the most general superpotential for the superfields of the MSSM, compatible with renormalizability, gauge symmetry and R-parity.

The MSSM Lagrangian is completely given only if the most general soft terms allowed

superfield	**spin $\frac{1}{2}$**	**spin 1**	$\mathbf{SU(3)_c}$	$\mathbf{SU(2)_L}$	$\mathbf{U(1)_Y}$
V_3	λ_G^a	G_μ^a	**8**	**1**	0
V_2	λ_W^i	W_μ^i	**1**	**3**	0
V_1	λ_B	B_μ	**1**	**1**	0

Table 2.2: Gauge multiplets of the MSSM. Indices a and i run over the adjoint representations of $SU(3)$ and $SU(2)$, respectively.

by gauge symmetry are specified

$$\begin{aligned}
-\mathcal{L}_{\rm soft} = &\Big[(m_Q^{IJ})^2\left((\tilde{u}_L^I)^*\tilde{u}_L^J + (\tilde{d}_L^I)^*\tilde{d}_L^J\right) + (m_U^{IJ})^2(\tilde{u}_R^I)^*\tilde{u}_R^J + (m_D^{IJ})^2(\tilde{d}_R^I)^*\tilde{d}_R^J \\
&+(m_L^{IJ})^2\left((\tilde{\nu}_L^I)^*\tilde{\nu}_L^J + (\tilde{e}_L^I)^*\tilde{e}_L^J\right) + (m_E^{IJ})^2(\tilde{e}_R^I)^*\tilde{e}_R^J \\
&+ m_{H_u}^2\left((h_u^1)^*h_u^1 + (h_u^2)^*h_u^2\right) + m_{H_d}^2\left((h_d^1)^*h_d^1 + (h_d^2)^*h_d^2\right)\Big] \\
&+\frac{1}{2}\left(M_1\lambda_B\lambda_B + M_2\lambda_W^i\lambda_W^i + M_3\lambda_G^a\lambda_G^a + h.c.\right) \\
&+\Big(\epsilon_{ij}A_U^{IJ}(\tilde{u}_R^I)^*\tilde{q}_L^{Ji}h_u^j - \epsilon_{ij}A_D^{IJ}(\tilde{d}_R^I)^*\tilde{q}_L^{Ji}h_d^j \\
&- \epsilon_{ij}A_E^{IJ}(\tilde{e}_R^I)^*\tilde{l}_L^{Ji}h_d^j + B\epsilon_{ij}h_u^ih_d^j + h.c.\Big) \ . \qquad (2.7)
\end{aligned}$$

In formula (2.7) we have used the notation $\tilde{q} \equiv (\tilde{u}, \tilde{d})$ and $\tilde{l} \equiv (\tilde{\nu}, \tilde{e})$. We have already stress in sec. 2.1 that all the positive mass dimension parameters in eq. (2.7), generally indicated as $m_{\rm soft}$, must be around the TeV scale, in order to do not reintroduce fine-tuning.

The Higgs mechanism is performed by giving a v.e.v. to ad hoc scalar components of both the H_u and H_d superfields

$$H_u \to \begin{pmatrix} 0 \\ v_u \end{pmatrix} \quad , \quad H_d \to \begin{pmatrix} v_d \\ 0 \end{pmatrix} \ , \qquad (2.8)$$

where $v_u = v\sin\beta$, $v_d = v\cos\beta$ is the common parameterization A detailed treatment of the Higgs mechanism can be found in [Der], whereas the resulting mass formulas with the conventions usually adopted in the literature are collected in [Ros90].

This choice is dictated by the request to break $SU(2)_L \times U(1)_Y$ down to $U(1)_{\rm em}$. We will not enter here into the details of the calculations practically realizing this mechanism, since they are not important for our discussion. We only write down the final relations which link the weak parameters to the electromagnetic charge $e = g_1c_W = g_2s_W$, where $s_W = \sin\theta_W$, $c_W = \cos\theta_W$ define the Weinberg angle θ_W

$$M_W = \frac{e}{2s_W}v \quad , \quad M_Z = \frac{e}{2s_Wc_W}v \ . \qquad (2.9)$$

We now turn to analyze in more details the CP and flavour properties of the MSSM, since they are closely linked to the physical observables under investigation in this Thesis.

2.3. CP and Flavour properties of the MSSM

Looking at the superpotential in eq. (2.6) we note that, in order to generate diagonal mass terms for the fermion fields, suitable unitary transformations in the generation space must be performed on the superfields Q^I, U_c^I, D_c^I, L and E_c^I. Such transformations are defined as [HKR86]

$$\begin{aligned} Q_i^I &\to (V_{Q_i})^{IJ} Q_i^J \ , \\ U_c^I &\to (V_U^*)^{IJ} U_c^J \ , \\ D_c^I &\to (V_D^*)^{IJ} D_c^J \ , \\ L_i^I &\to (V_{L_i})^{IJ} L_i^J \ , \\ E_c^I &\to (V_E^*)^{IJ} E^J \ . \end{aligned} \tag{2.10}$$

The important point is that the up- and down-components of doublets rotate with separate matrices. In particular rotations for u and d quarks are those defining the CKM basis. Since the same rotations occur for squarks, the superfield basis on the right side of eq. (2.10) is usually referred to as the super-CKM basis. Proceeding exactly as in the Standard Model, by means of formulae (2.10), the Yukawa couplings Y^{IJ} in eq. (2.6) are reduced to their diagonal form

$$(Y_U)^d = (V_U Y_U V_{Q_1}^\dagger) \ \ , \ \ (Y_D)^d = (V_D Y_D V_{Q_2}^\dagger) \ \ , \ \ (Y_E)^d = (V_E Y_D V_{L_2}^\dagger) \ . \tag{2.11}$$

and correspondingly the mass terms are

$$m_u^d = Y_U^d v_u \ \ , \ \ m_d^d = Y_D^d v_d \ \ , \ \ m_e^d = Y_E^d v_d \ \ . \tag{2.12}$$

However, the misalignment of V_{Q_1} and V_{Q_2} induce tree-level mixing among quarks of different generations. In particular vertices connecting a pair of quarks with a charged boson or scalar Higgs and their supersymmetric counterparts (see eq. (2.3)) are weighted by the elements of the CKM matrix $K = V_{Q_1} V_{Q_2}^\dagger$. This phenomenologically almost-diagonal matrix give rise to all the CP- and flavour- violating observables in the SM. We postpone the discussion of the strong CP violation, also present in the SM, in section 4.2.

In the MSSM there are several additional contributions to flavour changing transition and CP violation which are absent in the SM. We first observe that squarks with the same electric charge, organized in a six component vector as

$$(\tilde{u}_L, \tilde{u}_R)^T = \left(\tilde{u}_L, \tilde{c}_L, \tilde{t}_L, \tilde{u}_R, \tilde{c}_R, \tilde{t}_R\right)^T \tag{2.13}$$

in the case of up squarks, can mix through 6×6 matrices only restricted to be hermitian. The latter receives contribution from the soft terms in eq. (2.7) and, after the EW symmetry breaking, also from the gauge and superpotential couplings. After the diagonalization of the fermionic mass terms via the rotations in eq. (2.10), the expression for the up and

down-type squark matrices in the Super-CKM basis read

$$\mathcal{M}_U^2 = \begin{pmatrix} V_{Q_1} m_Q^2 V_{Q_1}^\dagger + (m_u^d)^2 + \Delta_{\tilde{u}_L}\hat{1} & (V_{Q_1} A_U^\dagger V_{Q_1}^\dagger - \mu \cot\beta) \mathrm{m_u^d} \\ m_u^d (V_{Q_1} A_U V_{Q_1}^\dagger - \mu^* \cot\beta) & V_U m_U^2 V_U^\dagger + (m_u^d)^2 + \Delta_{\tilde{u}_R}\hat{1} \end{pmatrix} , \tag{2.14}$$

$$\mathcal{M}_D^2 = \begin{pmatrix} V_{Q_2} m_Q^2 V_{Q_2}^\dagger + (m_d^d)^2 + \Delta_{\tilde{d}_L}\hat{1} & (V_{Q_2} A_D^\dagger V_{Q_2}^\dagger - \mu \tan\beta) \mathrm{m_d^d} \\ m_d^d (V_{Q_2} A_D V_{Q_2}^\dagger - \mu^* \tan\beta) & V_D m_D^2 V_D^\dagger + (m_d^d)^2 + \Delta_{\tilde{d}_R}\hat{1} \end{pmatrix} , \tag{2.15}$$

where $\Delta_\phi = \left[(T_3)_\phi - Q_\phi \sin^2\theta_W\right] \cos 2\beta M_Z^2$ and we have re-parameterized the A-terms extracting the corresponding Yukawa matrix as $A_U \to Y_U A_U$, $A_D \to Y_D A_D$.

The only CP- and flavour-violating terms in eqs. (2.14-2.15) comes from the soft parameters embedded in eq. (2.7). The SUSY breaking mechanism introduces many new parameters. In particular, a careful count [DS95] reveals that there are 57 additional masses and mixing angles and 40 extra phases with respect to the Standard Model.

The quite severe experimental bounds on the new flavour and CP violating parameters require a precise theoretical explanation. Now we want briefly discuss two possible solutions of the supersymmetric flavour and CP problem.

The first one is given by the mSUGRA model, and corresponds to the universality idea for the soft parameters. The theoretical motivations to justify such a kind of models have been already discussed in sec. 2.1. Here we point out the further observation that this models are very clear from a phenomenological perspective, since they strongly reduce the amount of independent sources of CP violation generated by the supersymmetry breaking mechanism.

In this case, once an auxiliary field F living in the hidden sector gets a v.e.v., the soft-breaking parameters can be written in terms of only four parameters $\left\{m_{1/2}, m_0, A_0, B_0\right\}$ as follows

$$M_i = m_{1/2} \quad , \quad i = 1,2,3 \; ; \tag{2.16}$$

$$m_Q^2 = m_U^2 = m_D^2 = m_L^2 = m_E^2 = m_0^2 \; \hat{1} \quad , \quad m_{H_u}^2 = m_{H_d}^2 = m_0^2 \; ; \tag{2.17}$$

$$Y_U A_U = A_0 Y_U \quad , \quad Y_D A_D = A_0 Y_D \quad , \quad Y_E A_E = A_0 Y_E \; ; \tag{2.18}$$

$$B = B_0 \mu \; . \tag{2.19}$$

Eqs. (2.16-2.19) are universal boundary conditions at the Plank scale for the RG evolution, and their solution allows, together with the supersymmetric couplings given by the gauge and Yukawa interactions, to provide the entire MSSM spectrum at the EW scale.

In the mSUGRA models those phases can arise from 4 complex parameters

$$\phi_\mu \quad , \quad \phi_{B_0} \quad , \quad \phi_{m_{1/2}} \quad , \quad \phi_{A_0} . \tag{2.20}$$

However, only two of this are physical, since it is always possible to "rotate" away the other ones acting on the fields with two $U(1)$ global symmetry. The first symmetry is a Peccei-Quinn transformation which acts on the Higgs doublets and the right-handed

fields in such a way that all the interactions but those which mix the two doublets are invariant. It is customary to use this symmetry in order to choose the phase convention in which B_0 is real. The second $U(1)_R$ symmetry transforms the fields in such a way that all the dimension one parameter involved in the superpotential (2.6) and in the soft Lagrangian (2.7) are rotated by the same magnitude. As a consequence, we can set to be real by a $U(1)_R$ rotation one another parameter in (2.20) The common choice adopted in the literature is to keep $m_{1/2}$ real.

The mSUGRA models are the theoretical ground for our analysis of the EDM of the Neutron. The latter is a CP-violating observable, and consequently vanish in the limit of null new supersymmetric phases.

We observe that renormalization effects do not introduce further additional phases in the transition from the boundary scale Q_0 to the electroweak one. We observe that a popular approximation is to impose the boundary conditions (2.16-2.19 at the unification scale $M_U \sim 10^{16}$ GeV instead of M_P [Mar97].

This is clear for the gaugino masses, since the RG equations are

$$\frac{d}{dt}M_a = \frac{1}{8\pi^2} b_a g_a^2 M_a \quad , \quad b_a = 33/5, 1, -3 \tag{2.21}$$

in the one-loop approximation, with $t = \ln Q/Q_0$. Then it follows that

$$M_a(Q) = \frac{g_a^2(Q)}{g_a^2(Q_0)} m_{1/2} \ . \tag{2.22}$$

As for the other potentially complex couplings we start observing that the phase of μ and B_0 are RGE-invariants. Turning finally to the A-terms, even if the evolution from the boundary scale to the EW is different for up- and down- type flavour, resulting into a splitting of the phases ϕ_{A_u} and ϕ_{A_d}, however they are both calculable from the boundary conditions (2.16-2.19).

The baseline of this discussion is that, in its more economical version, mSUGRA models allow to put directly constraints on the magnitude of the two independent "gravity mediated" phases ϕ_μ and ϕ_{A_0}.

In our analysis of the Neutron EDM this phases enters the squark mass matrix. The latter have been already introduced in its general form at the EW scale in eq. (2.14). The crucial point here is that, assuming the universality conditions at the input scale, the squared mass matrix of the down-type squarks evolved to M_W can be written in the Super-CKM basis as

$$\mathcal{M}_D^2(M_W) = \begin{pmatrix} M_{DLL}^2 & M_{DLR}^2 \\ M_{DRL}^2 & M_{DRR}^2 \end{pmatrix} \tag{2.23}$$

where

$$M^2_{DLL} = (M^d_{DLL})^2(t) + c_1(t) K^\dagger (m^d_u)^2 K \ , \tag{2.24}$$

$$M^2_{DLR} = \left[M^d_{DLR}(t) + \frac{c_2(t)}{M_W} K^\dagger (m^d_u)^2 K \right] \ m^d_d \ , \tag{2.25}$$

$$M^2_{DRL} = \ m^d_d \ \left[M^d_{DRL}(t) + \frac{c_2(t)}{M_W} K^\dagger (m^d_u)^2 K \right] \ , \tag{2.26}$$

$$M^2_{DRR} = (M^d_{DRR})^2(t) \ . \tag{2.27}$$

Here $t = \ln M_P/M_W$, c_i are function of $(M_0/M_W)^2$, where M_0 indicates one of boundary masses in eqs. (2.16-2.19), that can be explicitely calculated using the RG equation for the MSSM parameters [MV94]. From eqs. (2.24-2.27) follows that (i) the RR sector is still diagonal after the RG evolution, (ii) flavour transitions in LL,LR,RL sectors are proportional to the ordinary CKM angles (iii) LR and RL transitions are also proportional to the mass of the corresponding right-handed quark. The asymmetric pattern in (i) is a consequence of the chiral structure of the MSSM. In the superpotential left down squarks, whose superpartners are left quarks embedded in a $SU(2)_L$ doublet, can couple to other fields either with the up and down Yukawa couplings as [MV94]

$$\frac{dm^2_Q}{dt} \propto c_U Y^\dagger_U Y_U + c_D Y^\dagger_D Y_D \ . \tag{2.28}$$

The first term on the right side of eq. 2.28 generates the second term in eq. (2.24), once the Yukawa matrices are diagonalized via eq. (2.11). The same term is instead not present for the right down squark.

The initial conditions have the explicit expressions

$$(M^d_{DLL})^2(0) = m_0^2 \ \hat{1} + (m^d_d)^2 + \Delta_{\tilde{d}_L} \ \hat{1} \ , \tag{2.29}$$

$$M^d_{DLR}(0) = A_0^* - \mu \tan\beta \ , \tag{2.30}$$

$$M^d_{DRL}(0) = A_0 - \mu^* \tan\beta \ , \tag{2.31}$$

$$(M^d_{DRR})^2(0) = m_0^2 \ \hat{1} + (m^d_d)^2 + \Delta_{\tilde{d}_R} \hat{1} \ . \tag{2.32}$$

Now we want to study the impact of such a very clean picture when applied to the EDM of the Neutron, The latter involves only up and down type quarks of the first generation as external states and moreover the dipole interaction violates chirality and consequently must be proportional to some quark mass. We consider for example the down quark.

Two possible scenarios are in order now for the LR and RL typical of the EDM transition to be generated.

The first option is to restrict the down-type squark mass matrix in eq. (2.23) to a 2×2 matrix in the basis $(\tilde{d}_L, \tilde{d}_R)$. In this case the LR and RL transition will be proportional to the light quark mass m_d, and we expect a natural suppression to the EDM of the Neutron. The off-diagonal entries of the squark mass matrix also contain the sensitivity to the new

supersymmetric CP violation phases, as is manifest looking at eqs. (2.29-2.32). This is the possibility we have considered in our subsequent calculations (see eq. (4.35)).

Alternatively, the first non-null contribution to the EDM interaction from flavour transitions, not proportional to m_d, is a third order effect given by the following chain:

$$\tilde{d}_L \to \tilde{b}_R \to \tilde{b}_L \to \tilde{d}_R \tag{2.33}$$

and is dimensionally suppressed with respect to the leading term by a factor m_b^2/M_{SUSY}^2. In the case of the u quark, the corresponding factor m_t^2/M_{SUSY}^2 can be of order one, but is not sufficient to compensate the suppression associated with the CKM elements in eq. (2.24-2.27). This observation justify our restriction of the squark mass matrix discussed above.

In our analysis of the EDM of the Neutron there are other sources of CP violation which arise after spontaneous symmetry breaking of $SU(2)_L \times U(1)_Y$, when higgsinos and electroweak gauginos with the same electric charge can mix. In particular, the four neutral fermions $(\lambda_B, \lambda_W^3, \tilde{h}_d^0, \tilde{h}_u^0)$ give rise to the mass matrix

$$M_{\tilde{\chi}^0} = \begin{pmatrix} M_1 & 0 & -\cos\beta \sin\theta_W M_Z & \sin\beta \sin\theta_W M_Z \\ 0 & M_2 & \cos\beta \cos\theta_W M_Z & -\sin\beta \cos\theta_W M_Z \\ -\cos\beta \sin\theta_W M_Z & \cos\beta \cos\theta_W M_Z & 0 & -\mu \\ \sin\beta \sin\theta_W M_Z & -\sin\beta \cos\theta_W M_Z & -\mu & 0 \end{pmatrix} , \tag{2.34}$$

while the charged ones $(\lambda_W^+, \tilde{h}_u^+)$ and $(\lambda_W^-, \tilde{h}_d^-)$ give rise to

$$M_{\tilde{\chi}^\pm} = \begin{pmatrix} M_2 & \sqrt{2}\sin\beta M_W \\ \sqrt{2}\cos\beta M_W & \mu \end{pmatrix} . \tag{2.35}$$

CP violation naturally enters in (2.34-2.35) through the μ parameter. The diagonalization of those matrices with

$$Z^* M_{\tilde{\chi}^0} Z^\dagger = M_{\tilde{\chi}^0}^d \quad , \quad U^* M_{\tilde{\chi}^\pm} V^\dagger = M_{\tilde{\chi}^\pm}^d \tag{2.36}$$

where Z, U and V are unitary matrix give rise to mass eigenstates for Majorana and Dirac particles, respectively called Neutralinos (N^0) and Charginos ($C^\pm$) The vertices neutralino/chargino-quark-squark enter the EDM interaction through loop-induced diagrams.

Another possible scenario to explain the suppression of FCNC is given by the already mentioned MFV hypothesis. According to it, the maximal flavour symmetry group of the SM, $SU(3)_q^3 \times SU(3)_l^2 \times U(1)^5$, is broken by the supersymmetric partners exactly in the same way as it is broken in the SM by the Yukawa couplings. The allowed terms for the positive mass dimension parameters in eq. (2.7) can be computed in a model-independent

fashion with the spurion technique [DGIS02], and turns out to be

$$m_Q^2 = m_0^2 \left(a_1 \hat{1} + b_1 Y_U Y_U^\dagger + b_2 Y_D Y_D^\dagger + b_3 Y_D Y_D^\dagger Y_U Y_U^\dagger + b_4 Y_U Y_U^\dagger Y_D Y_D^\dagger \right) \ , \quad (2.37)$$

$$m_U^2 = m_0^2 \left(a_2 \hat{1} + b_5 Y_U Y_U^\dagger \right) \ , \quad (2.38)$$

$$m_D^2 = m_0^2 \left(a_3 \hat{1} + b_6 Y_D Y_D^\dagger \right) \ , \quad (2.39)$$

$$Y_U A_U = A_0 \left(a_4 \hat{1} + b_7 Y_D Y_D^\dagger \right) Y_U \ , \quad (2.40)$$

$$Y_D A_D = A_0 \left(a_5 \hat{1} + b_8 Y_U Y_U^\dagger \right) Y_D \ , \quad (2.41)$$

where the terms quadratic in the down quark Yukawa coupling Y_D are negligible for small $\tan\beta$. The b_i coefficients introduce the deviations from the universality conditions for the soft terms introduced in eqs. (2.16-2.19). As a reference example, if we substitute eq. (2.37) in the Left-Left entry of the up squark mass matrix in eq. (2.14) and we use the definition of the CKM matrix K we arrive at

$$V_{Q_1} m_Q^2 V_{Q_1}^\dagger = m_0^2 \left[a_1 + b_1 (Y_U^d)^2 + b_2 K (Y_D^d)^2 K^\dagger + O(Y_D^2 Y_U^2) \right] \ . \quad (2.42)$$

Eq. (2.42) tell us that the flavour-violating effects in squark matrices are proportional to the entries of K. However, these effects are unphysical, since they can be rotated away with another simultaneous rotation of quark and squark under which the charged current interactions, mediated by the same matrix K, are invariant. As a consequence, in MFV the neutral currents remains flavour diagonal at tree level, as in the SM. The supersymmetric contributions to flavour transitions occur only in the charged current sector and are mediated by the known CKM angles. In particular, the MFV hypothesis implies the absence of tree-level flavor-changing gluino (FCG) interactions. This has deep phenomenological implications, because the strong coupling is much larger than the others at the energy around the TeV scale, where the new supersymmetric degrees of freedom, as the squarks and gluinos, can manifest. Consequently, the MFV hypothesis seems to be favored by the present absence of deviations from the SM of the FCNC processes. However, the pattern in eqs. (2.37-2.41) requires all the dynamics up to the cutoff (M_P in the gravity mediated case) to respect the MFV hypothesis. In addition, because the weak interactions affect the squark and quark mass matrices in a different way, their simultaneous diagonalization is not preserved by higher order corrections and can consistently imposed only at a certain scale μ_{MFV}, complicating the study of higher order contributions in this framework [CDGG98].

We now turn to the most pessimistic scenario for flavour (and CP) phenomenology. We take the most general situation, where there is no alignment of quark and squark mass matrices in the Super-CKM basis. We can diagonalize $\mathcal{M}_U$ and $\mathcal{M}_D$ with appropriate unitary transformations of the up- and down-type squarks

$$\begin{aligned} \tilde{u}_L^I = (Z_U^\dagger)^{Ik} U_k \ \ , \ \ \tilde{u}_R^I = (Z_U^\dagger)^{(I+3)k} U_k \ \ , \\ \tilde{d}_L^I = (Z_D^\dagger)^{Ik} D_k \ \ , \ \ \tilde{d}_R^I = (Z_D^\dagger)^{(I+3)k} D_k \ \ , \end{aligned} \quad (2.43)$$

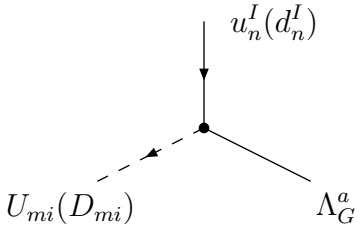

$$= -i\sqrt{2}g_s T^a_{mn}\left[(Z_{U(D)})^{iI}P_L - (Z_{U(D)})^{i(I+3)}P_R\right] \tag{2.46}$$

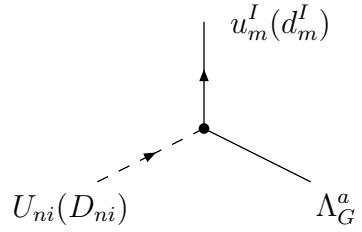

$$= -i\sqrt{2}g_s T^a_{mn}\left[(Z^\dagger_{U(D)})^{Ii}P_R - (Z^\dagger_{U(D)})^{(I+3)i}P_L\right] \tag{2.47}$$

Figure 2.1: Feynman rules for FCG tree level interactions.

where the index $k = 1, ..., 6$ and, recalling that $I = 1, ..., 3$ runs over the generations, the unitary conditions read as

$$(Z_{U,D})^{mI}(Z^\dagger_{U,D})^{In} + (Z_{U,D})^{m(I+3)}(Z^\dagger_{U,D})^{(I+3)n} = \delta^{mn}. \tag{2.44}$$

The mass matrix in the U basis is given by

$$Z_U \begin{pmatrix} (M_U^2)_{LL} & (M_U^2)_{LR} \\ (M_U^2)_{RL} & (M_U^2)_{RR} \end{pmatrix} Z_U^\dagger = \begin{pmatrix} \mathcal{M}^2_{U_1} & & 0 \\ & \ddots & \\ 0 & & \mathcal{M}^2_{U_6} \end{pmatrix} . \tag{2.45}$$

We have applied the consequences of this realization of the squark mass matrices in the case of the radiative B decays. Among the new supersymmetric interactions contributing to this process, the main role can naively be associated to the FCG. In fact, differently of the MFV picture, now the vertex quark-squark-gluino is directly present at tree level as shown in fig. 2.1 where we have introduced the Majorana spinor $\Lambda_G \equiv (-i\lambda_G\ ,\ +i\overline{\lambda}_G)^T$. In eqs. (2.46-2.47) the left- and right-handed projectors are defined as $P_{R,L} = (1 \pm \gamma_5)/2$ while index a run over generators T of the SU(3) group, whereas indices m, n run over its fundamental representation. Finally, indices I and i run over the generations of quarks and the squark bases U, D, respectively.

Using these vertices one can in principle perform a full computation of the FCG effects in the branching ratio of $B \to X_s\gamma$ [BGHW00]..

Such computation means keeping the Z_D, Z_U matrices in the final expressions, that will depend as well on all the squark masses $\mathcal{M}_{U_i}, \mathcal{M}_{D_i}$ in the mass eigenstates' basis. Comparing with the experimental data, one could provide exact constraints on all the entries of the Z matrices. Performing all the computations with full Z_D, Z_U matrices implies invoking a certain degree of fine tuning: off-diagonal entries in the Z's could be of $O(1)$ with respect to the diagonal ones but cancellations should occur so that the final FCNC effects arising be small. As a consequence, one could in general raise doubts on the

reliability of the resulting estimate of the Z entries, unless the abovementioned numerical problems are really kept under control.

One could even question whether the "exact" approach outlined above is really worthwhile after all, considering that the big number of free parameters ends up to spoil the real utility of formulae from a phenomenological point of view. A more practical strategy is to find a suitable approximation that could allow to account for the bulk of the effects while considerably simplifying the exact formulae.

Let us start rewriting eq. (2.45) as

$$\left(\mathcal{M}_U^2\right)_{ij} = (Z_U^\dagger)_{ik}\mathcal{M}^2_{U_k}\,(Z_U)_{kj}\ , \tag{2.48}$$

where values $1, ..., 3$ for the indices i, j stand for the corresponding flavours and left chirality, whereas values $4, ..., 6$ span the same flavours and right chirality.

Our goal is to bound the flavour-changing entries on the left side of eq. (2.48).

To this end we rewrite eq. (2.48) in the form

$$\begin{aligned}(Z_U^\dagger)_{ik}\mathcal{M}^2_{U_k}(Z_U)_{kj} = (\mathcal{M}_U^2)_{ij} &= \underbrace{(M^2)_i\ \delta_{ij}}_{\text{diagonal}} + \underbrace{\Delta_{ij}}_{\text{off-diagonal}} \\ &\simeq \left(\overline{M}^2\hat{1} + \Delta\right)_{ij} = \overline{M}^2(\hat{1} + \underbrace{\frac{\Delta}{\overline{M}^2}}_{\text{small}})_{ij}\ .\end{aligned} \tag{2.49}$$

We see that, after splitting the $(\mathcal{M}_U^2)_{ij}$ mass matrix into diagonal and off-diagonal parts, in the second line of eq. (2.49) we have

- introduced an average squark mass $\overline{M}$
- assumed the off-diagonal entries Δ_{ij} small with respect to $\overline{M}$

The two assumptions above form what is called the Mass Insertion Approximation (MIA) [HKR86], which is a very popular one in the literature.

The practical application of the MIA consists in expanding the theoretical amplitudes to the first non-null order in the parameter δ, defined as

$$\delta_{ij} \equiv \frac{\Delta_{ij}}{\overline{M}^2}\ . \tag{2.50}$$

This approach avoids the diagonalization of the 6×6 mass matrices of quarks. Moreover, the study of the (potentially) formidable sources of supersymmetric flavour changing translate in a study of the bounds on the δ's, when confronting with the experimental measures. In particular, the analysis of FCNC processes related to $\Delta F = 2$ Hamiltonians has recently witnessed allowed to put severe constraints on the corresponding $\delta' s$, particularly in the $K - \overline{K}$ case [C$^+$98], unless the squark masses dividing them are well above $O(1)$ TeV.

Turning to the radiative B decays, we will give the complete LO numerical factors for a phenomenological analysis within the MIA. To fix more clearly the notation, we define four different mass insertions, according to the chirality of the up and down squarks

$$(\delta_{LL})_{ij} \equiv \delta_{ij} \quad i,j = 1,\dots,3 \quad , \quad (\delta_{RR})_{i-3\ j-3} \equiv \delta_{ij} \quad i,j = 4,\dots,6 \ , \tag{2.51}$$

$$(\delta_{LR})_{i\ j-3} \equiv \delta_{ij} \quad i = 1,\dots,3 \quad j = 4,\dots,6 \quad , \quad (\delta_{RL})_{i-3\ j} \equiv \delta_{ij} \quad i = 4,\dots,6 \quad j = 1,\dots 3 \ .$$

In the formulae presented in chapter 6, the indices i, j specify the flavour and consequently run over u, c, t, d, s, b.

In summary, we have briefly summarized the aspects of SUSY, in particular of the MSSM, more closely related to the calculations presenter in this Thesis. Possible scenarios for the flavour and CP properties of the new supersymmetric degrees of freedom have been briefly reviewed in sec. (2.3), and prepare the theoretical ground for our analysis of the EDM of the Neutron and the radiative B decays in chapters 4-6. Of course, there are many specific models which do not belong to any of categories presented, and also inside these groups the phenomenological predictions strongly depend on how the parameters are arranged (see for instance [COPW94] for the popular case of large tan β).

3. Theoretical framework II: OPE & RGE

This chapter introduces the general theoretical framework in which our calculations have been done. It is the Operator Product Expansion (OPE) and the Renormalization Group Equations (RGE), two basic and powerful tools for the analysis of particle processes where many different physical scales come into play. The OPE allows to separate, rather factorize, the physical effects coming from the various energy regimes, as it will be clear shortly.

3.1. Effective Hamiltonian formalism

Our aim is to estimate the transition amplitude between the hadronic states we are interested in, mediated by supersymmetry as it is realized in the MSSM. They are the Neutron in the case of our EDMs analysis and the B meson for our study of the inclusive $B \to X_s\gamma$ decays. In these processes several different energy scales take part, and in each regime a different "kind of physics" plays the main role. To begin with, the short-distance interaction between the constituent quarks of our external bound states is generated − in the framework of the MSSM − by SUSY particles with typical mass $M_{\rm SUSY} \geq 1$ TeV. The various MSSM contributions − related to the different particles running in the loop − at these energy regimes can be safely treated in perturbation theory. An intermediate scale is represented by the momenta p of the external particles, typically in the GeV range. Finally, the external states − mesons or baryons − are not fundamental particles, but states built up of quarks and gluons strongly interacting among themselves. The typical energy scale $\Lambda_{\rm QCD}$ for such interactions can naively be obtained from the inverse of a meson size, resulting in $\Lambda_{\rm QCD} \equiv$ few $\times$ 100 MeV. Around and below this scale, QCD cannot be treated perturbatively, and to estimate physical effects − responsible for "building up" an hadron out of quarks and gluons − one has to resort to strictly non perturbative methods, as Lattice QCD (LQCD) or Heavy Quark Effective Theory (HQET). So we have to cope with a problem bearing three energy scales, with $\Lambda_{\rm QCD} \ll p \ll M_{\rm SUSY}$.

The OPE [WZ72] formalizes the separation of the physical effects occurring at the different scales. For a clear and exhaustive introduction to the OPE, see ref. [Bur98]. The simplest way − and the most popular as well − to introduce the OPE idea starts by considering two quark-antiquark currents interacting via a heavy intermediate boson. Let the initial and final currents be respectively $J_A^\mu = \bar\psi_1 \Gamma_A^\mu \psi_2$ and $J_B^\mu = \bar\psi_3 \Gamma_A^\mu \psi_4$. Γ_{AB}^μ are strings of gamma matrices and together with the external flavours specify the quantum numbers of the currents. Let the two gauge currents J_A, J_B interact with strength g

with a heavy vector boson B^μ, whose mass M_B is much higher than the four-momentum p carried by the external states coming out of $J_A,\ J_B$ themselves. For the amplitude in momentum space on can write

$$\mathcal{A}_{\text{full}} \propto g^2 J_A^\mu \frac{(-ig_{\mu\nu})}{p^2 - M_B^2} J_B^\nu \overset{p^2 \ll M_B^2}{=} +ig^2 \left(\frac{1}{M_B^2} J_A^\mu J_{\mu B} + O(p^2/M_B^2) \right) \tag{3.1}$$

where we have indicated by $O(p^2/M_B^2)$ generic contributions suppressed by integers of the small ratio p^2/M_B^2. The under-script "full" means that the amplitude is computed in a theory where all the degrees of freedom are present. The leading term on the right side is the product of two currents, with no dependence on the momentum carried by the vector boson. So in the x-space the two currents are on the same point and give rise to the four fermions local operator $J_A^\mu J_{\mu B}(x)$, that is of dimension 6. The other terms, proportional to $(p^2/M_B^2)^n$, are generated by higher dimensional operators and typically contains derivatives, in order to generate the factor p^{2n}. What happened in passing from the left to the right side of eq. (3.1) is that the propagation of the heavy boson B^μ as an explicit degree of freedom has been traded for an infinite series of local operators approximating the better such propagation the higher is the maximum dimensionality included.

Abstracting the discussion, we can say that our amplitude $\mathcal{A}_{\text{full}}$, which is an S-matrix element between some external states $|\text{in}\rangle$ and $|\text{out}\rangle$, can be reproduced by an effective Hamiltonian $\mathcal{H}_{\text{eff}}$, between the same external states, made up of a series of couplings C_i times increasing dimension operators $\mathcal{O}_i$

$$\mathcal{A}_{\text{full}} = \langle \text{out}|S|\text{in}\rangle = \sum_i C_i(\mu, M_B) \langle \text{out}|\mathcal{O}_i(\mu)|\text{in}\rangle \equiv \langle \text{out}|\mathcal{H}_{\text{eff}}|\text{in}\rangle \ , \tag{3.2}$$

where the $C_i(\mu, M_B)$, known as Wilson coefficients, depend on the masses M_B of the heavy degrees of freedom and $\langle \mathcal{O}_i(\mu) \rangle$ are matrix elements of local operators.

By construction such expansion makes sense when the energies of external states p satisfy the relation $p \ll M_B$. Then, the "order" of the expansion is given by the maximum dimension of the operators included, and at any given order the $\mathcal{O}_i$ must be all those allowed by the symmetries of the problem [BBL96]. It is possible to discard redundant operators as well as operators vanishing by the Equation Of Motion (EOM): in this process of selection, one chooses a set of independent operators usually referred to as a basis. Normally the higher order operators in p^2/M_B^2 turns out to be numerically negligible and are neglected.

The quantity μ, beyond playing the technical role of a renormalization scale, assumes in this context also the meaning of a factorization scale. What is factorized is the dependence on the various physical effects arising at the different energy scales [Bur98]. In particular, the coefficients $C_i(\mu, M_B)$, as coupling constants, will depend only on the high-energy part of the full theory, namely on energies $> \mu$. On the other hand, the low-energy dynamics, by definition that at energies $< \mu$, is encoded in the operator matrix elements $\langle \mathcal{O}_i(\mu) \rangle$. The latter represent local operators evaluated between the external physical states of interest. It follows that, in order to properly evaluate such matrix elements, one must take into

account also the non-perturbative regime of QCD described above. One way to cope with the latter is that of using QCD on the lattice, which, among the various methods on the market, is the only one relying exclusively on first principle. Alternatively, the matrix elements can be estimated for example with $1/N_c$-expansion, QCD- and hadronic sum rules or chiral perturbation theory.

From eq. (3.2) it is evident that, while couplings and matrix elements of the effective operators separately depend on the scale μ, $\mathcal{A}_{\text{full}}$ remains μ-independent as it is the case for physical observables.

Now let us look more closely at formula (3.2). According to it, in order to reproduce our amplitude we can use an effective theory, made up of a tower of couplings times operators with increasing dimension. We could ask what happens when one includes radiative corrections. Such a theory is not renormalizable, since, to start with, it contains an infinite number of couplings with negative mass dimension. Nonetheless it is renormalizable at any given order k in the dimension of the operators [Wei79]: after fixing the values assumed at a certain scale μ by all the couplings appearing in $\mathcal{H}_{\text{eff}}$ to order k, the effective Hamiltonian becomes predictive. Renormalization of $\mathcal{H}_{\text{eff}}$ cannot be performed by means of suitable redefinitions of the wave functions and couplings of the "full" theory. In fact in this case such a renormalization procedure is not sufficient to absorb all the divergences of an effective amplitude, since local composite operators bring in additional divergences. The latter can be taken care of by redefining the operator basis by means of a renormalization constant matrix Z, according to

$$\mathcal{O}_i^{(0)} = Z_{ij}\mathcal{O}_j \ , \tag{3.3}$$

where we have specified the unrenormalized operators with a superscript $^{(0)}$.

From the above discussion, it is evident that the $C_i(\mu, M_B)$ are the unknowns objects in $\mathcal{H}_{\text{eff}}$. Since by construction our effective Hamiltonian reproduces the full amplitude $\mathcal{A}_{\text{full}}$ at some low energy scale below M_B (recall eq. (3.1)), one should exploit equality (3.2) to find the $C_i(\mu, M_B)$. A fundamental observation helps out: the $C_i(\mu, M_B)$ depend only on energy scales above μ and are always the same independently of the low-energy dynamics, in particular independently from the choice of the external states. This means that, for the purpose of evaluating the couplings $C_i(\mu, M_B)$, instead of taking as external states the physical degrees of freedom we are interested in, we can choose states of quarks and massless bosons such as gluons and photons, possibly with unphysical kinematic conditions. So the equality to exploit in order to determine the $C_i(\mu, M_B)$ is the following

$$\mathcal{A}'_{\text{full}} = \langle b|S|a\rangle = \sum_i C_i(\mu, M_B)\langle b|\mathcal{O}_i|a\rangle(\mu) \equiv \mathcal{A}'_{\text{eff}} \ , \tag{3.4}$$

where we have substituted our states of interest $|\text{in(out)}\rangle$ with "suitable" states $|a(b)\rangle$ and the primes indicate amplitudes calculated with such external states. This way both $\mathcal{A}'_{\text{full}}$ and the matrix elements $\langle b|\mathcal{O}_i|a\rangle(\mu)$ are analytically computable using QCD, and relation (3.4) translates into a number of algebraic equalities, as many as are the operators $\mathcal{O}_i$. A relation like (3.4) is usually called a matching condition of the full theory onto the effective one, and allows to determine the couplings $C_i(\mu, M_B)$.

Even if the matching condition can be enforced at any μ, in practice the scale at which the $C_i(\mu, M_B)$ are determined by the above condition (3.4) must be $\mu \sim M_B$. This is due to the following reason. In the above discussion we have stressed that coefficient functions depend only on the high energy part of the whole problem. Thus they will have a functional dependence on the mass M_B, but not on the external particles' momentum p. Moreover a dependence on the quantity $\ln \mu^2$ will inevitably come out when computing divergent loop corrections. So, supposing that coefficient functions are finite to LO, their structure to NLO must be the following

$$C_i(\mu, M_B) = A_i^{(0)} + \frac{\alpha_s}{4\pi}\left(A_i^{(1)} + B_i^{(1)} \ln \frac{M_B}{\mu}\right) \ , \tag{3.5}$$

where A_i, B_i are Ultra-Violet (UV) finite quantities, possibly depending on the mass M_B, and the NLO corrections was indicated by an explicit overall α_s factor. The above equation is the result of a naive dimensional argument. From eq. (3.5) one sees that even if $\alpha_s(\mu) \ll 1$, the logarithm can be very large whenever scales M_B and μ are vastly different. This is in turn the case for our physical observables, since we can identify $M_B \sim M_{\rm SUSY}$ and $\mu \sim \Lambda_{\rm QCD}$ where matrix elements are computed. The result is that the product $\alpha_s \times \ln M_{\rm SUSY}/\mu$ turns out to be of $O(1)$, and the perturbative expansion in α_s does not make sense any longer.

To avoid this problem one is forced to choose the scale μ, at which the Wilson coefficients are calculated via the matching procedure, not too far from the high energy scale $M_{\rm SUSY}$. In other words, $\mu_{\rm matching} \equiv \mu_{\rm S} \sim M_{\rm SUSY}$. On the other hand, we need at the end the $C_i(\mu, M_{\rm SUSY})$ evaluated at the low energy scale μ_H in order to match it with the operator matrix elements and to consistently reconstruct the physical amplitude. The evolution of the $C_i(\mu)$ from $\mu_{\rm S}$ to μ_H is realized by means of the Renormalization Group Equations (RGE) [Sym70]. The latter are first order differential equations in $\ln \mu$, to be solved with initial conditions the $C_i(\mu_{\rm S})$. The power of these equations lies in the fact that they permit a resummation of the large logarithms introduced above to all orders in perturbation theory. More specifically, the Leading Order (LO) solution provides a resummation of all the leading logarithmic terms

$$\sim \alpha_s^n \left(\ln(\mu_{\rm S}/\mu_H)\right)^n \ , \tag{3.6}$$

while the Next-to-Leading Order (NLO) corresponds to the resummation of the terms

$$\sim \alpha_s^{n+1} \left(\alpha_s \ln(\mu_{\rm S}/\mu_H)\right)^n \ . \tag{3.7}$$

Since we are interested in the analysis of the EDM of the Neutron at the NLO precision, in the next section we will specialize to the matching conditions as they must be imposed in our case of interest. Then in sec. 3.2 we will briefly discuss the RGE equation up to NLO precision and focalize on their numerical implementation.

3.1.1. Master Formula for the matching conditions

In this section we give a complete picture of all the ingredients entering the calculation of the Wilson coefficients, both in the full as well as in the effective theory. Since in this

Thesis we present the NLO calculation only for the (chromo)magnetic operators (see sec. 4.2 and eq. (4.13) for the definition of these operators), in the following we will write formulae specialized for matrix elements of operators with two external fermions and one external gluon.

Let us look back at eq. (3.4). On the left handed side we have $\mathcal{A}_{\rm full}$, the full amputated amplitude among the relevant external states. Such amplitude, before renormalization, has UV and as well as InfraRed (IR) divergences. To regularize the ultraviolet ones we have used Naive Dimensional Regularization (NDR) and define operators in the $\overline{\rm MS}$ scheme, while light quark masses will play the role of IR regulator, as it will be described in chapter 5. The result of the full theory calculation after renormalization can be written in the following form

$$\mathcal{A}'_{\rm full} = Z^{(f)}_{\psi,\rm full}(Z^{(f)}_{3,\rm full})^{1/2}\left(F^{(0)} + \frac{\alpha_s}{4\pi}F^{(1)}\right)_i \langle\mathcal{O}_i\rangle^{(0)} \ , \tag{3.8}$$

in terms of the tree level matrix elements $\langle\mathcal{O}_i\rangle^{(0)}$ of an operator set $\mathcal{O}_i$ between the external states. In eq. (3.8) $F^{(0)}$ represents the LO contributions, whereas $F^{(1)}$ contains the NLO corrections and an explicit factor of α_s has been factored out for the latter. Now, $F^{(0)}$ is finite by itself and so regularization independent. On the other hand $F^{(1)}$ depends on the regularization chosen to cope with the UV singularities, in this case NDR-$\overline{\rm MS}$, and moreover it contain logarithms and inverse powers of light masses as IR regulators. The diagrams generating the functions $F^{(0)}$ and $F^{(1)}$ are depicted in figs. 4.1 and 5.1-5.6, respectively.

On the right side of eq. (3.8) there are two $Z's$ factors for which an explanation is in order. They are defined as the pole residue of the two point-correlator functions for the quark and gluon field and allow to define the corresponding renormalized propagator of a massless quark and gluon in the full theory as

$$S(p)_{\rm full} = Z^{(f)}_{\psi,\rm full}\frac{i}{\not p} \ , \quad G(p)_{\rm full} = Z^{(f)}_{3,\rm full}\frac{-ig^{\mu\nu}}{p^2} \ . \tag{3.9}$$

The presence of these factors is a consequence of the LSZ reduction formula [LSZ55]. The latter provides the relation between the Green functions we have calculated in the language of Feynman diagrams and the S-matrix elements which is the physical amplitude we are interested in. In our case, since we have evaluated amputated Green functions, the prescription of the LSZ formula is to multiply the final result for a factor

$$(Z^{(f)}_{\psi})^{n_f/2}(Z^{(f)}_{3})^{n_g/2} \ , \tag{3.10}$$

where n_f and n_g represent the number of external quark and gluonic legs. Such operation is necessary in the present calculation because external fields have a different normalization in the effective theory with respect to the full one. In particular, one loop corrections to the quark and gluon propagator include a squark-gluino loop as well as a quark-gluon loop, whereas only the latter appears in the effective theory. In other words, defining in analogy with (3.9) the residue $Z^{(f)}_{\psi,\rm eff}$ and $Z^{(f)}_{3,\rm eff}$ as

$$S(p)_{\rm eff} = Z^{(f)}_{\psi,\rm eff}\frac{i}{\not p} \ , \quad G(p)_{\rm eff} = Z^{(f)}_{3,\rm eff}\frac{-ig^{\mu\nu}}{p^2} \ , \tag{3.11}$$

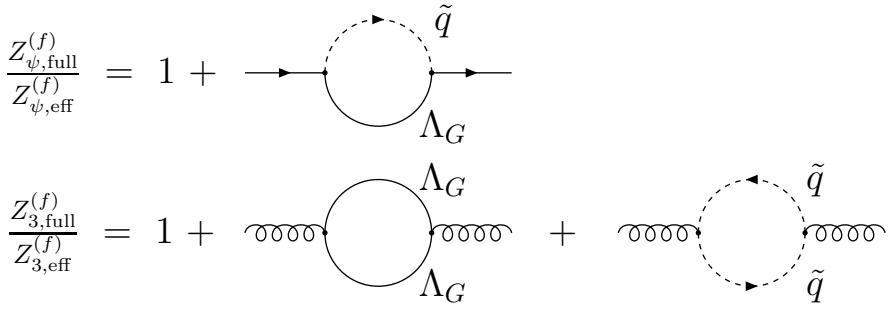

Figure 3.1: Feynman diagrams for the calculation of the ratio of the renormalization constant for the external fields. See text.

we have $Z^{(f)}_{\psi,\text{full}} \neq Z^{(f)}_{\psi,\text{eff}}$ and $Z^{(f)}_{3,\text{full}} \neq Z^{(f)}_{3,\text{eff}}$. The mismatch ΔZ between the renormalization constants in the full and effective theories is not cancelled in the matching and remains in the Wilson coefficients, as we will derive in a moment.

Now let us go to the right handed side of eq. (3.4), containing the amplitude in the effective theory:

$$\mathcal{A}'_{\text{eff}} = \sum_i C_i \langle \mathcal{O}_i \rangle \ . \tag{3.12}$$

Note again that all quantities in (3.12) are renormalized ones. In particular the $\langle \mathcal{O}_i \rangle$ are renormalized matrix elements of the operators $\mathcal{O}_i$ between the same external states adopted in the full theory. What is relevant to our present discussion is that such matrix elements can be written as follows

$$\langle \mathcal{O}_i \rangle = Z^{(f)}_{\psi,\text{eff}} (Z^{(f)}_{3,\text{eff}})^{1/2} r_{ij} \langle \mathcal{O}_j \rangle^{(0)} \ , \tag{3.13}$$

in terms of the tree level matrix elements of the same operator basis used in the evaluation of the full theory amplitude in eq. (3.8). r_{ij} is a matrix of UV-renormalized 1-loop corrections to the (chromo)magnetic vertices, explicitely given by the diagrams depicted in fig. 5.7. Note that such corrections will be dependent from the IR regulators in our chosen setup, in exact analogy with the full theory case. These dependences, being IR effects, must cancel out between the full and the effective theories in the matching procedure. This is consequence of the already mentioned fact that the OPE factorizes the UV and IR regions of the full amplitude in the Wilson coefficients and the hadronic matrix elements respectively. In particular, the C_i carry no dependences at all on IR effects like the choice of the kinematic conditions for the external states.

Now one can put together eqs. (3.8) and (3.12), taking into account eq. (3.13). Solving for the Wilson coefficients, that are our unknowns, one finally gets

$$C_j = \frac{Z^{(f)}_{\psi,\text{full}} \ (Z^{(f)}_{3,\text{full}})^{1/2}}{Z^{(f)}_{\psi,\text{eff}} \ (Z^{(f)}_{3,\text{full}})^{1/2}} \left(F^{(0)} + \frac{\alpha_s}{4\pi} F^{(1)} \right)_i \ (r^{-1})_{ij} \ , \tag{3.14}$$

representing the reference formula for the matching condition of the dipole operators. An important remark is in order here.

We observe that the two ratios $Z^{(f)}_{\psi,\text{full}}/Z^{(f)}_{\psi,\text{eff}}$ and $Z^{(f)}_{3,\text{full}}/Z^{(f)}_{3,\text{eff}}$ collects perturbatively the contributions to the residue of the quark and gluon propagators poles in the full theory that do not have a counterpart in the effective one. At the one loop level such ratio is just the finite part of the squark and/or gluino correction to the quark and gluon propagator, as depicted in fig. 3.1.

To summarize, eq. (3.14) is our master formula for the matching. It will be used in chapters 4-6 to obtain the Wilson coefficients at $\mu_S \sim M_{\text{SUSY}}$ as stressed above. In the next section we will finally address the issue of how to use the RGE to move the Wilson coefficients from μ_S to a different scale μ.

3.2. RGE for the Wilson coefficients

The RGE for the Wilson coefficients can be simply derived imposing the independence of $\mathcal{H}_{\text{eff}}$ from the factorization scale μ. Introducing row vectors for the Wilson coefficients and the corresponding operators, we can write the effective Hamiltonian as

$$\mathcal{H}_{\text{eff}} = \vec{\mathcal{O}}^T(\mu)\vec{C}(\mu) \ . \tag{3.15}$$

Using eq. (3.3) and the fact that bare operators $\mathcal{O}^{(0)}_i$ are μ-independent, the RGE follows from

$$\mu\frac{d}{d\mu}\mathcal{H}_{\text{eff}} = \mu\frac{d}{d\mu}\left[\vec{\mathcal{O}}^{(0)T}(Z^{-1})^T\vec{C}\right] = 0 \quad \Rightarrow \quad \mu\frac{d}{d\mu}\vec{C} = \gamma^T\vec{C} \tag{3.16}$$

where we have defined the so-called anomalous dimension matrix (ADM) for the operator basis $\mathcal{O}_i$ as

$$\gamma = Z^{-1}\mu\frac{d}{d\mu}Z \ . \tag{3.17}$$

The ADM γ admits an expansion in α_s as

$$\gamma = \frac{\alpha_s}{4\pi}\gamma^{(0)} + \left(\frac{\alpha_s}{4\pi}\right)^2\gamma^{(1)} + ... \ , \tag{3.18}$$

whose coefficients are linked to the renormalization constant matrix Z, as derived in eq. (3.17). The extraction of the LO and NLO terms $\gamma^{(0)}$ and $\gamma^{(1)}$ starts from an expansion in power of α_s and $1/\epsilon$ as follows

$$Z = 1 + \frac{\alpha_s}{4\pi}Z^{(1)} + \left(\frac{\alpha_s}{4\pi}\right)^2 Z^{(2)} + ... \quad , \quad Z^{(i)} = \sum_{j=0}^{i}\left(\frac{1}{\epsilon}\right)^j Z^{(i)}_j \ . \tag{3.19}$$

Substituting eqs. (3.18-3.19) into (3.17) we obtain the master formulae

$$\gamma^{(0)} = -2Z^{(1)}_1 \ , \tag{3.20}$$

$$\gamma^{(1)} = -4Z^{(2)}_1 - 2\beta_0 Z^{(1)}_0 + 2\left(Z^{(1)}_1 Z^{(1)}_0 + Z^{(1)}_0 Z^{(1)}_1\right) \ , \tag{3.21}$$

$$Z^{(2)}_2 = \frac{1}{2}Z^{(1)}_1 Z^{(1)}_1 - \frac{1}{2}\beta_0 Z^{(1)}_1 \ . \tag{3.22}$$

The first two equations tell us that it is sufficient to compute the pole and finite part of $Z^{(1)}$ and the single pole of $Z^{(2)}$ in order to obtain the ADM to NLO. The second term in eq. (3.21) automatically add the renormalization of the strong coupling constant.

The third one is a condition which must be satisfied in order to have a finite ADM as $\epsilon \to 0$. From this condition one obtains a relation between the one- and two- loop coefficients of Z which constitute a useful check of the calculation of the ADM.

We now want briefly discuss the method commonly used to solve the RGE up to NLO [Bur98]. In order to find a LO solution to eq. (3.16), one first defines a matrix V diagonalizing γ^T to first order

$$\gamma^{(0)d} = V^{-1}\gamma^{(0)T}V \ , \tag{3.23}$$

then reexpresses eq. (3.16) in terms of the diagonal basis $\overline{C} = V^{-1}C$ as

$$\mu\frac{d}{d\mu}\overline{C} = \gamma^{(0)d}\overline{C} \ . \tag{3.24}$$

Eq. (3.24) has the simple solution

$$\frac{\overline{C}_i(\mu)}{\overline{C}_i(\mu_0)} = \left(\frac{\alpha_s(\mu_0)}{\alpha_s(\mu)}\right)^{\frac{(\gamma^{(0)d})_i}{2\beta_0}} \ , \tag{3.25}$$

where β_0 is the first term of the β-function for the g_s coupling. Finally, rotating back to the original C_i, we find

$$C_i(\mu) = \left[V \ \left(\frac{\alpha_s(\mu_0}{\alpha_s(\mu)}\right)^{\frac{(\gamma^{(0)d})_i}{2\beta_0}} V^{-1}\right]_{ij} C_j(\mu_0) \ . \tag{3.26}$$

The matrix in square brackets on the right side of eq. (3.26) represents the LO terms of the so-called evolution matrix $U(\mu, \mu_0)$ for the $C_i(\mu)$, and generally defined as

$$\begin{aligned} C_i(\mu) &= U(\mu, \mu_0)_{ij}C_i(\mu_0) \ , \\ U^{(0)}(\mu, \mu_0) &= V \ \left(\frac{\alpha_s(\mu_0)}{\alpha_s(\mu)}\right)^{\frac{(\gamma^{(0)d})_i}{2\beta_0}} V^{-1} \ . \end{aligned} \tag{3.27}$$

Turning back to our case of interest, we can identify the initial condition $C_i(\mu_0)$ as the one calculated at the SUSY scale μ_S. Since we have calculated the Wilson coefficients up to the NLO, we need an expression for $U(\mu, \mu_S)$ including the NLO as well. To that end it is customary to start directly with the differential equation obeyed by $U(\mu, \mu_0)$, which is

$$\mu\frac{d}{d\mu}U(\mu, \mu_S) = \gamma^T(\alpha_s)U(\mu, \mu_S) \ . \tag{3.28}$$

The general solution can be written down iteratively in the form of a Dyson series as follows

$$U(\mu, \mu_S) = 1 + \int_{\alpha_s(\mu_S)}^{\alpha_s(\mu)} \frac{\gamma^T(\alpha_s')}{\beta(\alpha_s')}d\alpha_s' + \int_{\alpha_s(\mu_S)}^{\alpha_s(\mu)}\int_{\alpha_s(\mu_S)}^{\alpha_s'} \frac{\gamma^T(\alpha_s')\gamma^T(\alpha_s'')}{\beta(\alpha_s')\beta(\alpha_s'')}d\alpha_s'd\alpha_s'' + ... \tag{3.29}$$

One should notice that matrices γ^T at different values of the coupling constant do not commute, because for example $[\gamma^{(0)}, \gamma^{(1)}] \neq 0$. As a consequence, integrands on the right handed side of (3.29) must be written from right to left in order of increasing argument, provided that $\mu_S > \mu$, as we are supposing.

Now, a NLO formula for the evolution matrix, indicated as $U^{(1)}$, can be found following the procedure described in appendix A of ref. [BJLW92]. The result is

$$U^{(1)}(\mu, \mu_S) = \left(\hat{1} + \frac{\alpha_s(\mu)}{4\pi} J\right) U^{(0)}(\mu, \mu_S) \left(\hat{1} - \frac{\alpha_s(\mu_S)}{4\pi} J\right) , \tag{3.30}$$

where again, an ordering of the coupling constants in increasing values from right to left was maintained. The matrix J is defined by the formula

$$J = V S V^{-1} , \tag{3.31}$$

where V is the matrix diagonalizing the ADM to LO, see eq. (3.23), and S is defined by [BJLW92]

$$S_{ij} = \delta_{ij} (\gamma^{d(0)})_i \frac{\beta_1}{2\beta_0^2} - \frac{(V^{-1}\gamma^{(1)}V)_{ij}}{2\beta_0 + (\gamma^{d(0)})_i - (\gamma^{d(0)})_j} . \tag{3.32}$$

In the previous equation one should notice the presence of the matrix $\gamma^{(1)}$, representing the NLO in the expression of the ADM (see eq. (3.18)), as obvious since we want a NLO solution for the evolution matrix. It is evident that, while V diagonalizes $\gamma^{(0)}$ by definition, in general it does not simultaneously diagonalize $\gamma^{(1)}$ as well.

3.2.1. "Magic Numbers"

In the previous section we have derived the general formulae for the evolution of the Wilson coefficients from the matching scale μ_S to a general low scale μ. In the phenomenogical analysis of the EDM of the Neutron and of the radiative B decays under investigation in this work, the RGE techniques described above must be used to translate the Wilson coefficients at the low scale μ_H, where the hadronic matrix elements are evaluated.

To this end, we have used the common choice of expressing the general formula for the solution of the RGE, eq. (3.30), in terms of the following analytic formulae

$$C_i^{(0)}(\mu_H) = \sum_{j=1} \sum_{a=1} \sum_{b=1} \alpha_s(\mu_S)^{Y_a} \eta^{Z_b} X_{ij}^{ab} C_j^{(0)}(\mu_S) , \tag{3.33}$$

$$C_i^{(1)}(\mu_H) = \sum_{j=1} \sum_{a=1} \sum_{b=1} \alpha_s(\mu_S)^{Y_a} \eta^{Z_b} \left(X_{ij}^{ab} C_j^{(1)}(\mu_S) + N_{ij}^{ab} C_j^{(0)}(\mu_S) \right) , \tag{3.34}$$

where $\eta = \alpha_s(\mu_S)/\alpha_s(\mu_H)$. In eqs. (3.33-3.34), the index i, j run over the operator basis of the effective Hamiltonian while a, b run over the eigenvalues of the $\gamma^{(0)T}$ matrix, as dictated by eq. (3.23). The coefficients Y_a, Z_b, X_{ij}^{ab} and N_{ij}^{ab} in eqs. (3.33-3.34) are commonly called "magic numbers". In sec. 4.3 and 5.1 we will provide their explicit expression for the Electric Dipole Moment of the Neutron. Moreover, in sec. 6.3 we will discuss the leading order results for the magic numbers related to the radiative B decays in supersymmetric models with FCG interactions.

3.3. Concluding remarks

In this chapter we have described the theoretical tools that allow to build an effective Hamiltonian describing a physical multi-scale process in the framework of the OPE. Starting from the rewriting of the full amplitude according to eq. (3.2) the whole calculation can be summarized in a three step procedure as follows:

1. A matching calculation of the full theory with the effective one at the high energy scale $\mu = \mu_S$ for Wilson coefficients, as discussed in sec. 3.1. In our case of interest μ_S is identified as the scale of the supersymmetric partners of the SM particles, and lies around or over the electroweak one.

2. RG evolution of the $C_i(\mu_S)$ down to $\mu_H \sim$ few GeV using the ADM to order α_s (LO) or α_s^2 (NLO), as discussed in sec. 3.2. We have introduced the magic numbers as the practical numerical objects we have used in our subsequent phenomenological analysis.

3. Non-perturbative evaluation of the hadronic matrix elements $\mathcal{O}(\mu)_i$ between the external states defining the given process under investigation.

The results of this various steps for the Electric Dipole Moment of the Neutron and for the radiative B decays will be discussed in the chapter 4-6, the original part of this Thesis work.

4. Neutron EDM at Leading Order

In this chapter we specialize the OPE techniques described in the previous chapter to the Electric Dipole Moment (EDM) of the Neutron, which is a member of a class of observables actually under experimental investigation. We first shortly recall the non-relativistic definition of the EDM of a particle, and then introduce the relevant operator basis and all the ingredients for a complete LO analysis.

4.1. The Electric Dipole Moment interaction

The electric dipole moment $\vec{d}$ of an elementary particle is defined, in the non relativistic limit, from the interaction Hamiltonian

$$\mathcal{H}_{\text{int}} = -\vec{d}\cdot\vec{E}\ , \tag{4.1}$$

where $\vec{E}$ is an external electric field. Moreover, since the only vector which characterize a particle is its spin $\vec{J}$, in analogy with the magnetic moment we can write

$$\vec{d} = d\frac{\vec{J}}{|\vec{J}|}\ . \tag{4.2}$$

We finally note that $\mathcal{H}_{\text{int}}$ in (4.1) is odd under CP or T symmetry

$$\begin{array}{l} d \xrightarrow{C} -d\ ,\ \ \vec{E} \xrightarrow{C} -\vec{E}\ , \\ \vec{J} \xrightarrow{P} \vec{J}\ ,\quad \vec{E} \xrightarrow{P} -\vec{E}\ , \\ \vec{J} \xrightarrow{T} -\vec{J}\ ,\ \vec{E} \xrightarrow{T} \vec{E}\ . \end{array} \tag{4.3}$$

Passage to a relativistic interaction

In the relativistic quark field theory the interaction described by (4.1) corresponds, for a 1/2 spin particle, to an effective Lagrangian

$$\mathcal{L}_{\text{eff}} = -\frac{i}{2}d^E\overline{\psi}\sigma^{\mu\nu}\gamma_5\psi F_{\mu\nu}\ . \tag{4.4}$$

To show this statement one can confront the scattering amplitude from an external potential $A^\mu(x) = (\phi(\vec{x}), \vec{A}(\vec{x}))$ generated by (4.4) in the non relativistic limit with the analogous amplitude obtained using (4.1) in the Born approximation.

The first amplitude is governed by the following Feynman amplitude

$$\mathcal{M} = \frac{1}{2} d^E \overline{u}(p') \sigma^{\mu\nu} \gamma_5 u(p) F_{\mu\nu}(q) \quad , \quad q = p - p' \ . \tag{4.5}$$

In the non-relativistic limit ($|p|, |p'| \ll m$) the spinors u satisfies the following relations

$$\begin{aligned} u &\approx \sqrt{m} \begin{pmatrix} \chi \\ \chi \end{pmatrix} \ , \\ \overline{u}(p') \sigma^{ij} \gamma_5 u(p) &= \begin{pmatrix} -\epsilon^{ijk}\sigma^k & 0 \\ 0 & \epsilon^{ijk}\sigma^k \end{pmatrix} u(p) \approx 0 \ , \\ \overline{u}(p') \sigma^{0k} \gamma_5 u(p) &= \begin{pmatrix} i\sigma^k & 0 \\ 0 & i\sigma^k \end{pmatrix} u(p) \approx i2m\chi' \sigma^k \chi \ . \end{aligned} \tag{4.6}$$

Recalling that $F_{0k} = \partial_0 A_k - \partial_k A_0 = E^k$ we finally obtain

$$\mathcal{M} = i2md^E \chi' \vec{\sigma} \chi \cdot \tilde{\vec{E}}(q) \ , \tag{4.7}$$

where χ and χ' are the two component spinors describing the particle polarization and $\tilde{\vec{E}}(q)$ is the Fourier transform of $\vec{E}(x)(q = p - p')$. As regards the second, we start from the general formula

$$f(p', p)|_{\text{Born}} = -2m(2\pi)^3 \langle p', \chi' | \mathcal{H}_{\text{int}} | p, \chi \rangle \ . \tag{4.8}$$

where the states normalization is $\langle p'|p\rangle = \delta^{(3)}(p' - p)$. For an explicit derivation the reader is referred to [Sak85]. Specializing eq. (4.8) to interaction (4.1) we obtain

$$f(p', p)|_{\text{Born}} = 2md \ \langle \chi' | \frac{\vec{J}}{|J|} | \chi \rangle \cdot \tilde{\vec{E}}(q) \ . \tag{4.9}$$

From eqs. (4.7) and (4.9) it is clear that $d = id^E$.

CP behavior of the EDM transition

To explicitly verify that L_{eff} in eq. (4.4) violates CP we must consider the ψ and A^μ fields transformation properties under charge conjugation

$$C\psi C = C\overline{\psi}^T \quad , \quad CA^\mu C = -A^\mu \quad , \tag{4.10}$$

where $C = i\gamma^0\gamma^2$. Turning to the EDM operator, we have

$$\begin{aligned} C \left[\overline{\psi} \sigma^{\mu\nu} \gamma_5 F_{\mu\nu} \right] C &= \psi^T C \sigma^{\mu\nu} \gamma_5 C \overline{\psi}^T (-F_{\mu\nu}) \\ &= \psi^T (\sigma^{\mu\nu} \gamma_5) \overline{\psi}^T (-F_{\mu\nu}) \\ &= +\overline{\psi} \sigma^{\mu\nu} \gamma_5 \psi F_{\mu\nu} \ . \end{aligned} \tag{4.11}$$

This operator conserve C, but violates P since $\overline{\psi}\sigma^{\mu\nu}\gamma_5\psi$ is a pseudo-tensor and consequently gives a pseudo-scalar after the contraction with $F_{\mu\nu}$.

4.2. Operator basis for the Neutron EDM

In this section we generalize the relativistic EDM interaction (4.4) to non elementary systems, specializing to our case of interest, the EDM of the Neutron. We write the relevant CP-violating effective low-energy Hamiltonian as

$$\mathcal{H}_{\rm CPV} = \sum_q C_1^q(\mu) O_1^q(\mu) + \sum_q C_2^q(\mu) O_2^q(\mu) + C_3(\mu) O_3(\mu) \quad , \tag{4.12}$$

where

$$\begin{aligned} O_1^q &= -\frac{i}{2} e\, Q_q m_q\, \bar{q} \sigma^{\mu\nu} \gamma_5 q\, F_{\mu\nu} \ , \\ O_2^q &= -\frac{i}{2} g_s m_q \bar{q}\, \sigma^{\mu\nu} t^a \gamma_5 q\, G^a_{\mu\nu} \ , \\ O_3 &= -\frac{1}{6} g_s f^{abc} G^a_{\mu\rho} G^{b\rho}_{\nu} G^c_{\lambda\sigma} \epsilon^{\mu\nu\lambda\sigma} \quad . \end{aligned} \tag{4.13}$$

The index q runs over light quarks, and $Q_q = (2/3, -1/3)$ for up- and down-type quarks respectively. With this choice, all the operators have dimension six. Four fermion operators can in principle also appear in $\mathcal{H}_{\rm CPV}$. These new operators are parameterized by Wilson coefficients

$$\mathcal{H}_{\rm eff} = \sum_{i,j=e,d,s,b} C_{ij} \left(\overline{q}_i q_j\right) \left(\overline{q}_j i\gamma_5 q_j\right) \ , \tag{4.14}$$

where i, j run over flavor indices and the second index always indicates the fermion flavor that enters eq. 4.14 via a pseudoscalar bilinear. For simplicity we don't take into account these contributions that in many SUSY models are usually suppressed unless $\tan\beta$ is very large [LP02, DLO$^+$04].

Before starting the analysis of the Neutron EDM in the framework of the MSSM we shortly consider other possible contributions already present in the SM. A beautiful review of this subject can be found in [Dar00].

Standard Model electroweak contribution to the Neutron EDM

The calculation of the Neutron EDM is proportional to δ_{CKM}, the only source of CP violation in the $SU(2) \times U(1)$ Weinberg-Salam Model. Adopting a quark model (see section 4.4) to parameterize the internal structure of the Neutron, it is necessary to compute the coefficients $C_i(\mu)$ in eq. (4.12), the EDM of a single free quark. However, it is known [EGN76] that the unitarity of the CKM matrix give rise to cancellation mechanism between different diagrams. The one loop graphs are self-conjugated and cannot contribute to CP-violating observables. It was shown [Sha80] that the two loop diagrams sum up to zero and consequently there is no contribution to quark EDM up to three loops.

The theoretical predictions gives

$$|d_n| \sim 10^{-33}\ e \cdot cm\ , \tag{4.15}$$

which is at least 7 orders of magnitude below the present experimental limit (recall eq. (1.4)).
Consequently, it is always possible to safely forget the possible contribution to the EDM transitions coming from the SM weak phase.

Strong contribution to the Neutron EDM

The Neutron EDM is in principle sensible to another SM operator, emerging when considering the properties of the QCD vacuum [Jar], given by

$$\mathcal{L}_{\rm QCD} = \theta \frac{g_s^2}{64\pi^2} \epsilon^{\mu\nu\rho\sigma} G^a_{\mu\nu} G^a_{\rho\sigma}\ , \tag{4.16}$$

where θ is a free parameter, not a priori predicted by the theory. This operator should be eliminated performing a chiral transformation, provided that at least one massless quark exists. This is no longer true in a general texture for the quark mass matrix, since a chiral transformation would modify the phases of the Yukawa matrix.

The most common choice is to work with a real quark mass matrix and parameterize the two effects inside a $\mathcal{L}^{\rm eff}_{QCD}$ defining an effective parameter $\theta_{\rm eff}$.

The effect of θ_{eff} on the Neutron EDM can be estimated with non perturbative techniques [Bal79]

$$|d_n| \sim 10^{-16} \theta_{\rm eff}\ e \cdot cm\ . \tag{4.17}$$

Confronting eq. (4.17) with the experimental limit in eq. (1.4) a very stringent constraint over $\theta_{\rm eff}$ can be provided

$$\theta_{\rm eff} < 10^{-9}\ . \tag{4.18}$$

This requires a huge fine tuning of the pure QCD angle θ and the phase of the quark mass matrices. That one has such a small value for θ_{eff} instead of a naively expected order of unity poses the well known strong CP problem [Che]. Many efforts have been done to find solutions to this issues, mainly linked to two main ideas.

The first, initially proposed in ([PQ77]), is based on the introduction of an effective potential for the dynamical variable θ_{eff} which relaxes it to zero at all orders in perturbation theory.

The second is based on an appropriate choice of the quark mass matrix such that the interplay between the original QCD vacuum angle and that of the quark mass matrix is lost and it is possible to put $\theta = 0$ from the beginning.

The baseline of this short review is that one can advance some theoretical hints to assert that the Neutron EDM is a good vehicle to analyze new sources of CP violation beyond those present in the SM. In the following we specialize this analysis to the MSSM models, applying the OPE and RGE methods to the Hamiltonian in (4.12).

4.3. Magic Numbers at LO

Let us now discuss the LO anomalous dimensions of the operators in eq. (4.13). The anomalous dimensions of operators O_1^q and O_2^q can be easily gleaned from that of the operators O_7 and O_8 relevant in the $b \to s\gamma$ process (see ref. [CFM+93]). The anomalous dimension of the Weinberg operator O_3 [Wei89] and of its mixing with O_2 was derived in ref. [BLY90a]. Therefore we get the following LO anomalous dimension matrix:

$$\gamma^{(0)} \equiv \begin{pmatrix} \gamma_e & 0 & 0 \\ \gamma_{qe} & \gamma_q & 0 \\ 0 & \gamma_{Gq} & \gamma_G \end{pmatrix} = \begin{pmatrix} 8\,C_F & 0 & 0 \\ 8\,C_F & 16\,C_F - 4\,N_c & 0 \\ 0 & -2\,N_c & N_c + 2n_f + \beta_0 \end{pmatrix} \tag{4.19}$$

where $C_F = 4/3$, $N_c = 3$, $\beta_0 = \frac{1}{3}(11N_c - 2n_f)$ with n_f the number of active flavours. The Wilson coefficients at the hadronic scale μ_H can be easily obtained from those at a high scale μ_S from

$$C_1^q(\mu_H) = \eta^{\kappa_e} C_1^q(\mu_S) + \frac{\gamma_{qe}}{\gamma_e - \gamma_q}\left(\eta^{\kappa_e} - \eta^{\kappa_q}\right) C_2^q(\mu_S) + \left[\frac{\gamma_{Gq}\gamma_{qe}\,\eta^{\kappa_e}}{(\gamma_q - \gamma_e)(\gamma_G - \gamma_e)} + \frac{\gamma_{Gq}\gamma_{qe}\,\eta^{\kappa_q}}{(\gamma_e - \gamma_q)(\gamma_G - \gamma_q)} + \frac{\gamma_{Gq}\gamma_{qe}\,\eta^{\kappa_G}}{(\gamma_e - \gamma_G)(\gamma_q - \gamma_G)}\right] C_3(\mu_S)\ , \tag{4.20}$$

$$C_2^q(\mu_H) = \eta^{\kappa_q} C_2^q(\mu_S) + \frac{\gamma_{Gq}}{\gamma_q - \gamma_G}\left(\eta^{\kappa_q} - \eta^{\kappa_G}\right) C_3(\mu_S)\ , \tag{4.21}$$

$$C_3(\mu_H) = \eta^{\kappa_G} C_3(\mu_S)\ , \tag{4.22}$$

where $\eta = \alpha_s(\mu_S)/\alpha_s(\mu_H)$ and $\kappa_i = \gamma_i/(2\beta_0)$.

The operator basis in eq. (4.13) is very suitable to discuss the anomalous dimension matrix. However, in order to avoid the explicit appearance of the strong coupling at the low scale in the operators, it is more convenient to introduce a slightly different operator basis

$$\begin{aligned} O_e^q &= -\frac{i}{2} e\, Q_q m_q\, \bar{q}\sigma^{\mu\nu}\gamma_5 q\, F_{\mu\nu}, \\ O_c^q &= -\frac{i}{2} m_q \bar{q}\,\sigma^{\mu\nu} t^a \gamma_5 q\, G^a_{\mu\nu}, \\ O_G &= -\frac{1}{6} f^{abc} G^a_{\mu\rho} G^{b\rho}_{\nu} G^c_{\lambda\sigma} \epsilon^{\mu\nu\lambda\sigma} \end{aligned} \tag{4.23}$$

that defines our electric dipole (O_e), chromoelectric dipole (O_c) and Weinberg operator (O_G) and whose corresponding Wilson coefficients can be easily obtained from eqs. (4.20–4.22) by redefining the coefficients as follows:

$$\begin{aligned} g_s(\mu_H)\, C_2^q(\mu_S) &= \eta^{-(1/2)} C_c^q(\mu_S), \\ g_s(\mu_H)\, C_3(\mu_S) &= \eta^{-(1/2)} C_G(\mu_S). \end{aligned} \tag{4.24}$$

X_{11}^{23}	1.25857	X_{12}^{12}	-9.78321	X_{12}^{23}	10.06853
X_{13}^{12}	-4.63415	X_{13}^{23}	5.33040	X_{13}^{35}	-1.60476
X_{13}^{43}	7.76606	X_{13}^{52}	-7.05911	X_{22}^{11}	1.22290
X_{23}^{11}	0.57927	X_{23}^{34}	-1.30387	X_{23}^{51}	0.88239
X_{33}^{34}	2.17311				

Table 4.1: Magic numbers X_{ij}^{ab} for the evolution from six to four flavours. See the text for details.

To illustrate in a simple way the relation between the Wilson coefficients at the μ_S scale and those at the μ_H scale we take $\mu_S \sim m_t$ and assume five flavours of light quarks between the scales μ_S and μ_H, obtaining

$$C_e^q(\mu_H) = \eta^{\frac{16}{23}} C_e^q(\mu_S) + 8\left(\eta^{\frac{16}{23}} - \eta^{\frac{14}{23}}\right) \frac{C_c^q(\mu_S)}{g_s(\mu_S)} + \frac{24}{85}\left[17\,\eta^{\frac{16}{23}} - 15\,\eta^{\frac{14}{23}} - 2\,\eta^{\frac{31}{23}}\right] \frac{C_G(\mu_S)}{g_s(\mu_S)}, \tag{4.25}$$

$$C_c^q(\mu_H) = \eta^{\frac{5}{46}} C_c^q(\mu_S) + \frac{9}{17}\left(\eta^{\frac{5}{46}} - \eta^{\frac{39}{46}}\right) C_G(\mu_S), \tag{4.26}$$

$$C_G(\mu_H) = \eta^{\frac{39}{46}} C_G(\mu_S). \tag{4.27}$$

It is interesting to note that in eqs. (4.25–4.27) all the η's are raised to a positive power and then act as suppression factors.

In general, SUSY masses are expected to be above m_t while the hadronic matrix element is evaluated at a scale of the order of the Neutron mass. In this situation it is more appropriate to consider the evolution from $\mu_S > m_t$ to $\mu_H < m_b$, i.e. from the six- to the four-flavour theory, that can be summarized via the already introduced magic numbers. In this case, the low-energy coefficients $\vec{C}(\mu_H) \equiv (C_e^q, C_c^q, C_G)$ are given in terms of the high energy ones as

$$\mathrm{C}_i(\mu_H) = \sum_{j=1}^{3} \sum_{a,b=1}^{5} X_{ij}^{ab} \alpha_s(\mu_S)^{Y_a} \eta^{Z_b} g_s(\mu_S)^{\delta_{i1}(\delta_{j1}-1)} \mathrm{C}_j(\mu_S)\,, \tag{4.28}$$

with Y_a and Z_b given by:

$$Y_a = \left\{\frac{8}{75}, \frac{64}{525}, \frac{72}{175}, \frac{163}{175}, \frac{177}{175}\right\},$$
$$Z_b = \left\{\frac{3}{50}, \frac{14}{25}, \frac{16}{25}, \frac{33}{50}, \frac{29}{25}\right\} \tag{4.29}$$

and the nonvanishing entries in X_{ij}^{ab} are listed in Table 4.1. These magic numbers have been obtained using the average values $\overline{m}_t(m_t) = 168.5$ GeV, $\overline{m}_b(m_b) = 4.28$ GeV and $\alpha_s(M_Z) = 0.119$.

A comparison with previous evaluations of the LO anomalous dimension matrix is now in order. Several partial LO results are present in the literature [BGTW90, DF90,

BLY90a, ALN90] although the work of ref. [ALN90], to be called ALN, can be regarded as the standard reference for the QCD correction to the Neutron EDM with its numerical estimates of the QCD correction factors that have been and are still widely used in the literature. With respect to ALN our analysis differs in two aspects: i) we have included the mixing between the operators O_e and O_c that is neglected in ALN. ii) Our definition of the operator basis (eq. (4.23)) is different from that employed in ALN. In particular, we write explicitly in the definition of the operators O_e and O_c the mass of the quark, as well as in O_e the charge of quark, while in the operator basis of ALN the quark mass and charge is not present. Correspondingly the anomalous dimension matrix of ALN should differ from ours by a factor $\gamma_m = -6\,C_F$. Taking into account this difference we find agreement with ALN in the anomalous dimension result for the chromoelectric and Weinberg operators. Instead, for the electric dipole operator we find that, with the conventions employed by ALN, the anomalous dimension should read $\gamma_e = -8/3$, i.e. it has the opposite sign with respect to the one quoted in ref. [ALN90]. As a consequence, the QCD renormalization factor of the dipole operator, $\eta^{\rm ED}$, that is estimated in ALN to be $\eta^{\rm ED} = 1.53$, should be $\eta^{\rm ED} < 1$, i.e it does not enhance the CP violating effect but actually suppresses it. Employing the same values for strong coupling at the high and low scale used in ALN we get $\eta^{\rm ED} \sim 0.61$.

In our view the definition of the operator basis we employ (eq. (4.23)) has the advantage to make more transparent the behavior of the perturbative QCD corrections to the Neutron EDM that in general give correction factors that decrease the amount of CP violation generated at the high scale. In the ALN operator basis this effect is somewhat hidden by the fact that the quark mass entering their Wilson coefficients has to be taken at the high scale and $m_q(\mu_{\rm S}) < m_q(\mu_H)$. It should be noticed that the dependence of the Wilson coefficients upon the quark mass can also appear in an indirect way, e.g. through the matrices that diagonalize squark masses (see eqs. (2.25-2.26)).

4.4. Hadronic Matrix Elements

In order to compute the EDM of the Neutron the matrix elements of O_e^q, O_c^q, O_G between Neutron states are also needed. At the moment a result from Lattice QCD is not yet available, although first steps in this direction have been recently made [S$^+$05]. Several alternative approaches have been used to estimate these matrix elements, as QCD sum rules [PR01] or chiral Lagrangians [PdR91]. In this paper we are mainly concerned about perturbative aspects of the EDM calculation, thus we are going to use the simplest estimates of the operator matrix elements. In particular, for the electric dipole operator, we use the chiral quark model where the Neutron is seen as a collection of three valence quarks described by an $SU(6)$ symmetric spin-flavour wave function. In this model the Neutron EDM is related to that of the valence quarks by

$$d_n^e = \frac{1}{3}\,(4d_d^e - d_u^e)\,, \tag{4.30}$$

where

$$d_q^e = e\, Q_q\, m_q(\mu_H)\, C_e^q(\mu_H) \tag{4.31}$$

is the quark EDM. Concerning the contribution of the chromoelectric and Weinberg operators to d_n the simplest estimate is obtained via naive dimensional analysis [GM84] giving

$$d_n^c = \frac{e}{4\pi}\left(m_u(\mu_H)\, C_u^c(\mu_H) + m_d(\mu_H)\, C_d^c(\mu_H)\right), \tag{4.32}$$

$$d_n^G = \frac{e}{4\pi}\,\Lambda\, C_G(\mu_H) \tag{4.33}$$

where $\Lambda \approx 1.19$ GeV is the chiral-symmetry-breaking scale. We notice that in eqs. (4.31) and (4.32) m_q is computed at the hadronic scale, while in the expressions for the Wilson coefficients at the $\mu_{\rm S}$ scale the masses, as well as g_s, are computed at the high scale.

4.5. Wilson coefficients at LO

We now turn to the analysis of the amplitude of the EDM transition via MSSM interactions to the LO.

Extraction of the EDM interaction

We work in an off-shell kinematical configuration in which all external momenta are assumed to be much smaller than the masses of the particles running inside the loops. To extract C_e^q and C_c^q we notice that the most general vertex diagram having as external particles two fermions and one boson can be decomposed in 12×2 objects, where 12 are the possible combinations of one Lorentz index and two momenta. Using standard techniques one can construct projectors for each of these 24 objects and then take the appropriate combination of them which, after the use of EOM and the Gordon identity, contributes to the operators (4.23). We observe that this projectors depend on the kinematical configuration assumed. We work in the configuration defined by $p_1^2 = p_2^2 = 0,\ p_1 \cdot q = q^2/2$ where p_1 and q are the momentum carried by the incoming quark and the external boson, respectively, and $q^2 \ll m_q^2$. In this framework the projector for the tensor part read

$$\begin{aligned} P_{EDM}^{\mu} = \frac{1}{2\, q^6\, (n-2)} \Big\{ & q^2(n-2)(q^2 - \not{q}\not{p}_1 + m_q\, \not{q})(2p_1 - q)^{\mu} \\ & + m_q^2 \left[(n-1)(4\, \not{q}\not{p}_1(2\, p_1 - q)^{\mu} - 4\, q^2 p_1^{\mu}) + 2\, n\, q^2 q^{\mu} - 2\, q^2 \gamma^{\mu}\, \not{q}\right] \Big\}\, \gamma_5 \ , \end{aligned} \tag{4.34}$$

and works by contacting it with the amplitude and taking the trace. In eq. (4.34) n is the dimension of the space-time and μ is the index carried by the external boson. As it can be seen from eq. (4.34), the projector contains power of q^2 in the denominators. However, because the assumption $q^2 \ll m_q^2$, we can perform ordinary Taylor expansion to eliminate unphysical poles when $q^2 \to 0$. Consequently, the actual computation of

the one and two loop graphs both for the full and the effective theory is reduced to the calculation of massive self-energy integrals with no external momenta. Explicit results on two-loop integrals of this kind are known [DT93].

Parameterization of the squark propagator

To present our results in a transparent way we perform the computation of the Wilson coefficients using current eigenstates for squark fields. In this basis the propagator for the squark of the first generation, relevant for the EDM of the Neutron as discussed in sec. 2.3, is a 2×2 matrix given by (see eqs. (2.24-2.27))

$$\Delta_{\tilde{q}}(k) = \frac{i}{(k^2 - M^2_{\tilde{q}_1})\,(k^2 - M^2_{\tilde{q}_2})} \begin{pmatrix} k^2 - M^2_{\tilde{q}_R} & m_q X_q^* \\ m_q X_q & k^2 - M^2_{\tilde{q}_L} \end{pmatrix} \tag{4.35}$$

where $M_{\tilde{q}_i}$ are the eigenvalues of $\mathcal{M}^2_{\tilde{q}} = \mathcal{M}^2_{U,D}$ and $X_q = A_q^* - \mu \tan\beta$.

Neglecting $\mathcal{O}(m_q^2)$ terms we have that $M_{\tilde{q}_1} \simeq M_{\tilde{q}_L}$, $M_{\tilde{q}_2} \simeq M_{\tilde{q}_R}$ so that $\Delta_{\tilde{q}}(k)$ reduces to

$$\Delta_{\tilde{q}}(k) \simeq i \begin{pmatrix} \frac{1}{k^2 - M^2_{\tilde{q}_1}} & \frac{m_q X_q^*}{(k^2 - M^2_{\tilde{q}_1})\,(k^2 - M^2_{\tilde{q}_2})} \\ \frac{m_q X_q}{(k^2 - M^2_{\tilde{q}_1})\,(k^2 - M^2_{\tilde{q}_2})} & \frac{1}{k^2 - M^2_{\tilde{q}_2}} \end{pmatrix}. \tag{4.36}$$

We notice that within this approximation the left-right propagator is still exact.

Results for gluino, chargino and neutralino exchange

The Wilson coefficients of the operators O_e, O_c are generated at the one-loop order through the first diagram in fig. 4.1 while that of O_G appears for the first time at the two-loop level (second diagram in fig. 4.1). At the LO we can then set $C_G(\mu_S) = 0$ and write

$$C_e^q(\mu_S) = C^q_{e\tilde{g}}(\mu_S) + C^q_{e\tilde{\chi}^-}(\mu_S) + C^q_{e\tilde{\chi}^0}(\mu_S) \tag{4.37}$$

and similarly for C_c^q.

We find for the gluino contribution [1]

$$C^q_{e\tilde{g}}(\mu_S) = \frac{\alpha_s}{4\pi\, M^2_{\tilde{g}}} \mathrm{Im}\left(\frac{X_q}{M_{\tilde{g}}}\right) \frac{8}{3}\, \tilde{B}\,(x_1, x_2)\,, \tag{4.38}$$

$$C^q_{c\tilde{g}}(\mu_S) = \frac{g_s\, \alpha_s}{4\pi\, M^2_{\tilde{g}}} \mathrm{Im}\left(\frac{X_q}{M_{\tilde{g}}}\right) \tilde{C}\,(x_1, x_2) \tag{4.39}$$

where $x_i = M^2_{\tilde{g}}/M^2_{\tilde{q}_i}$. The explicit expressions for the functions $\tilde{B}$ and $\tilde{C}$ as well as those entering in the chargino and neutralino contributions are collected in the Appendix C.

[1] Note that gluino mass is indicated with $M_{\tilde{g}}$ instead of M_3 from now on as a common choice in the literature.

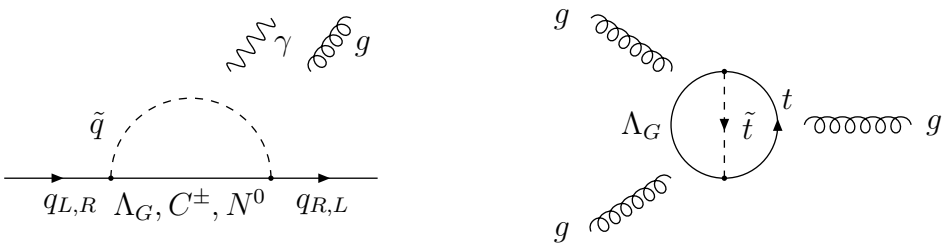

Figure 4.1: Leading SUSY contributions to the quark EDMs. The photon and gluon lines are to be attached to the loop in all possible way.

For the chargino we have

$$C^u_{e\tilde{\chi}^-}(\mu_S) = \frac{\alpha\, Q_u^{-1}}{4\pi s_W^2} \sum_{i=1}^{2} \frac{1}{\sqrt{2}\, s_\beta\; M^2_{\tilde{\chi}_i{}^-}} \left(\frac{M_{\tilde{\chi}_i{}^-}}{M_W}\right) \Big\{ \mathrm{Im}\,(V_{i2}\, U_{i1}) \Big[(Q_d - Q_u)\, A(y^i_{\tilde{d}_1}) + Q_d\, B(y^i_{\tilde{d}_1}) \Big] \\ -\mathrm{Im}\left(\frac{m_d X_d^*}{M^2_{\tilde{\chi}_i{}^-}} V_{i2}\, U_{i2}\right) Y_d \Big[(Q_d - Q_u)\, \tilde{A}(y^i_{\tilde{d}_1}, y^i_{\tilde{d}_2}) + Q_d\, \tilde{B}(y^i_{\tilde{d}_1}, y^i_{\tilde{d}_2}) \Big] \Big\}, \quad (4.40)$$

$$C^d_{e\tilde{\chi}^-}(\mu_S) = \frac{\alpha\, Q_d^{-1}}{4\pi s_W^2} \sum_{i=1}^{2} \frac{1}{\sqrt{2}\, c_\beta\; M^2_{\tilde{\chi}_i{}^-}} \left(\frac{M_{\tilde{\chi}_i{}^-}}{M_W}\right) \Big\{ \mathrm{Im}\,(V_{i1}\, U_{i2}) \Big[(Q_u - Q_d)\, A(y^i_{\tilde{u}_1}) + Q_u\, B(y^i_{\tilde{u}_1}) \Big] \\ -\mathrm{Im}\left(\frac{m_u X_u^*}{M^2_{\tilde{\chi}_i{}^-}} V_{i2}\, U_{i2}\right) Y_u \Big[(Q_u - Q_d)\, \tilde{A}(y^i_{\tilde{u}_1}, y^i_{\tilde{u}_2}) + Q_u\, \tilde{B}(y^i_{\tilde{u}_1}, y^i_{\tilde{u}_2}) \Big] \Big\}, \quad (4.41)$$

$$C^u_{c\tilde{\chi}^-}(\mu_S) = \frac{g_s\, \alpha}{4\pi s_W^2} \sum_{i=1}^{2} \frac{1}{\sqrt{2}\, s_\beta\; M^2_{\tilde{\chi}_i{}^-}} \left(\frac{M_{\tilde{\chi}_i{}^-}}{M_W}\right) \Big\{ \mathrm{Im}\,(V_{i2}\, U_{i1})\, B(y^i_{\tilde{d}_1}) \\ -\mathrm{Im}\left(\frac{m_d X_d^*}{M^2_{\tilde{\chi}_i{}^-}} V_{i2}\, U_{i2}\right) Y_d \tilde{B}(y^i_{\tilde{d}_1}, y^i_{\tilde{d}_2}) \Big\}, \quad (4.42)$$

$$C^d_{c\tilde{\chi}^-}(\mu_S) = \frac{g_s\, \alpha}{4\pi s_W^2} \sum_{i=1}^{2} \frac{1}{\sqrt{2}\, c_\beta\; M^2_{\tilde{\chi}_i{}^-}} \left(\frac{M_{\tilde{\chi}_i{}^-}}{M_W}\right) \Big\{ \mathrm{Im}\,(V_{i1}\, U_{i2})\, B(y^i_{\tilde{u}_1}) \\ -\mathrm{Im}\left(\frac{m_u X_u^*}{M^2_{\tilde{\chi}_i{}^-}} V_{i2}\, U_{i2}\right) Y_u \tilde{B}(y^i_{\tilde{u}_1}, y^i_{\tilde{u}_2}) \Big\} \quad (4.43)$$

where $y^i_{\tilde{q}_j} = M^2_{\tilde{\chi}_i^-}/M^2_{\tilde{q}_j}$, U and V are the matrices that diagonalize $M_{\tilde{\chi}^\pm}$ according to $U^* M_{\tilde{\chi}^\pm} V^{-1} = M^d_{\tilde{\chi}^\pm}$ and $Y_{u,d}$ are the Yukawa couplings of the up and down quarks in units of $e/\sin\theta_W$.

In eqs. (4.40–4.43) we have also written explicitly the contributions proportional to the mass and the Yukawa coupling of the light quarks to show that the phase combination that enters in the gluino contribution is actually present in the chargino term in a suppressed way. Indeed, in the chargino contribution the only relevant phase is ϕ_μ, hidden

inside the matrices U and V. This can be seen explicitly in the following simplified expression, obtained by neglecting the contributions proportional to quark masses and Yukawa couplings:

$$C^u_{e\tilde{\chi}^-}(\mu_S) = \frac{\alpha\, Q_u^{-1}}{4\pi s_W^2} \sum_{i=1}^{2} \frac{1}{\sqrt{2}\, s_\beta\; M^2_{\tilde{\chi}_i{}^-}} \left\{ \mathrm{Im}\left(\frac{U^*_{i2}\, U_{i1}\mu}{M_W} \right) \left[(Q_d - Q_u)\, A(y^i_{\tilde{d}_1}) + Q_d\, B(y^i_{\tilde{d}_1}) \right] \right\} . \tag{4.44}$$

Analogous expressions can be obtained from eqs. (4.41)-(4.43) with the substitutions:

$$\begin{aligned} M_{\tilde{\chi}_i{}^-}\, \mathrm{Im}\,(V_{i2}\, U_{i1}) &\to \mathrm{Im}\,(U^*_{i2}\, U_{i1}\mu)\ , \\ M_{\tilde{\chi}_i{}^-}\, \mathrm{Im}\,(V_{i1}\, U_{i2}) &\to \mathrm{Im}\,(V^*_{i2}\, V_{i1}\mu)\ . \end{aligned} \tag{4.45}$$

Finally the neutralino contribution, neglecting terms proportional to the the quark masses, is given by:

$$\begin{aligned} C^q_{e\tilde{\chi}^0}(\mu_S) = \frac{\alpha}{4\pi s_W^2} \sum_{i=1}^{4} \frac{1}{M^2_{\tilde{\chi}_i{}^0}} \Bigg\{ & \mathrm{Im}\left(\frac{K^a_{qi} K^b_{qi} X_q}{M_{\tilde{\chi}^0_i}} \right) \tilde{B}(z^i_1, z^i_2) \\ & + \left(\frac{M_{\tilde{\chi}_i{}^0}}{M_W} \right) \left(\mathrm{Im}\left(K^b_{qi} K^c_{qi} \right) B(z^i_2) - \mathrm{Im}\left(K^a_{qi} K^c_{qi} \right) B(z^i_1) \right) \Bigg\} , \end{aligned} \tag{4.46}$$

$$C^q_{c\tilde{\chi}^0}(\mu_S) = g_s\, C^q_{e\tilde{\chi}^0} \tag{4.47}$$

where $z^i_j = M^2_{\tilde{\chi}^0_i}/M^2_{\tilde{q}_j}$, and

$$K^a_{ui} = \sqrt{2} \left[\left(Q_u - \frac{1}{2} \right) \tan\theta_W\, Z^{i1} + \frac{1}{2} Z^{i2} \right] , \tag{4.48}$$

$$K^b_{ui} = \sqrt{2} \tan\theta_W\, Q_u\, Z^{i1} , \tag{4.49}$$

$$K^c_{ui} = \frac{1}{\sqrt{2} s_\beta} Z^{i4} , \tag{4.50}$$

$$K^a_{di} = \sqrt{2} \left[\left(Q_d + \frac{1}{2} \right) \tan\theta_W\, Z^{i1} - \frac{1}{2} Z^{i2} \right] , \tag{4.51}$$

$$K^b_{di} = \sqrt{2} \tan\theta_W\, Q_d\, Z^{i1} , \tag{4.52}$$

$$K^c_{di} = \frac{1}{\sqrt{2} c_\beta} Z^{i3} . \tag{4.53}$$

In eqs. (4.48-4.53) Z is the matrix that diagonalizes M_{χ_0} according to $Z^* M_{\chi_0} Z^{-1} = M^d_{\chi_0}$. As can be seen from eq. (4.46) in the neutralino contribution both ϕ_μ, through the matrix Z, and the X_q phase combination are actually present.

We noticed that the results reported in eqs. (4.38)-(4.43) and (4.46)-(4.53) are fully in agreement with those in ref. [IN98, PRS00] and represent the lowest order approximation.

4.6. LO results

In this section we investigate, at the LO, the effect of QCD corrections on the Neutron EDM, to assess whether they can significantly reduce the individual gluino, chargino and neutralino contributions making the EDM constraint on SUSY phases less severe.

To discuss in a simple way the effect of the QCD corrections and in particular the importance of the mixing between O_e and O_c that was neglected in previous analyses, we consider eqs. (4.25-4.27) assuming $\eta = 0.3$ and setting $C_G = 0$. Then

$$C_e^q(\mu_H) = 0.43\, C_e^q(\mu_S) - 0.38\, \frac{C_c^q(\mu_S)}{g_s(\mu_S)}, \tag{4.54}$$

$$C_c^q(\mu_H) = 0.88\, C_c^q(\mu_S), \tag{4.55}$$

$$C_G(\mu_H) = 0. \tag{4.56}$$

Thus, if $C_e^q(\mu_S) \simeq C_c^q(\mu_S)/g_s(\mu_S)$ the resulting $C_e^q(\mu_H)$ is strongly suppressed. With our definition of the operators the above situation is achieved when the gluon in a diagram contributing to C_c^q is attached to a squark of the same charge of the external quark. This case is realized in the neutralino contribution (see eq. (4.47)). Indeed, we can estimate the neutralino contribution to d_n^e, d_n^c, as given in eqs. (4.30,4.32), by employing the Wilson coefficient at the low scale evaluated via eqs. (4.25-4.27) with $g_s(\mu_S) = 1.22$. We get

$$\begin{aligned} d_n^{e,\tilde{\chi}^0} &\simeq \frac{e}{3}\left[4\, m_d(\mu_H)\left(-\frac{1}{3}0.05\right) C^d_{e\tilde{\chi}^0}(\mu_S) - m_u(\mu_H)\left(\frac{2}{3}0.05\right) C^u_{e\tilde{\chi}^0}(\mu_S)\right] \\ &\approx e\left[-m_d(\mu_H)\, 0.02\, C^d_{e\tilde{\chi}^0}(\mu_S) - 0.01\, m_u(\mu_H)\, C^u_{e\tilde{\chi}^0}(\mu_S)\right] \quad , \end{aligned} \tag{4.57}$$

$$\begin{aligned} d_n^{c,\tilde{\chi}^0} &\simeq 0.88\frac{e}{4\pi}\left[m_u(\mu_H)\, g_s(\mu_S)\, C^u_{e\tilde{\chi}^0}(\mu_S) + m_d(\mu_H)\, g_s(\mu_S)\, C^d_{e\tilde{\chi}^0}(\mu_S)\right] \\ &\approx e\, 0.08\, \left[m_u(\mu_H)\, C^u_{e\tilde{\chi}^0}(\mu_S) + m_d(\mu_H)\, C^d_{e\tilde{\chi}^0}(\mu_S)\right]. \end{aligned} \tag{4.58}$$

Eqs. (4.57-4.58) show that the individual quark EDMs are strongly suppressed by the QCD corrections. A so large effect is actually specific to the neutralino contribution because of the simple relation between $C^q_{e\tilde{\chi}^0}$ and $C^q_{c\tilde{\chi}^0}$ (eq. (4.47)). The general case is more complicated and the resulting effect depends upon the relative sign between $C_e^q(\mu_S)$ and $C_c^q(\mu_S)$.

It is not our purpose here to perform a general analysis of EDM constraints on SUSY models. Rather, our aim is to illustrate the impact of QCD corrections on the computation of the EDM. To do so, we study a specific point in the SUSY parameter space that we choose with a mass spectrum similar to that of the benchmark point 1a of the Snowmass Points and Slopes [2] (SPS) [A+02]. The SPS benchmark points are actually defined assuming real parameters, however we take the mass spectrum of point 1a as indicative, also in the case of complex parameters, of possible mass values of a "typical" mSUGRA scenario

[2] We use the low-energy spectrum obtained from the tool [AKP03] available on the Web at the URL: `http://kraml.home.cern.ch/kraml/comparison/`

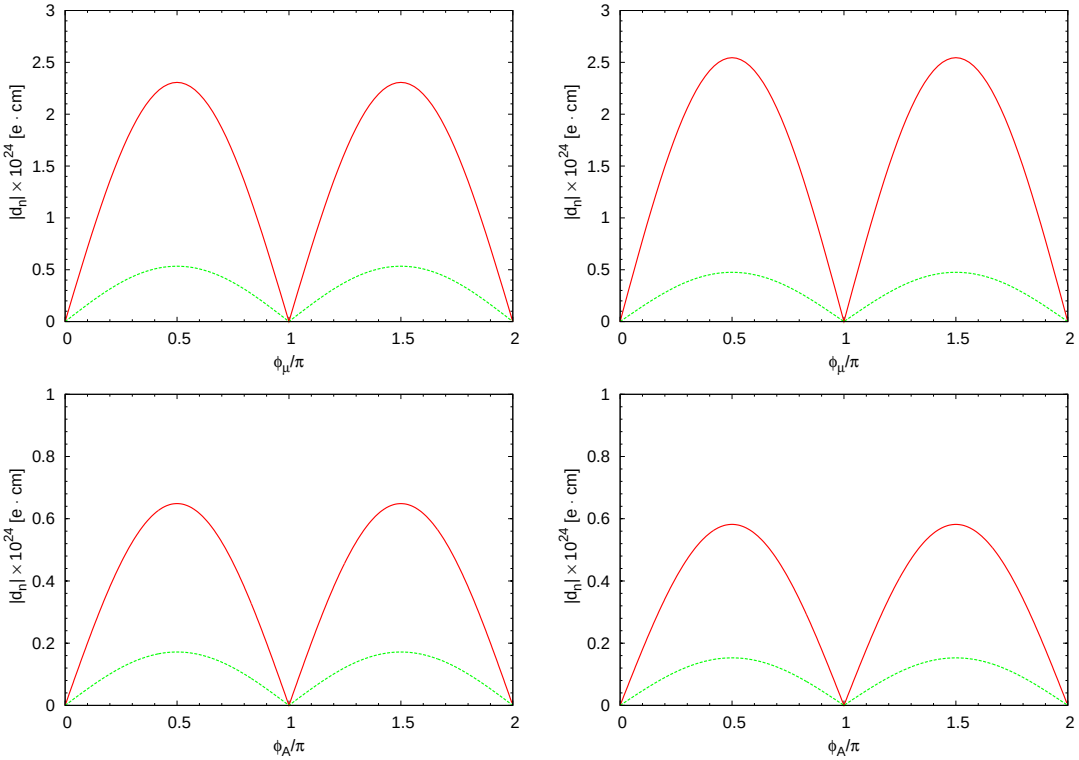

Figure 4.2: Gluino contribution to the Neutron EDM versus ϕ_μ (top) and $\phi_{A_u} = \phi_{A_d}$ (bottom), without (left) and with (right) QCD corrections. The red line is the d_n^e contribution, while the green one the corresponding d_n^c contribution.

with an intermediate value of $\tan\beta$. We take $M_{\tilde{g}} = 585$ GeV, $M_1 = 100$ GeV, $M_2 = 190$ GeV, $M_{\tilde{u}_1} = 540$ GeV, $M_{\tilde{u}_2} = 525$ GeV, $M_{\tilde{d}_1} = 550$ GeV, $M_{\tilde{d}_2} = 520$ GeV, $|\mu| = 355$ GeV, $\tan\beta = 10$, $|A_d| = 855$ GeV, $|A_u| = 675$ GeV and $\mu_S = 465$ GeV. To obtain d_n we have chosen the hadronic scale $\mu_H = 2$ GeV with $m_d(\mu_H) = 7$ MeV and $m_u(\mu_H) = 3$ MeV. In fig. (4.2) we show the effect of QCD corrections on the gluino contribution to the EDM of the Neutron. In the figure we plot the absolute value of d_n as a function of ϕ_A and ϕ_μ with the other SUSY parameters set to the values listed above. As can be seen comparing the plots on the left, which are obtained without QCD corrections, to the ones on the right, where QCD corrections are included, the effect in this case amounts to $\sim 10\%$. Fig. (4.3) and fig. (4.4) show the corresponding analysis for chargino and neutralino contributions, respectively. Fig. (4.3) shows that for chargino contributions the inclusion of QCD corrections reduces the amount of CP violation generated at the μ_S scale by a factor $\sim 50\%$. Finally, the simple analysis of the neutralino contribution discussed above is substantiated by fig. (4.4) where this strong reduction is clearly visible.

A popular mechanism [IN98] invoked to suppress the Neutron EDM without resorting to extremely small phases or very heavy SUSY particles is the search for regions of the parameter space where cancellations among the three different contributions are active. It is always possible to find regions of the parameter space where contributions depending upon different parameters cancel each other, although it can be questioned if these regions

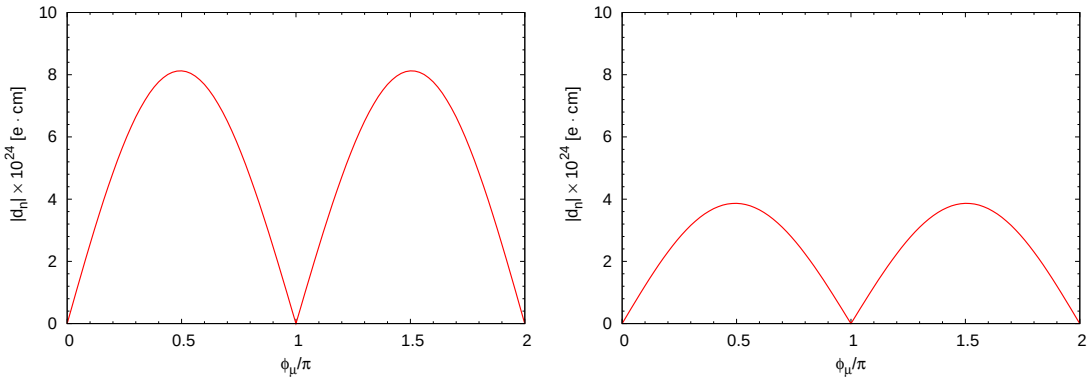

Figure 4.3: Chargino contribution to the Neutron EDM versus ϕ_μ, without (left) and with (right) QCD corrections. We show only the d_n^e contribution because the d_n^c one is negligible.

can be representative of general situations. With respect to this, it is interesting to note that, since the neutralino contribution is always much more suppressed by QCD corrections than the gluino and chargino ones, the cancellation mechanism among different contributions invoked in ref. [IN98] should actually work between the gluino and chargino only. However, these two contributions depend upon different phase combinations. As an example, ϕ_A is only present in the gluino contribution.

Uncertainties of the LO analysis

In the above analysis all the uncertainties of the LO computation have been neglected. The uncertainties connected to the nonperturbative evaluation of the hadronic matrix elements go beyond the scope of this work, since we focus our analysis on the perturbative aspects of QCD effects. Therefore, let us assume that some nonperturbative method such as Lattice QCD will produce in the future the necessary matrix elements at a scale $\mu_H = 2$ GeV, so that we fix the hadronic scale in our analysis. Then, we are left with the uncertainties connected to the matching between the full and the effective theory at the scale μ_S.

It is well known that in the RGE improved perturbation theory there remain unphysical μ_S-dependences which are of the order of the neglected higher order terms. Usually, this uncertainty can be estimated by varying the matching scale in a (arbitrarily chosen) given range. However, for the EDM computation, there are further sources of uncertainty. All contributions depend upon the squark masses, but the precise definition of these masses cannot be fixed at LO, so that one can use pole, $\overline{\rm DR}$ or any other squark mass. Indeed, the difference between the results obtained using two different mass definitions is of higher order in α_s and provides an estimate of this additional LO uncertainty. Furthermore, the gluino contribution also depends on the gluino mass and, more important, on the strong coupling. Neither the definition of the gluino mass nor, in principle, the scale of α_s is fixed at LO, so that they constitute another source of uncertainty. All these uncertainties can be ameliorated only by a NLO calculation.

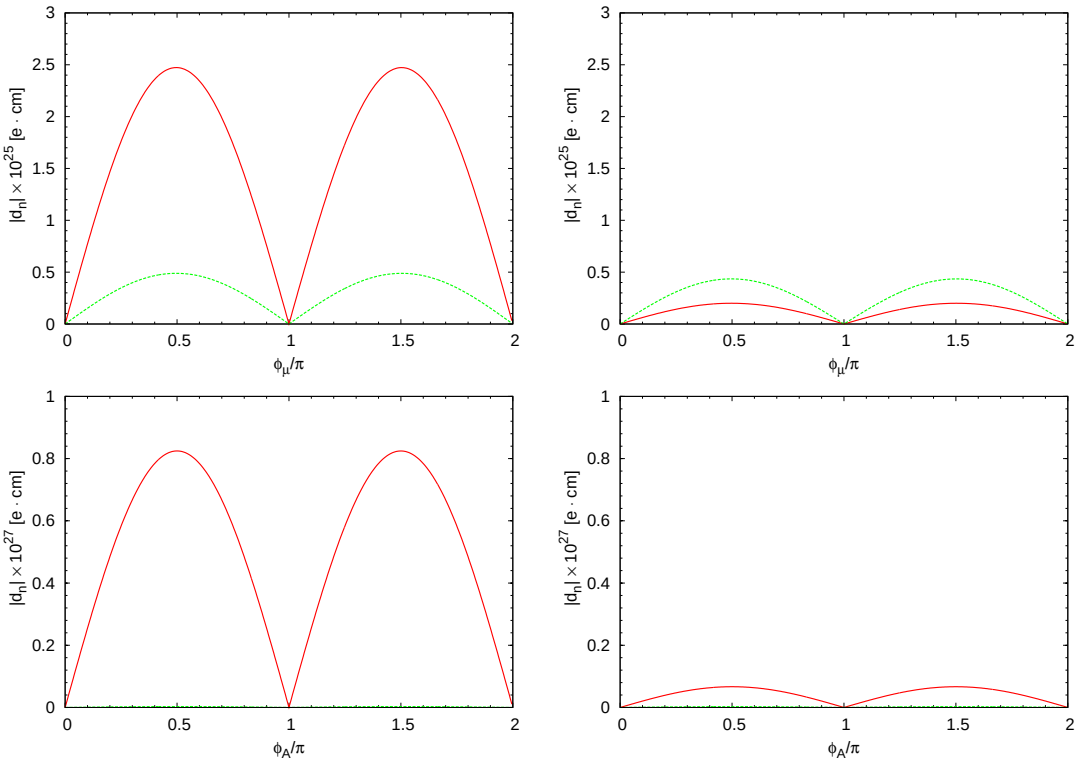

Figure 4.4: Neutralino contribution to the Neutron EDM versus ϕ_μ (top) and $\phi_{A_u} = \phi_{A_d}$ (bottom), without (left) or with (right) QCD corrections. The red line is the d_n^e contribution, while the green one the corresponding d_n^c contribution.

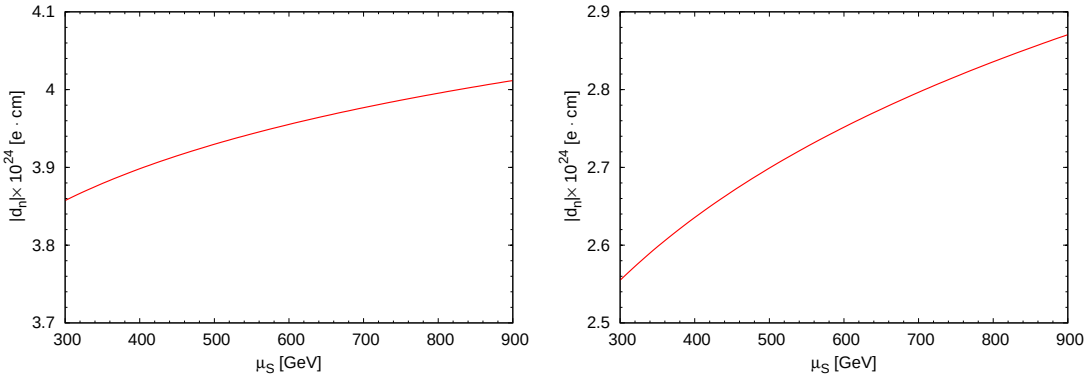

Figure 4.5: The μ_S scale dependence of the chargino (left) and gluino (right) contributions to d_n^e at LO.

In fig. (4.5) we illustrate the LO uncertainty only due to the choice of the matching point. Here and in the following NLO analysis we will use an average squark mass $M_{\tilde{q}}^2 = (M_{\tilde{q}_1}^2 + M_{\tilde{q}_2}^2)/2$. In the figure we plot the LO gluino (right) and chargino (left) contributions to $|d_n| \simeq |d_n^e|$ as a function of the matching scale with α_s and $\overline{\text{MS}}$-DRED masses evaluated, for simplicity, at the scale μ_{S}. As expected the μ_{S} dependence is more pronounced in the gluino case and amounts to 10-15 % while in the chargino contribution it reaches at most 4 %.

The LO gluino contribution shows a substantial uncertainty that, including all effects, can be expected to be $\sim 20\%$. To reduce it to a level comparable to that of the chargino contribution one needs the NLO computation of this contribution that will be discussed in the next chapter.

5. Neutron EDM at Next-to-Leading Order

This chapter is devoted to the explanation of the computational steps we have performed to compute the NLO Wilson coefficients of the Neutron EDM in the MSSM.

We do not attempt to perform a complete NLO analysis of the QCD corrections to the Neutron EDM, instead we focus on the relevant pieces needed to discuss the reduction of the scale dependence of the gluino contribution, as already discussed in sec. 4.6.1 We present the NLO anomalous dimension matrix for the electric and chromoelectric operators and the NLO Wilson coefficients for the gluino contribution. For completeness we present also the Wilson coefficients of the Weinberg operator. We recall that at the LO $C_G(\mu_H) = 0$, therefore to obtain the NLO result it is sufficient to know the LO γ_G, γ_{Gq} entries of the anomalous dimension matrix.

5.1. Magic Numbers at NLO

The discussion of the NLO anomalous dimension matrix is more easily accomplished in the O_1^q–O_3 basis of eq.(4.13). Indeed in this basis the anomalous dimension matrix can be organized in powers of α_s as

$$\gamma = \frac{\alpha_s}{4\,\pi}\gamma^{(0)} + \left(\frac{\alpha_s}{4\,\pi}\right)^2 \gamma^{(1)}, \tag{5.1}$$

where $\gamma^{(0)}$ is given in eq.(4.19) and

$$\gamma^{(1)} = \begin{pmatrix} \left(\frac{548}{9}N_c - 16\,C_F - \frac{56}{9}n_f\right) C_F & 0 & 0 \\ \left(\frac{404}{9}N_c - 32\,C_F - \frac{56}{9}n_f\right) C_F & -\frac{458}{9} - \frac{12}{N_c^2} + \frac{214}{9}N_c^2 + \frac{56}{9}\frac{n_f}{N_c} - \frac{13}{9}N_c\,n_f & 0 \\ * & * & * \end{pmatrix}. \tag{5.2}$$

We have computed the NLO anomalous dimension in eq.(5.2) and our results are in complete agreement with those obtained from the known NLO anomalous dimension of the O_7 and O_8 operators in the $b \to s\gamma$ process [MM95].

The entries in the third row are unknown but not needed at the NLO, since they contribute only to the $(i3)$ sector of the NLO magic numbers, and the initial coefficient of the Weinberg operator is vanishing at the LO. The corresponding Wilson coefficients in the O_e^q–O_G basis can be easily obtained using eq.(4.24). The simplest way to present

ab	43	43	54	55	63
ij	11	12	12	22	12
W_{ij}^{ab}	11.301	85.158	-79.353	9.9191	0
R_{ij}^{ab}	-8.7762	-70.209	65.693	-6.9887	0
δX_{ij}^{ab}	-0.39785	-3.1828	3.7203	-0.65874	-0.46504

Table 5.1: Magic numbers R_{ij}^{ab} , W_{ij}^{ab} and δX_{ij}^{ab} for the NLO evolution from six to four flavours.

the NLO evolution of the Wilson coefficients is via the magic numbers. Referring to the O_e^q–O_G basis we can write for a generic scale μ

$$\vec{\mathrm{C}}(\mu) = \vec{\mathrm{C}}^{(0)}(\mu) + \frac{\alpha_s(\mu)}{4\pi}\,\vec{\mathrm{C}}^{(1)}(\mu) \tag{5.3}$$

where $\mathrm{C}_i^{(0)}(\mu_\mathrm{S})$ is the LO Wilson coefficient at the scale μ_S and its evolution from $\mu_\mathrm{S} > m_t$ to $\mu_H < m_b$ is given by eq.(4.28). The evolution of $\vec{\mathrm{C}}^{(1)}(\mu)$ from $\mu_\mathrm{S} > m_t$ to $\mu_H < m_b$ can be summarized in the following way

$$\begin{aligned}\mathrm{C}_i^{(1)}(\mu_H) = \eta \sum_{j=1}^{3}\sum_{a=1}^{6}\sum_{b=1}^{5} \alpha_s(\mu_\mathrm{S})^{Y_a}\eta^{Z_b} g_s(\mu_\mathrm{S})^{\delta_{i1}(\delta_{j1}-1)} \Big[X_{ij}^{ab}\,\mathrm{C}_j^{(1)}(\mu_\mathrm{S}) \\ + \left(\delta X_{ij}^{ab}/\alpha_s(\mu_\mathrm{S}) + W_{ij}^{ab} + \eta^{-1}R_{ij}^{ab}\right)\mathrm{C}_j^{(0)}(\mu_\mathrm{S})\Big]\,.\end{aligned} \tag{5.4}$$

The relevant entries of the NLO magic numbers δX_{ij}^{ab} , W_{ij}^{ab} and R_{ij}^{ab} are given in Table 5.1. As expected, the evolution of $\vec{\mathrm{C}}^{(1)}(\mu_\mathrm{S})$ is dictated by the magic numbers derived in the LO case (see eq.(4.28)).

5.2. Full theory calculation

The computational steps we must follow to evaluate the full amplitude to the NLO are basically the same as those described for the LO case. For this reason we can take the LO calculation of the previous chapter as a reference and move on from it to tackle the various complications emerging when one more loop is included.

Step 1: Feynman diagrams

In order to include the next order in perturbation theory, we have to generate all the two loop diagrams with the same amputated external legs, and having as vertices and internal propagators all those belonging to the MSSM. It goes without saying that at NLO a major difficulty is to be sure "not to forget any diagrams" as well as to have all combinatorial factors under control.

Such problems were addressed and resolved by taking advantage of FeynArts [Hah01], an open-source Mathematica [Wol88] package for the generation and visualization of Feynman diagrams and amplitudes. A presentation and a list of the main features of FeynArts

can be found at the URL in [Hah01]. Here we will address only those that are particularly relevant to our discussion.

1. Given a theory, hence a set of vertices, and a particular process, thus a set of external states, FeynArts allows first to generate all the diagrams entering the corresponding amplitude, up to three loop order. Afterwards, it permits to automatically substitute Feynman rules in any generated diagram, or, in other words, to "write it down" in the form of an *inserted amplitude*. Such amplitude is printed in a Mathematica form whence subsequent custom manipulations are possible. In the present work the latter were implemented in a Mathematica program that basically automatizes the various computational steps involved. More technical details will be given in due curse, when singly addressing each step. The starting point "links" the FeynArts output to the rest of the program by feeding inserted amplitudes to appropriate pattern-matching-recognition based code.

2. FeynArts allows to deal with Dirac as well as with Majorana fermions. Concerning the latter, we point out that Majorana particles imply vertices where the fermion number is violated [1]. This causes an ambiguity when trying to fix the fermion flow in fermion lines containing propagators of Majorana particles. In our case this problem emerges, because of the presence of gluino-quark-squark vertices (see (2.46-2.47)) and similar neutralino-quark-squark ones. To tackle this difficulty, we outlined the simple procedure introduced by the authors of ref. [DEHK92]. The same algorithm is the one adopted in the present work, since it is part of the FeynArts code: it is automatically implemented when substituting Feynman rules inside a given diagram, to generate the corresponding *inserted amplitude*.

3. The theory FeynArts should use to generate Feynman diagrams is specified in a "model file", through the full set of propagators and interaction vertices it entails. In our MSSM case, a model file is already implemented. However the existing version has a limitation in squark vertices involving the unitary matrices Z_D, Z_U that allow to pass from the squark mass eigenstates' basis to the flavour$\times$chirality eigenstates' one (see eq. (2.43)). In the original version of the MSSM model file, vertices with Z_D's and Z_U's are implemented as general in chirality, but diagonal in flavour. The latter limitation was removed within the present work with suitable modifications to the model file, given that flavour diagonal squark interactions would obviously not be able to generate the $\Delta B = 1$ transition analyzed in chapter 6.

The full set of diagrams entering the NLO amplitude can be first divided into six subsets:

[1] A Majorana fermion coincides with its own antiparticle, at variance with a Dirac one.

1. **Gluon corrections** connecting *different legs* in A-type and B-type diagrams. Such corrections are collected in fig. 5.1 and do not involve self-energies with gluon insertion, since in this case the gluon propagator would start and end on the same leg.

2. Gluon corrections to $\mathbf{q \to q}$ **transition**, where $q = u, d$, collected in fig. 5.2.

3. **Self-energy corrections** of internal legs only, since we are calculating amputated amplitudes. Such corrections include self-energies due to gluons and are collected in fig. 5.3.

4. Diagrams involving the **squark-squark-gauge-gauge vertices**, depicted in fig. 5.4.

5. **Squark corrections**, due to the addition to A-type and B-type topologies of more squark propagator, via the quark-squark-gluino interactions. They are reported in fig. 5.5.

6. **Other topologies**. These include other diagrams that cannot be included in the abovementionated categories, and are collected in fig. 5.6.

Looking at figs. (5.1-5.6), beyond the "graph" column, there are a "diagram" and a "#" column, for which some words of explanation are mandatory.

The "diagram" column reports the diagrams' names. Within all the diagrams that come out of A-type and B-type topologies with the inclusion of more one loop in all possible way, the name has the form A_S or B_S, with S a subscript. The form $A(B)$ is due to the observation that such subsets are generated from A-type and B-type topologies. Turning to the subscript S, the latter classifies the additional loop that is included starting from A and B, to produce the given NLO diagram. In the case of gluon and self-energy corrections, the subscript is a pair of numbers ij, referring to the pair of legs that corrections themselves connect, according to the following labels

and in particular self-energies corrections to a leg i are indexed with ii.

Now let us turn to the "#" column. It reports the diagram degeneracy. The latter represents the total number of distinct corrections of the kind of that depicted in the given graph [2]. All such corrections are obtained by 180° rotation of the graph about the axis connecting the top-left corner to the bottom-right one and by the $4 \leftrightarrow 5$ exchange (see labels in the above diagrams).

Several comments are in order here. First, the diagrams depicted with an external photon are those contributing to the matching of the electric dipole operator, while for

[2]Including the one in the graph.

extracting the chromoelectric operator the diagrams with an external gluon must be added. Concerning diagram $B_{44q}, A_{66q}, B_{V_2}, B_{V_3}$, we see that, notwithstanding the number of distinct rotations, the latter must be also multiplied by 2 N_f. This is because the quark-squark loop can be done with an up- or a down-quark of either flavour (in total N_f possibilities) and with arrow in either sense of the loop. In this sense the top quark is a special case, since it can induce in the supergravity model under our investigation a chirality-violating transition proportional to its mass (see the LR and RL entries of the squark mass matrix in eqs. (2.25-2.26)). This insertion is an effect entering for the first time at the two-loop level and allow the (chromo)-electric dipole operators to be generated by a different combinations of CP-violating phases.

A further comment, before proceeding in our discussion of the calculation, concerns the neglect in our listing of the two loop diagrams that are generated by FeynArts but are zero. Trivial diagrams are generated by LO boxes with insertion of a tadpole in a squark or a gluino leg. The possibilities for the squark case are the following

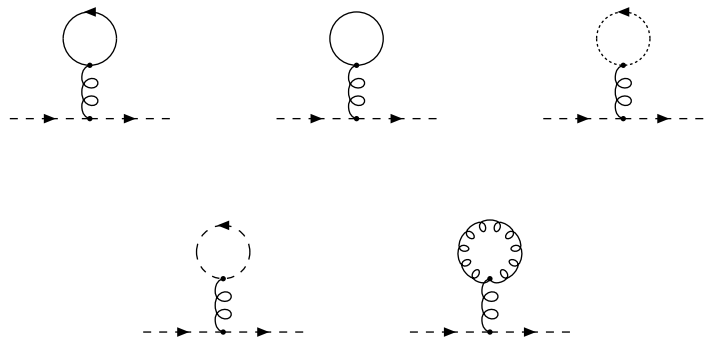

(5.5)

where the dotted propagator refers to a $SU(3)_c$ ghost. All the tadpoles in (5.5) vanish because the particle in the loop belongs either to the fundamental or to the adjoint representation of $SU(3)_c$ and in both cases generators are traceless. Tadpoles insertions for a gluino propagator are exactly the same as those for the squark case. One should also mention that the diagrams of the kind of $A(B)_{44s}$ (fig. 5.3) with a gluon loop in place of the squark one are possible, but null in dimensional regularization because gluons are massless.

Step 2: Inserted amplitudes

The next step, after the generation and the classification of all the Feynman diagrams arising at NLO, is to substitute Feynman rules in each of them. Given the number of diagrams and the algebraic complexity of at least some of the MSSM rules, this is a very tedious task to do by hand. However, as seen above, this can be done within FeynArts, with a special function that reads a given graph and generates the corresponding amplitude (within the MSSM in our case). Such amplitude is printed in a human-readable Mathematica format and in a suitable way to prevent other Mathematica simplifications.

A-type	graph	B-type	graph	#
A_{12}	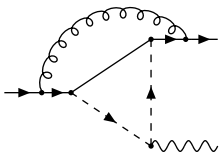	B_{12}	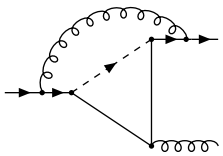	1 / 1
A^a_{13}	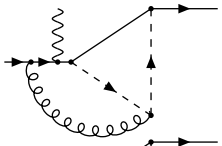	B^a_{13}	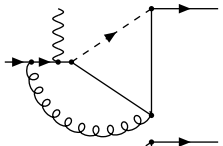	2 / 2
A^{na}_{13}	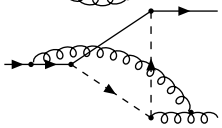	B^{na}_{13}	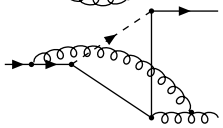	2 / 2
A_{14}	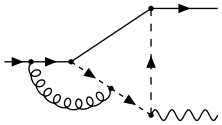	B_{14}	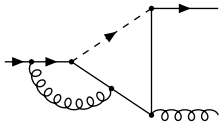	4 / 4
A_{16}	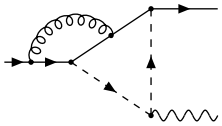	B_{16}	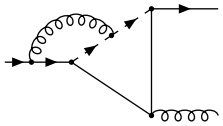	2 / 2
A^a_{45}	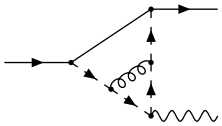	B^a_{45}	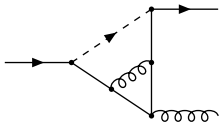	1 / 1
A^{na}_{45}	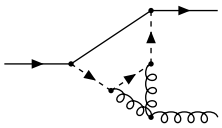	B^{na}_{45}	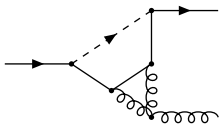	2 / 2
A_{46}	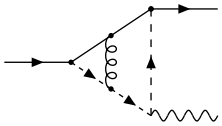	B_{46}	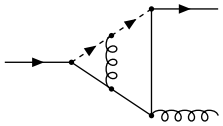	1 / 1

Figure 5.1: NLO diagrams generated from gluon corrections connecting different legs. The last diagram is not generated from the LO topologies.

diagram	graph	#
X_1	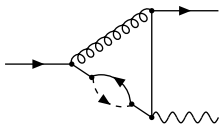	2
X_2	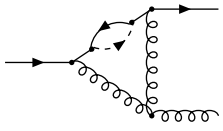	1

Figure 5.2: NLO diagrams generated from corrections to $q \to q$ transitions.

A-type	graph	B-type	graph	#
A_{44g}	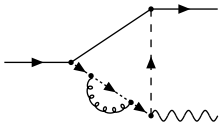	B_{44g}	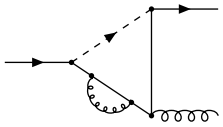	2 / 2
A_{44q}	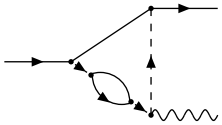	B_{44q}	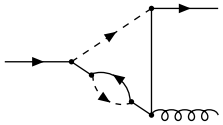	2 / 4 N_f
A_{44s}	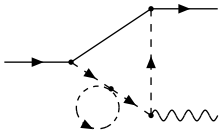	B_{66s}	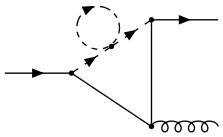	4 / 2
A_{66g}	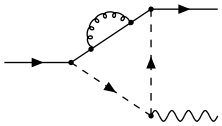	B_{66g}	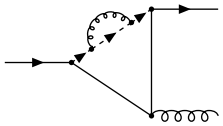	1 / 1
A_{66q}	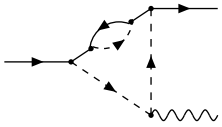	B_{66q}	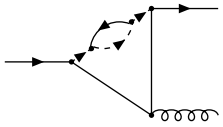	2 N_f/ 1

Figure 5.3: NLO diagrams generated from self-energy corrections to A-type and B-type magnetic topologies.

diagram	graph	#
Y_1	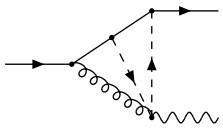	2
Y_2	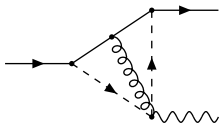	1
Y_3	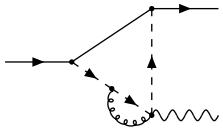	2
Y_4	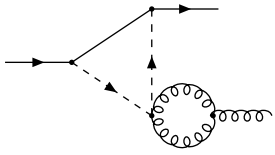	1

Figure 5.4: NLO diagrams involving the squark-squark-gauge-gauge vertices.

A-type	graph	B-type	graph	#
A_{V_1}	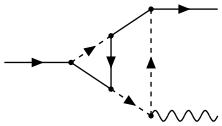	B_{V_1}	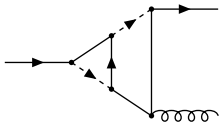	2 / 2
A_{V_2}	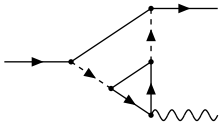	B_{V_2}	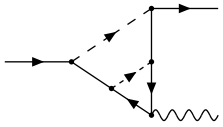	1 / 2 N_f
A_{V_3}	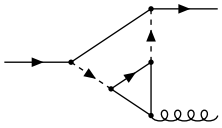	B_{V_3}	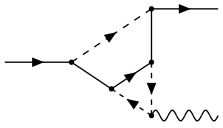	1 / 2 N_f

Figure 5.5: NLO diagrams generated from squark corrections to A-type and B-type magnetic diagrams.

diagram	graph	#
Z_1	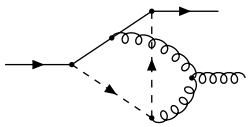	1
Z_2	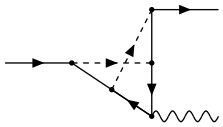	2
Z_3	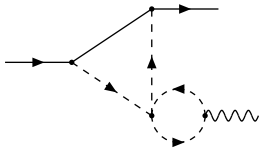	1

Figure 5.6: Other topologies.

Step 3: Algebraic manipulations

Given the inserted amplitude of an NLO diagram, the algebraic manipulations that have to be done to simplify it are

1. Contraction with the projector.

2. Color matrices simplifications and contraction with external spinors.
   Afterwards, before summing diagrams, one has to perform the

3. Two loop scalar integrals.

The last step of performing loop integrations is addressed in a later discussion. In the present work, all the above manipulations are dealt with in the framework of Mathematica by means of suitable routines. To make every step automatic and trustworthy for all the various topologies encountered, the following working procedure was adopted. The inserted amplitude generated by FeynArts is read by some pattern-matching based functions and each of its terms is split into a color, a Dirac, a flavour part and what is left over. Each of the latter terms is then separately reduced, and taken back together at the end to rebuild the initial term.

Final manipulations

The only operations left are the scalar integration in the loop variables and the amplitude renormalization. We address the two issues in turn.

Loop integration

As explained in the previous chapter, loop integrations call for evaluation of vacuum integrals. In addition there are no uncontracted Lorentz indices and integrals are of scalar form. We also mention that, after well known algebraic manipulations like the partial fractioning decomposition

$$\frac{1}{(q^2-m_1^2)\ (q^2-m_2^2)} = \frac{1}{m_1^2-m_2^2}\left[\frac{1}{(q^2-m_1^2)} - \frac{1}{(q^2-m_2^2)}\right] \ , \tag{5.6}$$

each of these integrals can be reduced to the master form

$$\mathcal{I}(m_1,m_2,m_3;n_1,n_2,n_3) \equiv$$
$$\int \frac{d^dq_1}{(2\pi)^d}\frac{d^dq_2}{(2\pi)^d}\frac{1}{(q_1^2-m_1^2)^{n_1}\ (q_2^2-m_2^2)^{2_1}\ ((q_1-q_2)^2-m_3^2)^{n_3}} \ . \tag{5.7}$$

The analytic solution of integrals like (5.7) can be found in [DT93]. In particular, $\mathcal{I}(m_1,m_2,m_3;1,1,1)$ is calculated explicitly, and then the one with generic n_1,n_2,n_3 is "connected" to it via recursion relations. The latter are obtained using the so-called "partial p" operation [tHV72] and allow to calculate an integral with $n_1+n_2+n_3=\sigma+1$ in terms of those with $n_1+n_2+n_3=\sigma$ [DT93].

Diagram renormalization

Renormalization has been performed according to the so-called BPHZ prescription, introduced in refs. [BP57, Hep66, Zim69]. According to this procedure, UV divergences are subtracted on a digram-by-diagram basis, by building suitable counterterms. So we have

to classify all diagrams to NLO, as collected in figs. 5.1-5.6, according to their UV and IR behavior. One has

$$\begin{aligned}
\text{UV divergent}: \quad & \{A_{14}, A_{16}, A_{45}^{a}, A_{45}^{na}, A_{46}, A_{44g}, A_{44q}, A_{44s}, A_{66g}, A_{66q}, Y_3, Y_4, A_{V_2}, A_{V_3}, Z_3\} \\
& + \{A \to B\} \\
\text{IR divergent}: \quad & \{A_{12}, A_{13}^{a}, A_{13}^{na}, A_{14}, A_{16}, A_{34}, C_{36}, X_1, Y_1, Y_2\} + \{A \to B\} \ , \qquad (5.8)
\end{aligned}$$

whereas all the other diagrams are finite. Looking at the divergent graphs (basically all the self-energies and some of the gluon insertions), one realizes that divergences are brought about by one-loop vertex and self-energies corrections only. So one just calculates such corrections, singles out the $1/\epsilon$ part, substitute it into the one-loop magnetic diagrams and subtracts the obtained diagram to the corresponding UV divergent NLO one.

We have already observed that light m_q masses plays the role of infrared regulators. However Feynman diagrams involving the three gluon vertex present additional infrared divergences that are not regulated by this procedure. The simplest regulator in our approach are masses, so we have computed this diagrams with a fictitious gluon mass λ.

The sum of all the NLO diagrams, with renormalization by subtraction of the BPHZ counterterms, gives the connected renormalized amputated NLO amplitude A'_{full}, one of the ingredient needed in the matching procedure (3.14). The other one is A'_{eff}, and is the subject of the next section.

5.3. Effective theory calculation

From a conceptual point of view, the effective theory calculation is completely analogous to the full theory one. The LO in the effective theory case is by definition represented by the tree level matrix elements of the dipole operators. The NLO is correspondingly given by gluon corrections to the effective vertices, since the quark-quark-gluon interactions are the only ones present after integrating out the heavy MSSM degrees of freedom. So the NLO entails simply a one-loop calculation.

However, there are some theoretical subtleties related to our choose of the implementation of the matching conditions. As we have already explained, we work with an off-shell kinematical configuration such that the relevant Feynman diagrams can be evaluated using ordinary Taylor expansions in the external momenta. This is in contrast with to the on-shell case, in which asymptotic expansion [Smi95] must be employed.

This requires to consider, beside the on-shell operators in eqs. (4.13), other ones implementing a linearly independent basis when ignoring relations due to the EOM. Following ref. [Sim94], it is possible to construct a complete set of gauge invariant dimension five and six operators for the EDM transition. We can then restrict to the only operator with

the same chirality of those in eqs. (4.13):

$$O^q_m = -\frac{i}{2} m_q \, \bar{q}\gamma_5 q \ ,$$
$$O^q_{p^2} = -\frac{i}{2} m_q \, \bar{q} \ \not{D} \not{D} \gamma_5 q \ . \tag{5.9}$$

This operators generates, besides the on-shell $q \to q\gamma$ and $q \to qg$ vertices, the $q \to q$, $q \to q\gamma g$ and $q \to qgg$ ones. The corresponding contribution can be worked out either through the use of the Ward identities that relate the self-energies vertex to the tensor ones, or by direct computation of the Feynman diagrams rules from the relevant operators.

The off-shell operators must be inserted in all the possible effective diagrams. Since we are enforcing the matching procedure between q and $q, \gamma(g)$ external states, at this point it is sufficient to use the projector in eq. (4.34) to extract the (chromo)magnetic form factor.

At the one loop order in the effective theory there are only seven diagrams with gluon exchange. They are depicted in fig. (5.7), and are in one-to-one correspondence with the two loop diagrams in which an heavy loop is contracted in a local operator. Since, as already stressed, the full and effective theory has the same infrared behavior, the above-mentioned correspondence is extended to the terms the behave as $1/m_q^2, 1/\lambda^2, \ln m_q^2, \ln \lambda^2$ as $m_q, \lambda \to 0$.

We only mention that the first operator in eq. (5.9) has the dimension of a mass term for the quark fields. Its introduction, besides the cancellation of the power-like IR divergences, guarantees the quark masses to remain real beyond the tree level.

Operator renormalization

In the previous section we have discussed the enlargement of the operator basis in our off-shell Hamiltonian. The "effective theory side" of the calculation requires, in analogy with the full one, a procedure to define renormalized operators. This is a clear consequence to the fact that the two theories only differs in the UV regime.

However, the renormalization procedure must be the same between theories which yeld the same on-shell amplitude, usually referred as "on-shell equivalent theory". For a detailed explanation of this statement see [Sim94]. In our case this applies to Effective Hamiltonians obtained with or without the use of EOM. Consequently, we can use the well known renormalization constant evaluated restricting the operator basis to the on shell-operators in eq. (4.23).

Specializing formula (3.3) to our operator basis, this constants reads

$$O^{e(0)}_q = Z_\psi \left(Z_{O,11} O^e_q + Z_{O,12} O^c_q \right) \ ,$$
$$O^{c(0)}_q = Z_\psi Z_3^{1/2} Z_g^{1/2} \left(Z_{O,21} O^e_q + Z_{O,22} O^c_q \right) \ , \tag{5.10}$$

where $Z_{12,Q} = 0$ since we have neglected electromagnetic corrections.

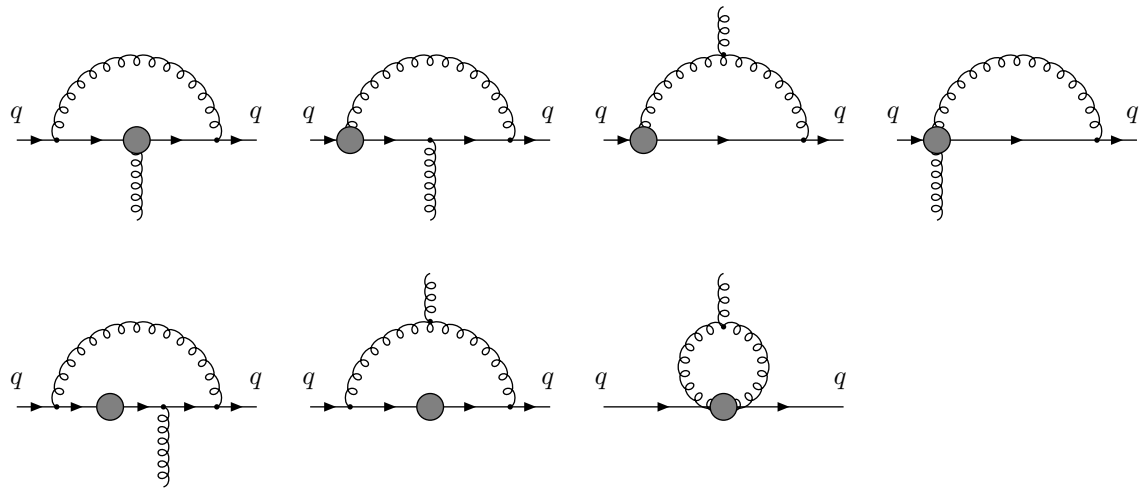

Figure 5.7: Diagrams in the effective theory contributing to the C_c^q. Rotated diagrams by 180° about the horizontal axe are not reported. The subset linked to C_e^q can be obtained eliminating the three gluon vertices and substituting the external gluon with a photon.

As an explicit check of the correctness of the effective theory calculation, we have checked that the $1/\epsilon$ ultraviolet divergences arising from the evaluation of the diagrams in fig. (5.7) fit with the renormalization constants in eq. (5.10).

After the $\overline{\text{MS}}$ subtraction of the $1/\epsilon$ poles, the results for the diagrams in fig. (5.7), multiplied for the corresponding LO Wilson coefficients, have the form $F_i^{(0)} r_{ij}$ requested for the matching (see eq. (3.14)) and must be subtracted to the full theory result in accord to (3.14) for being able to solve it in terms of our quantities of interest, the NLO Wilson coefficients.

This last operation have provided us the expression of the NLO Wilson coefficients in the $\overline{\text{MS}}$-NDR renormalization scheme.

5.4. Comparison of the results between different schemes

In the specific instance of our computation, the $\overline{\text{MS}}$-NDR renormalization scheme cannot be used to provide the final result for the Wilson coefficients. In fact, as first demonstrated in refs. ([Sie79, CJvN80]), NDR breaks supersymmetry. The problem is that, by requiring that the gluon field G_μ^a and the Dirac matrices carry a d-dimensional Lorentz index, NDR necessarily introduces a mismatch between fermion and boson degree of freedom. A way out of this difficulty, when dealing with supersymmetric theories, is given by the DRED scheme ([Sie79, CJvN80]). In DRED one requires that only momenta p^μ bear d-dimensional indices, while all the other tensors be 4-dimensional. This clearly avoids the problem of mismatch in the number of degrees of freedom outlined above.

We now discuss the relation between our calculation performed in the NDR scheme and the passage to the DRED one. A careful one-loop analysis of all the transformations

needed when comparing NDR with DRED was performed by Martin and Vaughn [MV93] in the framework of a general softly-broken $\mathcal{N} = 1$ supersymmetric theory. Concerning the way loop calculations performed in DRED and in NDR differ, the main observation [MV93] is that they

> *"only differ for graph in which there is at least one internal gauge boson line which does not terminate (at either end) in a scalar-scalar-gauge boson vertex".*

This analysis translates in our case into shifts of the form $1 + O(\alpha_s)$ for the gluino mass, and for the coupling constant g_s. Concerning the latter, in NDR one should in particular distinguish between the gauge coupling g_s appearing in the interactions of quarks, squarks and gluinos with gluons, and the coupling $\hat{g}_s$ appearing in the quark-squark-gluino interactions as a consequence of the "supersimmetrization" of the theory. In fact, while it is gauge invariance that guarantees the equality among couplings involving Yang-Mills interactions, only supersymmetry implies $g_s = \hat{g}_s$. As a consequence, DRED is the only scheme which allows the existence of supersymmetric Ward identities. .

The bottom line of the above discussion is that the NDR quantities undergoing redefinition are the gluino mass and the couplings g_s and $\hat{g}_s$, each by distinct finite $O(\alpha_s)$ terms. On the other hand squark masses do not vary to $O(\alpha_s)$ between the two schemes. The relevant formulae read [MV93]

$$\begin{aligned} M_{\tilde{g}}^{\rm NDR} &= M_{\tilde{g}}^{\rm DRED}\left(1+\frac{\alpha_s}{4\pi}N_c\right) \ , \\ g_s^{\rm NDR} &= g_s^{\rm DRED}\left(1-\frac{\alpha_s}{24\pi}N_c\right) \ , \\ \hat{g}_s^{\rm NDR} &= \hat{g}_s^{\rm DRED}\left(1+\frac{\alpha_s}{8\pi}(N_c-C_F)\right) \ , \end{aligned} \tag{5.11}$$

where N_c is the Casimir of the adjoint representation of the gauge group ($N_c = 3$ in our $\mathrm{SU(3)_c}$ case) and C_F is the Casimir in the fundamental representation (in our case $C_F = 4/3$). In formula (5.11) we have consistently neglected distinctions in the couplings definition for the $O(\alpha_s)$ terms.

Now, in our full theory calculation, the abovementioned transformations must obviously be done only on the LO part $C_{e\tilde{g}}^q$ and $C_{c\tilde{g}}^q$ (see eq. (4.38-4.39)), since the corresponding ones in $C_{e\tilde{g}}^{q(1)}$ and $C_{c\tilde{g}}^{q(1)}$ would amount to a NNLO effect. Looking at the one loop graph, we must distinguish between the electric and the chromoelectric transition. The former contains two $\hat{g}_s$ couplings, while the second two $\hat{g}_s$ couplings and one g_s coupling. In addition there is of course the gluino mass shift. As for the latter, the prescription is just to apply the first of eq. (5.11) to the leading order Wilson coefficients, in order to have the results with all the masses in the $\overline{\rm MS}$-DRED regularization-renormalization scheme. This is required by the fact that the tool we have used in our phenomenological analysis within the mSUGRA models to obtain a low-energy supersymmetric spectrum provides all the masses in such a scheme.

We have chosen instead to express the strong coupling constant in the $\overline{\rm MS}$-NDR scheme

through the following shift

$$\hat{g}_s^{NDR} = g_s^{NDR}\left[1+\frac{\alpha_s}{4\pi}\left(\frac{4N_c-3C_F}{6}\right)\right] , \tag{5.12}$$

which correspond to the difference of using NDR versus DRED and consequently restore the supersymmetric Ward identities.

We finally remark that also the pole residue of the quark and gluon propagator introduced in eqs. (3.9-3.11) are scheme-dependent quantity, different in the DRED and NDR schemes. However, the gluon corrections to the quark and gluon propagator, responsible for the shift of the pole residue when changing scheme, cancel in the master formula for the Wilson coefficients, as they are present both in the full and in the effective theory.

5.5. Wilson coefficients in the DRED scheme

We are now ready to present the general expressions of the Wilson coefficients in the $\overline{\text{MS}}$-DRED.
To simplify the calculation we have computed the NLO gluino contribution to the matching conditions retaining only one source of CP violation, namely we keep only one power of X_q, discharging terms X_q^n with $n>1$. We also work in the limit of $M_{\tilde{q}_L}=M_{\tilde{q}_R}\equiv M_{\tilde{q}}$ with $M_{\tilde{q}}$ common to all squark flavours and taking all quarks massless but the top one. Within this framework the NLO gluino corrections can be written as

$$\begin{aligned} C_{e\tilde{g}}^{q(1)}(\mu_S) = \frac{\alpha_s}{4\pi\, M_{\tilde{g}}^2}\Bigg\{ &\text{Im}\left(\frac{X_q}{M_{\tilde{g}}}\right)\left[F_1\left(x_{\tilde{g}}\right)+4F_2\left(x_{\tilde{g}}\right)+F_2\left(x_{\tilde{g}},x_t\right)+\text{Re}\left(\frac{m_t\,X_t}{M_{\tilde{g}}^2}\right)N_1\left(x_{\tilde{g}},x_t\right)\right] \\ &+\text{Im}\left(\frac{m_t\,X_t}{M_{\tilde{g}}^2}\right)\text{Re}\left(\frac{X_q}{M_{\tilde{g}}}\right)N_2\left(x_{\tilde{g}},x_t\right)\Bigg\}, \end{aligned} \tag{5.13}$$

$$\begin{aligned} C_{c\tilde{g}}^{q(1)}(\mu_S) = \frac{g_s\,\alpha_s}{4\pi\, M_{\tilde{g}}^2}\Bigg\{ &\text{Im}\left(\frac{X_q}{M_{\tilde{g}}}\right)\left[F_3\left(x_{\tilde{g}}\right)+4F_4\left(x_{\tilde{g}}\right)+F_4\left(x_{\tilde{g}},x_t\right)+\text{Re}\left(\frac{m_t\,X_t}{M_{\tilde{g}}^2}\right)N_3\left(x_{\tilde{g}},x_t\right)\right] \\ &+\text{Im}\left(\frac{m_t\,X_t}{M_{\tilde{g}}^2}\right)\text{Re}\left(\frac{X_q}{M_{\tilde{g}}}\right)N_4\left(x_{\tilde{g}},x_t\right)\Bigg\} \end{aligned} \tag{5.14}$$

where in the above equations the upper line represents the CP violation induced by the left-right entry in the mass matrix of the squark of type q while the lower one the corresponding effect due to the stops. We have further divide the former contribution into the the part due to the quark and squark of type q, that of the other four squarks and massless quarks (the first two terms), and that due to the top and stops including the mixing (the last two terms). In eqs.(5.13-5.14) $x_{\tilde{g}}=M_{\tilde{g}}^2/M_{\tilde{q}}^2$, $x_t=m_t^2/M_{\tilde{q}}^2$ and

$$F_i = G_i+\Delta_i\,\ln\frac{\mu_S^2}{M_{\tilde{q}}^2} \quad , \quad \lim_{x_t\to 0}F_i(x_{\tilde{g}},x_t)=F_i(x_{\tilde{g}}). \tag{5.15}$$

The explicit expressions of the functions G_i , Δ_i, N_i are reported in the Appendix C.

Finally, for completeness, we consider also the Weinberg operator. At the scale μ_S two-loop diagrams where top and stops together with the gluino are exchanged contribute to $C_G^{(1)}$ (see fig. 4.1). The relevant expressions can be gleaned from ref. [DDL$^+$90] obtaining

$$C_{G\tilde{g}}^{(1)}(\mu_S) = \frac{g_s\,\alpha_s}{4\pi\,M_{\tilde{g}}^2}\mathrm{Im}\left(\frac{X_t}{M_{\tilde{g}}}\right)\,H\left(x_{\tilde{g}},x_t\right), \tag{5.16}$$

where the function H is found in the Appendix C. However, when the evolution down to a four-flavour theory is considered one has to take into account also the shift in $C_G^{(1)}$ induced by the O_c operator at the m_b threshold [BGTW90, BLY90b, DDL$^+$90] or

$$C_{G\tilde{g}}^{(1)}(m_b^-) = C_{G\tilde{g}}^{(1)}(m_b^+) + \frac{\alpha_s(m_b)}{8\,\pi}C_{c\tilde{g}}^{b(0)}(m_b)\ , \tag{5.17}$$

where

$$C_{G\tilde{g}}^{(1)}(m_b^+) = \eta_b{}^{\frac{39}{46}}C_{G\tilde{g}}^{(1)}(\mu_S), \tag{5.18}$$

$$C_{c\tilde{g}}^{b(0)}(m_b) = \eta_b{}^{\frac{5}{46}}C_{c\tilde{g}}^{b(0)}(\mu_S) \tag{5.19}$$

with $\eta_b = \alpha_s(\mu_S)/\alpha_s(m_b)$.

5.6. Equation for the μ-dependence

Beyond LO, our calculated coefficient functions acquire a dependence on the renormalization scale μ. Such dependence must obey a Callan-Symanzik equation that can be used as a check of correctness for the results obtained.

The equation for the μ-dependence of the Wilson coefficients can be obtained simply observing that in the product $C_i(\mu)\,\langle Q_i\rangle(\mu)$ (no sum over i) the μ-dependence itself must cancel out up to the maximum order included in perturbation theory for the calculation of the C_i, in our case NLO. So one can write

$$\begin{aligned}
0 &= \frac{d}{d\ln\mu^2}\,C_i(\mu)\,\langle Q_i\rangle(\mu)\\
&= \left(\frac{d}{d\ln\mu^2}C_i(\mu)\right)\,\langle Q_i\rangle(\mu) + C_i(\mu)\,\left(\frac{d}{d\ln\mu^2}\langle Q_i\rangle(\mu)\right)\\
&= \left(\frac{dM_{\tilde{q}}^2}{d\ln\mu^2}\frac{\partial}{\partial M_{\tilde{q}}^2}C_i(\mu) + \frac{dM_{\tilde{g}}^2}{d\ln\mu^2}\frac{\partial}{\partial M_{\tilde{g}}^2}C_i(\mu) + \frac{dX_q}{d\ln\mu^2}\frac{\partial}{\partial X_q}C_i(\mu)\right.\\
&\quad\left. + \frac{dg_s^2}{d\ln\mu^2}\frac{\partial}{\partial g_s^2}C_i(\mu) + \frac{\partial}{\partial\ln\mu^2}C_i(\mu)\right)\,\langle Q_i\rangle(\mu) + C_i(\mu)\left(\frac{d}{d\ln\mu^2}\langle Q_i\rangle(\mu)\right)\ ,
\end{aligned} \tag{5.20}$$

where in the last equality we have taken into account that the μ-dependence within the $C_i(\mu)$ is also brought about by all the renormalized objects on which the C_i themselves obviously depends, in particular the constant g_s, the masses $M_{\tilde{q}}, M_{\tilde{g}}$ and the mass insertions X_q, with $q = u, d$.

Eq. (5.20) can now be simplified by using the RGE equations for the single terms. In particular, for the very last one, the equation reads

$$\frac{d}{d\ln\mu^2}\langle Q_i\rangle(\mu) = -\frac{\gamma_{ij}}{2}\langle Q_j\rangle(\mu) \tag{5.21}$$

where we have taken into account eq. (3.16). We observe that the ADM γ is in turn defined for the basis in eq.(4.23) and its explicit expression is the following

$$\gamma = \frac{\alpha_s}{4\pi}\begin{pmatrix} 8C_f & 0 \\ 8C_f & 16C_f - \frac{23}{3}N_c + \frac{2}{3}n_f \end{pmatrix} . \tag{5.22}$$

Turning to the RGE of the coupling constant g_s in eq. (5.20), it is dictated by

$$\frac{dg_s^2}{d\ln\mu^2} = g_s\beta^{MSSM}(g_s) = -\beta_0^{MSSM}\frac{g_s^4}{16\pi^2} \quad , \quad \beta_0^{MSSM} = 3N_c - n_f \tag{5.23}$$

where we have used the MSSM version of the β-function for g_s.

In exactly the same fashion, one can work out the explicit expression for the running of the masses $m_{\tilde{q}}$ and $m_{\tilde{g}}$ in eq. (5.20). The relevant expression are the following

$$\frac{dM_i^2}{d\ln\mu^2} = -\gamma_{M_i}M_i^2 = -\gamma_{M_i}^{(0)}\frac{g_s^2}{16\pi^2}M_i^2 , \tag{5.24}$$

where $\gamma_{M_{\tilde{g}}}^{(0)} = 2\,(3\,N_c - n_f)$ and $\gamma_{M_{\tilde{q}}}^{(0)} = 4\,C_F\,M_{\tilde{g}}^2/M_{\tilde{q}}^2$.

Finally, we must derive the RG equation for the mass insertion X_q. Now, recalling Lagrangian (2.7) and the corresponding squark mass matrices in eq. (2.14-2.15), it is clear, in the approximation where only the strong sector of the MSSM is considered, chirality- and flavour- changing mass insertions can be written as products of quark masses m_q times $A_{U,D}$ terms. Consequently, the ADM for X_q can be identified with those of the A-terms:

$$\frac{dX_q}{d\ln\mu^2} = -\frac{1}{2}\frac{g_s^2}{16\pi^2}\gamma_{X_q}^{(0)}X_q = -\frac{1}{2}\frac{g_s^2}{16\pi^2}(-2C_F)X_q . \tag{5.25}$$

We notice that the 1/2 factor in the second of eqs. (5.25) is due to the derivative being computed with respect to $\ln\mu^2$ in place of $\ln\mu$.

In conclusion, putting together results in eqs. (5.21) and (5.23)-(5.25) and dropping the operator matrix elements $\langle Q_i\rangle$, we can rewrite formula (5.20) as

$$\begin{aligned}
&\frac{\partial}{\partial\ln\mu^2}C_i(\mu)\delta_{ij} = \\
&\frac{g_s^2}{16\pi^2}\left[\left(\gamma_{M_{\tilde{g}}^2}^{(0)}M_{\tilde{g}}^2\frac{\partial}{M_{\tilde{g}}^2} + \gamma_{M_{\tilde{q}}^2}^{(0)}M_{\tilde{q}}^2\frac{\partial}{M_{\tilde{q}}^2} + \frac{\gamma_{X_q}^{(0)}}{2}\frac{\partial}{\partial X_q}\right.\right. \\
&\qquad\left.\left. +\beta_0^{MSSM}g_s^2\frac{\partial}{\partial g_s^2}\right)C_i(\mu)\delta_{ij} + \frac{\gamma_{ij}^{(0)}}{2}C_i(\mu)\right] .
\end{aligned} \tag{5.26}$$

Using eq. (5.26) and defining

$$\tilde{\Delta}_1 = \frac{\alpha_s}{4\pi\, M_{\tilde{g}}^2}\mathrm{Im}\left(\frac{X_q}{M_{\tilde{g}}}\right)(\Delta_1 + 5\Delta_2) \ ,$$

$$\tilde{\Delta}_2 = \frac{g_s\,\alpha_s}{4\pi\, M_{\tilde{g}}^2}\mathrm{Im}\left(\frac{X_q}{M_{\tilde{g}}}\right)(\Delta_3 + 5\Delta_4) \ ,$$

we have explicitely checked that the coefficients of the $\ln(\mu_{\rm S}^2/M_{\tilde{q}}^2)$ terms in eqs. (5.13)-(5.14) must satisfy the following relation

$$\tilde{\Delta}_i = \frac{1}{2}\left[(1+i)\ \beta_0^{SUSY} + \sum_{k=\tilde{g},\tilde{q}} \gamma_{M_k}^{(0)} M_k \frac{\partial}{\partial M_k} + \gamma_{X_q}^{(0)}\right] C_i^{(0)} + \frac{1}{2}\sum_{j=1}^{2} \gamma_{ji}^{(0)} C_j^{(0)} \ , \qquad (5.27)$$

guaranteeing the cancellation of the $\mu_{\rm S}$ dependence to $\mathcal{O}(\alpha_s^2)$ in eq. (5.3).

We observe that the effect of the term in the square brackets in eq.(5.27) is to shift the coupling and the mass parameters appearing in $C_i^{(0)}$ from the scale $\mu_{\rm S}$ to $M_{\tilde{q}}$.

5.7. Comparison with analysis using LO Hamiltonian

Combining the Wilson coefficients with the ADM and the matrix elements of the operators we obtain the expression of the gluino contribution to the EDM of the Neutron. We want to quantify the effect of the NLO coefficients with respect to the LO ones. We have studied the same specific point in the SUSY parameter already introduced in sec. 4.6.

As we anticipated in sec. 4.6, the inclusion of the NLO matching for the gluino contributions reduces the perturbative uncertainties down to a completely negligible level [DFMS05]. In fig. 5.8 we plot the scale dependence of the gluino contribution at the LO (upper line) and at the NLO (lower line) level. As shown in the figure the inclusion of the NLO contribution greatly reduces the scale dependence of the gluino contribution. Moreover, for what concerns the central numerical value, the inclusion of NLO corrections produces a non-negligible effect, lowering $|d_n|$ of about 10%. However, the gap between the LO and NLO curves is within the LO uncertainty in nearly all the range plotted.

As a closing remarks for our analysis of the EDM of the Neutron, we would like to stress the general results found in chap. 4-5. The operators in eq. 4.12, together with dimension six bilinear operators in eq. 4.14, form a complete basis for the EDM transition. We have already observed that the contribution to the EDM of the Neutron from the coefficients C_{ij} in eq. 4.14 is negligible in SUSY models, unless $\tan\beta$ is taken to be a large parameter. The important point connected to the formulae we have provided for the magic numbers and the matrix elements of the EDM operators is that they are completely general and allows for any phenomenological analysis of the new CP-violating phases embedded in the MSSM at a low or intermediate value of $\tan\beta$. In fact they do not depend on the high

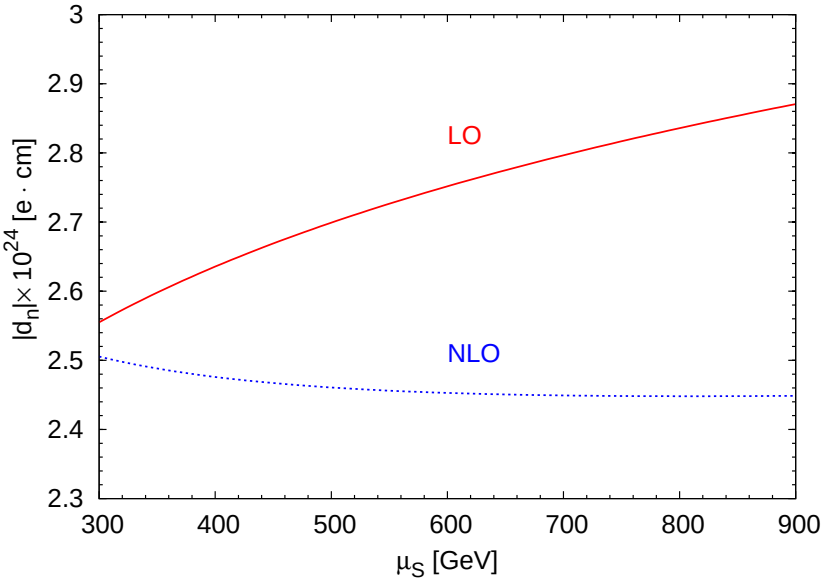

Figure 5.8: The μ_S scale dependence of the gluino contribution to d_n^e at LO (upper curve) and NLO (lower curve). See text for the reference values of the input parameters.

energy dynamics and can be used with Wilson coefficients computed in any hypothesis for the pattern of the supersymmetric spectrum.

We have then specialized the calculation of the Wilson coefficients to the mSUGRA models, since they provide a very clear and economical picture for the analysis of the new CP-violating couplings. A number of analysis have been presented in the literature during the years in the framework of the same models [IN98, PRS00], using LO results for the anomalous dimension matrix and the Wilson coefficients. However, as already observed in sec. 4.3, a wrong value for one of the entries of the anomalous dimension matrix has been long time used. We have corrected this long time mistake and merged together all the ingredients to obtain the reference plot for the EDM of the Neutron at LO in sec. 4.6.

In addition, we have analyzed the dependence of our predictions to the matching scale μ_S, showing the importance of an explicit computation of the NLO corrections for the gluino contribution to the Wilson coefficients. This has been the subject of the present chapter, and our effort is summarized in fig. 5.8, where the reduction of the dependence from the matching scale is manifest. This conclude our theoretical study of the EDM of the Neutron, and we address to the conclusive chapter for a brief look to some possible developments and enlargements of our analysis.

6. FCG contribution to $\mathrm{B} \to \mathrm{X_s}\gamma$ at LO

In this chapter we address the calculation of the gluino-induced contributions to the decay $b \to s\gamma$ in the MSSM, generated by the flavour changing tree level vertices in eqs. (2.46-2.47). We give all the ingredient needed in the evaluation of the branching ratio $B \to X_s\gamma$ at the LO in the so-called Mass Insertion Approximation (MIA), introduced in sec. 2.3. We confirm the results of Borzumati et al. [BGHW00] obtained in the mass-eigenstate basis for the up and down-type squark mass matrix.

6.1. $\Delta\mathrm{B} = 1$ effective Hamiltonian

The application of the OPE techniques in B decays begins with the decoupling of the heavy degrees of freedom. In the SM these are the electroweak bosons and the top quark. The resulting effective Hamiltonian has the form

$$\mathcal{H}_{\rm eff}^{W} = -\frac{4G_F}{\sqrt{2}}\, V_{tb}V_{ts}^{*} \sum_{i=1}^{8} C_i(\mu) P_i(\mu) \ , \tag{6.1}$$

and contains the following set of flavour changing operators

$$\begin{aligned}
&P_1 = (\overline{s}\gamma^{\mu} T^a P_L c)\,(\overline{c}\gamma_{\mu} T^a P_L b) \quad , \quad P_2 = (\overline{s}\gamma^{\mu} c)\,(\overline{c}\gamma_{\mu} b) \ , \\
&P_3 = (\overline{s}\gamma^{\mu} b)\sum_q (\overline{q}\gamma_{\mu} q) \quad , \quad P_4 = (\overline{s}\gamma^{\mu} T^a b)\sum_q (\overline{q}\gamma_{\mu} T^a q) \ , \\
&P_5 = (\overline{s}\gamma^{\mu}\gamma^{\nu}\gamma^{\rho} P_L b)\sum_q (\overline{q}\gamma_{\mu}\gamma_{\nu}\gamma_{\rho} q) \quad , \quad P_6 = (\overline{s}\gamma^{\mu}\gamma^{\nu}\gamma^{\rho} T^a P_L b)\sum_q (\overline{q}\gamma_{\mu}\gamma_{\nu}\gamma_{\rho} T^a q) \ , \\
&P_7 = \frac{e}{16\pi^2} m_b\,(\overline{s}\sigma^{\mu\nu} P_R b)\, F_{\mu\nu} \quad , \quad P_8 = \frac{g_s}{16\pi^2} m_b\,(\overline{s}\sigma^{\mu\nu} P_R T^a b)\, G^a_{\mu\nu} \ ,
\end{aligned} \tag{6.2}$$

where $P_{R,L} = (1 \pm \gamma_5)/2$ are the chirality projectors used throughout this chapter. The choice of the Dirac structure of the operators $P_3 - P_6$ allow to safely choose a regularization scheme with a fully anticommuting γ_5 [CMM98]. Indeed, as usual, the CKM suppressed element $V_{ub}V_{us}^{*}$ has been neglected.

The contribution of the effective Hamiltonian in eq. (6.1) to $B \to X_s\gamma$ has been extensively studied in the last decade and it presently includes NLO perturbative QCD corrections as well as the leading non-perturbative and electroweak effects (see [Gam06] for a concise discussion and a complete list of references). The calculation of NNLO QCD

effects is currently under way [M$^+$06] and its expected to bring the theoretical accuracy to a level equal to that one expected at the B factories.

We just mention that it is more convenient to use the effective coefficients [BMMP94]

$$\begin{aligned} C_i^{eff} &= C_i \ , \qquad i = 1, ...6 \ , \\ C_7^{eff} &= C_7 + \sum_{i=1}^{6} y_i C_i \ , \quad C_8^{eff} = C_8 + \sum_{i=1}^{6} z_i C_i \ , \end{aligned} \tag{6.3}$$

where $y = (0, 0, -1/3, -4/9, -20/3, -80/9)$ and $z = (0, 0, 1, -1/6, 20, -10/3)$ are the NDR results for y_i and z_i, defined in such a way that the leading order matrix elements of the effective Hamiltonian for the transition $b \to s\gamma$ ($b \to sg$) is proportional to C_7^{eff} and C_8^{eff} only.

We just summarize the long established results [IL81] for the Wilson coefficients at the matching scale:

$$\begin{aligned} C_i^{(0)eff}(\mu_W) &= 0 \qquad i = 1, 3, 4, 5, 6 \ , \\ C_i^{(0)eff}(\mu_W) &= 1 \qquad i = 2 \ , \\ C_7^{(0)eff}(\mu_W) &= \frac{x(7 - 5x - 8x^2)}{24(x-1)^3} + \frac{x^2(3x-2)}{4(x-1)^4} \ln x \ , \\ C_8^{(0)eff}(\mu_W) &= \frac{x(2 + 5x - x^2)}{8(x-1)^3} - \frac{3x^2}{4(x-1)^4} \ln x \ , \end{aligned}$$

where $x = m_t^2/M_W^2$.

The evolution from the matching scale μ_W to a generic low-energy scale μ can be obtained as usual through the procedure described in section 3.3. At the LO accuracy the only term entering the branching ratio formula (see eq. (6.49) below) is [BMMP94]

$$C_7^{(0)eff}(\mu) = \eta^{\frac{16}{23}} C_7^{(0)eff}(\mu_W) + \frac{8}{3}(\eta^{\frac{14}{3}} - \eta^{\frac{14}{3}}) C_8^{(0)eff}(\mu_W) + \sum_{i=1}^{8} h_i \eta^{a_i} \ , \tag{6.4}$$

where $\eta = \alpha_s(M_W)/\alpha_s(\mu)$ and the scheme-independent magic numbers a_i and h_i are

$$\begin{aligned} a_i &= (\frac{14}{23}, \ \frac{16}{23}, \ \frac{6}{23}, \ -\frac{12}{23}, \ 0.4086, \ -0.4230, \ -0.8994, \ 0.1456) \ , \\ h_i &= (\frac{626126}{272277}, \ -\frac{56281}{51730}, \ \frac{3}{7}, \ -\frac{1}{14}, \ 0.6494, \ -0.0380, \ -0.0186, \ -0.0057) \ . \end{aligned} \tag{6.5}$$

Now we turn to analyze the effects of new physics on the radiative B decays. In the absence of new light degrees of freedom, physics beyond the SM manifests itself through (i) new contributions to coefficients of the operators involved in the SM (ii) the appearance of operators absent in the SM. (i) applies, for example, to the case of Two Higgs Doublet Models (THDM) [CDGG97], and to some supersymmetric scenarios with MFV [DGS06]. On the other hand, in left-right-symmetric models [CM94] and in presence of tree level FCG [BGHW00] additional operators with different chirality structures arise. The latter is the case we want to analyze in this chapter.

The effect of the matching of the supersymmetric strong particles must be added to the effective Hamiltonian as

$$\mathcal{H}_{\rm eff} = \mathcal{H}^W_{\rm eff} + \mathcal{H}^{\tilde{g}}_{\rm eff} \ , \tag{6.6}$$

$$\mathcal{H}^{\tilde{g}}_{\rm eff} = \sum_i C_{i,\tilde{g}}(\mu)\ O_{i,\tilde{g}}(\mu) + \sum_i \sum_q C^q_{i,\tilde{g}}(\mu)\ O^q_{i,\tilde{g}}(\mu) \ , \tag{6.7}$$

where the index q runs over all light quarks $q = u, d, cs, c, b$. The classification of the new operators can be found in [BGHW00] and reads (we follow the same notation)

- magnetic operators, with chirality violation coming from the b- or c- quark mass

$$\begin{aligned} Q_{7b,\tilde{g}} &= e g_s^2 m_b \left(\overline{s}\sigma^{\mu\nu}\ P_R b\right) F_{\mu\nu} \quad , \quad Q_{8b,\tilde{g}} = g_s^3 m_b \left(\overline{s}\sigma^{\mu\nu}\ P_R T^a b\right) G^a_{\mu\nu} \ , \\ Q_{7c,\tilde{g}} &= e g_s^2 m_c \left(\overline{s}\sigma^{\mu\nu}\ P_R b\right) F_{\mu\nu} \quad , \quad Q_{8c,\tilde{g}} = g_s^3 m_c \left(\overline{s}\sigma^{\mu\nu}\ P_R T^a b\right) G^a_{\mu\nu} \ , \end{aligned} \tag{6.8}$$

plus their primed counterparts $Q'_{7b,\tilde{g}}$ and $Q'_{8b,\tilde{g}}$ obtained by replacing $P_L \to P_R$.

- magnetic operators in which the gluino mass $m_{\tilde{g}}$ signals the chirality-violation

$$Q_{7\tilde{g},\tilde{g}} = e g_s^2 \left(\overline{s}\sigma^{\mu\nu}\ P_R b\right) F_{\mu\nu} \quad , \quad Q_{8\tilde{g},\tilde{g}} = g_s^3 \left(\overline{s}\sigma^{\mu\nu}\ P_R T^a b\right) G^a_{\mu\nu} \ , \tag{6.9}$$

plus $Q'_{7\tilde{g},\tilde{g}}$ and $Q'_{8\tilde{g},\tilde{g}}$ obtained by replacing $P_L \to P_R$.

- Vector Lorentz structure operators

$$\begin{aligned} Q^q_{11,\tilde{g}} &= g_s^4 \left(\overline{s}_\alpha \gamma_\mu P_L b_\alpha\right) \left(\overline{q}_\beta \gamma^\mu P_L q_\beta\right) \quad , \quad Q^q_{12,\tilde{g}} = g_s^4 \left(\overline{s}_\alpha \gamma_\mu P_L b_\beta\right) \left(\overline{q}_\beta \gamma^\mu P_L q_\alpha\right) \quad , \\ Q^q_{13,\tilde{g}} &= g_s^4 \left(\overline{s}_\alpha \gamma_\mu P_R b_\alpha\right) \left(\overline{q}_\beta \gamma^\mu P_R q_\beta\right) \quad , \quad Q^q_{14,\tilde{g}} = g_s^4 \left(\overline{s}_\alpha \gamma_\mu P_L b\right)_\beta \left(\overline{q}_\beta \gamma^\mu P_R q\right)_\alpha \ . \end{aligned} \tag{6.10}$$

plus $Q'_{11\tilde{g},\tilde{g}} - Q'_{14\tilde{g},\tilde{g}}$ obtained by replacing $P_L \to P_R$.

- Scalar and tensor Lorentz structure operators

$$\begin{aligned} Q^q_{15,\tilde{g}} &= g_s^4 \left(\overline{s}_\alpha P_R b_\alpha\right) \left(\overline{q}_\beta P_R q_\beta\right) \quad , \quad Q^q_{16,\tilde{g}} = g_s^4 \left(\overline{s}_\alpha P_R b_\beta\right) \left(\overline{q}_\beta P_R q_\alpha\right) , \\ Q^q_{17,\tilde{g}} &= g_s^4 \left(\overline{s}_\alpha P_R b_\alpha\right) \left(\overline{q}_\beta P_L q_\beta\right) \quad , \quad Q^q_{18,\tilde{g}} = g_s^4 \left(\overline{s}_\alpha P_R b_\alpha\right) \left(\overline{q}_\beta P_L q_\beta\right) , \\ Q^q_{19,\tilde{g}} &= g_s^4 \left(\overline{s}_\alpha \sigma_{\mu\nu} P_R b_\alpha\right) \left(\overline{q}_\beta \sigma^{\mu\nu} P_R q_\beta\right) \quad , \quad Q^q_{20,\tilde{g}} = g_s^4 \left(\overline{s}_\alpha \sigma_{\mu\nu} P_R b_\beta\right) \left(\overline{q}_\beta \sigma^{\mu\nu} P_R q_\alpha\right) \end{aligned} \tag{6.11}$$

plus $\tilde{Q}_{15\tilde{g},\tilde{g}} - \tilde{Q}_{20\tilde{g},\tilde{g}}$ obtained by replacing $P_L \to P_R$.

By inspection one finds that the eqs. (6.8-6.11) are a complete basis containing 12 magnetic and chromomagnetic and 5 times (one for each flavour q) 20 four-quark operators. In total 112 operators.

The larger number of operators in (6.8-6.11) with respect to SM operators in (6.2) comes from different chirality and dimensional behavior. The different chiralities are due to the fact that the gluino couples both to left- and right handed quarks and the associated squarks. In contrast, the W boson has only left-handed couplings and therefore right

handed fields only arise if their masses are not neglected. Usually only (chromo)magnetic operators with right-handed b-quarks are included. Similarly, the occurrence of five dim. operators with differing powers of the b and c quark mass can also be understood from the chirality structure of the FCG vertices in eqs. (2.46-2.47). Some of the new operators differ from the SM (chromo)magnetic operators only by an additional factor g_s^2. These were introduced as additional operators for practical reasons, as we explain in the next section.

6.2. Mixing of Operators with different dimensions

In sec. 3.2 we have briefly derived the master formulae relevant for the extraction of the ADM of a given effective Hamiltonian. Now, if we look at our observables of interest, an important remark is linked to the different canonical dimensions of the operators involved. This is a consequence of the fact that five and six operators appears in the effective Hamiltonian of the radiative B decays. In this respect, the following property is valid: the renormalization of an operator of a given dimension needs only operators as counter-terms of the same or lower dimension. The proof of this property is based essentially on dimensional analysis. It can be found on page 149 of the book by Collins [Col].

This means in particular that the magnetic penguin cannot mix into dimension six operators (6.10-6.11) and it is always possible to put to zero the connected entries of the ADM without performing any calculation. On the other hand, operator of dimension six can mix into (i) other six dimensional operators and (ii) five dimensional magnetic operators.

Another useful remarks is linked to the difference between (i) and (ii). We have seen that the RG evolution, governed by the ADM, allows to resum large logs of the form $L = \ln(\mu/\mu_0)$. Now, in the diagrams relevant for (i) the large logarithms L comes only from loops with gluons. This implies at least one factor of α_s for each large logarithm and the possibility of a RG evolution of the Wilson coefficients as described in section 3.4, and in particular using an ADM expanded as in eq. (3.18).

It turns out that in the case (ii) another possibility is at hand, namely the first large logarithm can arise without the exchange of gluons. This possibility has a concrete example already in the SM when one tries to calculate the amplitude of the decay $b \to s l\bar{l}$. In supersymmetric models these terms arise in the $b \to s\gamma$ case. To achieve technically the resummation of these terms, it has been suggested [Mis93, BGHW00] to choose a normalization of the operators that allows to proceed according to the standard method. This translate into the request for the powers of α_s in Z (see eq. (3.19)) to be equal to the number of loops of the contributing diagrams. We implement this request by adding one factor of α_s in the definition of the (chromo)magnetic operators and a factor α_s^2 in the definition of the four-quark operators. In particular, the one loop mixing of the operators Q_{11-20} with the operators Q_{7-8} appears formally at $O(\alpha_s)$.

We finally want to underline another important difference in determining the effective

Hamiltonian for $b \to s\gamma$ within and beyond the SM. With the redefinition discussed above one immediately sees that the Wilson coefficients have a perturbative expansion starting from $O(\alpha_s^0)$. The calculation of the matrix elements however, must be different to take into account the fact that the amplitude generated by H_{eff}^W and $H_{eff}^{\tilde{g}}$ differs for an overall α_s factor. In the SM it must be performed at $O(\alpha_s^0)$ and $O(\alpha_s)$ at the LO and NLO precision. We just mention that either five or six dimensions operators enters the LO matrix elements, even if, as already noticed, it is possible to define effective coefficients such that only the five operators has a non-null on-shell matrix element. On the other hand, the FCG contribution to $b \to s\gamma$ requires a similar calculation to $O(\alpha_s)$ and $O(\alpha_s^2)$ at the LO and NLO precision and in this case only five-dimension operators naturally enters to LO precision.

Finally, with this organization of the effective Hamiltonian, the SM and SUSY undergo separate renormalization and can be studied separately.

6.3. Magic Numbers for $B \to X_s\gamma$

Turning back to eq. (6.7), we have seen that it contains 112 operators. Therefore the ADM matrix γ_{ij} is a 112×112 matrix. However, this huge matrix is formed by not communicating sub-blocks. In order to identify them we first not that the primed and non-primed operators do not mix under QCD renormalization. This reduces the problem to the evaluation of two identical 56×56 matrices. Moreover, given their proportionality to $m_{\tilde{g}}$, the dimension-five operators $O_{7\tilde{g},\tilde{g}},\ O_{8\tilde{g},\tilde{g}}$ and their primed counterparts do not mix with dimension-six operators. The 4×4 submatrix for these operators is a block-diagonal matrix with 2×2 blocks. The block corresponding to $O_{7\tilde{g},\tilde{g}},\ O_{8\tilde{g},\tilde{g}}$ is

$$\gamma_{ij,\tilde{g}} = \begin{pmatrix} 2C_F + \frac{22}{3}N_c - \frac{4}{3}n_f & 0 \\ 8C_F Q_d & \frac{25}{3}N_c - \frac{5}{N_c} - \frac{4}{3}n_f \end{pmatrix} \tag{6.12}$$

and differs from the known [CFM+93] ADM of the SM operators P_7 and P_8 in eq. (6.2) just by anomalous dimension of the explicit mass m_b and of the coupling g_s^2 in the definition of the operators (see eq. (6.9)). This matrix checks with formula (37) of ref. [BGHW00], after one specialize it to $n_f = 5$.

Applying the standard integration procedure for the RG equation described in section 3.2, we parameterize the evolution between μ_S and $\mu_b \sim m_b$ via the magic numbers, in analogy with the analysis we have already presented for the EDM of the Neutron

$$C_{i\tilde{g},\tilde{g}}^{(0)}(\mu_b) = \sum_{j=7}^{8} \sum_{a,b=1}^{2} X_{ij}^{ab} \alpha_s(\mu_S)^{Y_a} \eta^{Z_b} C_{j\tilde{g},\tilde{g}}^{(0)}(\mu_S)\,, \tag{6.13}$$

with Y_a and Z_b given by:

$$Y_a = \left\{ \frac{8}{125}, \frac{16}{125} \right\}\ ,\ Z_b = \left\{ \frac{27}{25}, \frac{29}{25} \right\} \tag{6.14}$$

and the nonvanishing entries in X_{ij}^{ab} are given below:

$$X_{77}^{22} = 1.0592 \ , \ X_{78}^{11} = 2.7444 \ , \ X_{78}^{22} = -2.8245 \ , \ X_{88}^{11} = 1.0292 \ . \tag{6.15}$$

In general, the structure of the remaining 54×54 matrix, corresponding to the four-quark operators $Q_{i,\tilde{g}}^q$ $(i = 11, ..., 20; q = u, d, c, s, b)$, magnetic operators $O_{7b,\tilde{g}}$ and chromomagnetic operators $O_{8b,\tilde{g}}$ is rather complicated. The fact that the LO formula for the Branching Ratio (see eq. (6.49)) only contains the coefficients $C_{7b,\tilde{g}}$ and $C_{7c,\tilde{g}}$, evaluated at the low scale μ_b, simplifies the analysis. Among the four-quark operators, only those with scalar/tensor Lorentz structure, $O_{i,\tilde{g}}^q$ $(i = 15, ..., 20)$, mix into the magnetic and chromomagnetic operators at $O(\alpha_s)$. The vector operators $O_{i,\tilde{g}}^q$ $(i = 11, ..., 14)$ on the other hand mix neither into the magnetic and chromomagnetic operators nor into the scalar/tensor four quark operators. This implies that the presence of the four-quark operators with vector structure is completely irrelevant for the evolution of the coefficients of the magnetic operators. The observation that the scalar/tensor operators with the label q mix into $O_{7q,\tilde{g}}$ and $O_{8q,\tilde{g}}$, with the same q, together with the fact that scalar/tensor operators mix along themselves in a flavour-diagonal way, further simplify the situation. It is indeed possible to restrict the problem at the LO level to the calculation of two 8×8 matrices corresponding to the following basis:

$$\left\{O_{15,\tilde{g}}^q, \ O_{16,\tilde{g}}^q, \ O_{17,\tilde{g}}^q, \ O_{18,\tilde{g}}^q, \ O_{19,\tilde{g}}^q, \ O_{20,\tilde{g}}^q, \ O_{7q,\tilde{g}}, \ O_{8q,\tilde{g}}\right\} \quad , \quad q = b, c \ . \tag{6.16}$$

For the case $q = b$, the result for the ADM is the following

$$\gamma_{ij,\tilde{g}} = \begin{pmatrix} \gamma_r & \vec{\beta}_7^b & \vec{\beta}_8^b \\ \vec{0}^T & \gamma_{77} & 0 \\ \vec{0}^T & \gamma_{87} & \gamma_{88} \end{pmatrix} \ , \tag{6.17}$$

where the various entries are given by

$$\gamma_r = \begin{pmatrix} \frac{6}{N_c} + \frac{26}{3}N_c & 0 & 0 & 0 & \frac{1}{N_c} & -1 \\ -6 & \frac{6}{N_c} + \frac{44}{3}N_c & 0 & 0 & -\frac{1}{2} & \frac{1}{N_c} - \frac{N_c}{2} \\ 0 & 0 & \frac{6}{N_c} + \frac{26}{3}N_c & 0 & 0 & 0 \\ 0 & 0 & -6 & \frac{6}{N_c} + \frac{44}{3}N_c & 0 & 0 \\ \frac{48}{N_c} & -48 & 0 & 0 & \frac{50}{3}N_c - \frac{2}{N_c} & 0 \\ -24 & \frac{48}{N_c} - 24N_c & 0 & 0 & 6 & \frac{32}{3}N_c - \frac{2}{N_c} \end{pmatrix} - \frac{8}{3}n_f\hat{1} \ ,$$

$$\gamma_{77} = 8C_F + \frac{22}{3}N_c - \frac{4}{3}n_f \ , \ \gamma_{87} = 8C_F Q_d \ , \ \gamma_{88} = \frac{34}{3}N_c - \frac{8}{N} - \frac{4}{3}n_f \ ,$$

$$\vec{\beta}_7^b = Q_d\,(1, N_c, 0, 0, -4 - 8N_c, -4N_c - 8) \ , \ \vec{\beta}_8^b = (1, 0, 0, 0, -4, -8) \ , \tag{6.18}$$

while the case $q = c$ differs from the previous one in the submatrix responsible for mixing of the four-quark operators into the magnetic and chromomagnetic ones:

$$\vec{\beta}_7^c = Q_u\,(0, 0, 0, 0, -8N_c, -8) \ , \ \vec{\beta}_8^c = (0, 0, 0, 0, 0, -8) \ . \tag{6.19}$$

$X^{3,2}_{b,71}$	0.63563	$X^{4,3}_{b,71}$	-0.56175	$X^{7,3}_{b,71}$	-0.17712	$X^{8,2}_{b,71}$	0.37021
$X^{10,6}_{b,71}$	-0.26985	$X^{12,8}_{b,71}$	-0.0054636	$X^{15,3}_{b,71}$	-0.011676	$X^{16,2}_{b,71}$	0.0045594
$X^{3,2}_{b,72}$	-0.22109	$X^{4,3}_{b,72}$	0.3039	$X^{7,3}_{b,72}$	0.046421	$X^{8,2}_{b,72}$	-0.097029
$X^{10,6}_{b,72}$	0.070725	$X^{12,8}_{b,72}$	-0.083386	$X^{15,3}_{b,72}$	-0.1782	$X^{16,2}_{b,72}$	0.069585
$X^{3,2}_{b,75}$	-0.77381	$X^{4,3}_{b,75}$	-0.18418	$X^{7,3}_{b,75}$	0.33711	$X^{8,2}_{b,75}$	-0.70463
$X^{10,6}_{b,75}$	0.51361	$X^{12,8}_{b,75}$	0.68894	$X^{15,3}_{b,75}$	1.4723	$X^{16,2}_{b,75}$	-0.57492
$X^{3,2}_{b,76}$	-4.2007	$X^{4,3}_{b,76}$	3.2784	$X^{7,3}_{b,76}$	1.2313	$X^{8,2}_{b,76}$	-2.5736
$X^{10,6}_{b,76}$	1.8759	$X^{12,8}_{b,76}$	0.37725	$X^{15,3}_{b,76}$	0.80619	$X^{16,2}_{b,76}$	-0.31482
$X^{4,3}_{b,77}$	1.2586	$X^{3,2}_{b,78}$	3.2611	$X^{4,3}_{b,78}$	-3.3562		
$X^{3,2}_{b,81}$	0.23836	$X^{8,2}_{b,81}$	0.13883	$X^{10,6}_{b,81}$	-0.33961	$X^{12,8}_{b,81}$	0.0011667
$X^{3,2}_{b,82}$	-0.082909	$X^{8,2}_{b,82}$	-0.036386	$X^{10,6}_{b,82}$	0.089006	$X^{12,8}_{b,82}$	0.017806
$X^{3,2}_{b,85}$	-0.29018	$X^{8,2}_{b,85}$	-0.26424	$X^{10,6}_{b,85}$	0.64637	$X^{12,8}_{b,85}$	-0.14712
$X^{3,2}_{b,86}$	-1.5753	$X^{8,2}_{b,86}$	-0.9651	$X^{10,6}_{b,86}$	2.3608	$X^{12,8}_{b,86}$	-0.080559
$X^{3,2}_{b,88}$	1.2229						

Table 6.1: Magic numbers $X^{k,l}_{b,ij}$ for the evolution from six to four flavours.

The 6×6 submatrix for the four-quark operators can be gleaned from ref. [BMU00], taking care about the different normalization of the operators and the different definition of the $\sigma^{\mu\nu} \otimes \sigma_{\mu\nu}$ Dirac structure.

The Wilson coefficients of the dimension six operators $C_{7b,\tilde{g}}$ and $C_{8b,\tilde{g}}$ at the low scale are given by

$$C^{(0)}_{ib,\tilde{g}}(\mu_H) = \sum_{j=1}^{8}\sum_{k=1}^{16}\sum_{l=1}^{8} X^{k,l}_{b,ij}\alpha_s(\mu_S)^{Y_k}\eta^{Z_l}C^{(0)}_j(\mu_S)\,, \quad i = 7,8 \tag{6.20}$$

where the index j runs over the Wilson coefficients corresponding to the operators of eq. (6.16), and with Y_k and Z_l given by:

$$\begin{aligned} Y_k = \Bigg\{ & -\frac{32}{175}, \frac{4}{175}, \frac{8}{75}, \frac{64}{525}, \frac{-236-25\sqrt{241}}{525}, \frac{-194-25\sqrt{241}}{525}, \frac{214-25\sqrt{241})}{525}, \frac{256-25\sqrt{241}}{525}, \\ & \frac{-4(17+\sqrt{241})}{525}, \frac{4(1-\sqrt{241})}{525}, \frac{4(-17+\sqrt{241})}{525}, \frac{4(1+\sqrt{241})}{525} \\ & \frac{-236+25\sqrt{241}}{525}, \frac{-194+25\sqrt{241}}{525}, \frac{214+25\sqrt{241}}{525}, \frac{256\sqrt{241}}{525} \Bigg\} \end{aligned} \tag{6.21}$$

$$Z_l = \left\{ \frac{26}{25}, \frac{39}{25}, \frac{41}{25}, \frac{53}{25}, \frac{33-\sqrt{241}}{525}, \frac{51-\sqrt{241}}{525}, \frac{33+\sqrt{241}}{525}, \frac{51+\sqrt{241}}{525} \right\} \tag{6.22}$$

and the non vanishing entries in $X^{k,l}_{b,ij}$ are listed in tables (6.1).

$X^{3,2}_{c,71}$	0.12701	$X^{4,3}_{c,71}$	0.15798	$X^{5,3}_{c,71}$	0.0015923	$X^{6,2}_{c,71}$	−0.0022584
$X^{7,3}_{c,71}$	−0.064313	$X^{8,2}_{c,71}$	0.18511	$X^{9,5}_{c,71}$	0.0086213	$X^{10,6}_{c,71}$	−0.22196
$X^{11,7}_{c,71}$	−0.061025	$X^{12,8}_{c,71}$	0.0050979	$X^{13,3}_{c,71}$	−0.19544	$X^{14,2}_{c,71}$	0.054212
$X^{15,3}_{c,71}$	0.0048233	$X^{16,2}_{c,71}$	0.0022797	$X^{3,2}_{c,72}$	−0.45747	$X^{4,3}_{c,72}$	1.0223
$X^{5,3}_{c,72}$	0.0008719	$X^{6,2}_{c,72}$	−0.0012366	$X^{7,3}_{c,72}$	0.016856	$X^{8,2}_{c,72}$	−0.048514
$X^{9,5}_{c,72}$	0.0047209	$X^{10,6}_{c,72}$	0.058173	$X^{11,7}_{c,72}$	−0.22289	$X^{12,8}_{c,72}$	0.077805
$X^{13,3}_{c,72}$	−0.71384	$X^{14,2}_{c,72}$	0.19801	$X^{15,3}_{c,72}$	0.073614	$X^{16,2}_{c,72}$	0.034793
$X^{3,2}_{c,75}$	−2.3991	$X^{4,3}_{c,75}$	7.6938	$X^{5,3}_{c,75}$	0.00060611	$X^{6,2}_{c,75}$	−0.00085967
$X^{7,3}_{c,75}$	0.12241	$X^{8,2}_{c,75}$	−0.35232	$X^{9,5}_{c,75}$	0.0032818	$X^{10,6}_{c,75}$	0.42246
$X^{11,7}_{c,75}$	−1.539	$X^{12,8}_{c,75}$	−0.64283	$X^{13,3}_{c,75}$	−4.9289	$X^{14,2}_{c,75}$	1.3672
$X^{15,3}_{c,75}$	−0.6082	$X^{16,2}_{c,75}$	−0.28746	$X^{3,2}_{c,76}$	−2.2391	$X^{4,3}_{c,76}$	0.56355
$X^{5,3}_{c,76}$	0.0092506	$X^{6,2}_{c,76}$	−0.01312	$X^{7,3}_{c,76}$	0.44708	$X^{8,2}_{c,76}$	−1.2868
$X^{9,5}_{c,76}$	0.050087	$X^{10,6}_{c,76}$	1.543	$X^{11,7}_{c,76}$	0.40335	$X^{12,8}_{c,76}$	−0.352
$X^{13,3}_{c,76}$	1.2918	$X^{14,2}_{c,76}$	−0.35832	$X^{15,3}_{c,76}$	−0.33304	$X^{16,2}_{c,76}$	−0.15741
$X^{4,3}_{c,77}$	1.2586	$X^{3,2}_{c,78}$	3.2611	$X^{4,3}_{c,78}$	−3.3562		
$X^{3,2}_{c,81}$	0.047628	$X^{6,2}_{c,81}$	−0.00084689	$X^{8,2}_{c,81}$	0.069415	$X^{9,5}_{c,81}$	0.025683
$X^{10,6}_{c,81}$	−0.1698	$X^{11,7}_{c,81}$	0.013597	$X^{12,8}_{c,81}$	0.00058335	$X^{3,2}_{c,82}$	−0.17155
$X^{6,2}_{c,82}$	−0.00046374	$X^{8,2}_{c,82}$	−0.018193	$X^{9,5}_{c,82}$	0.014064	$X^{10,6}_{c,82}$	0.044503
$X^{11,7}_{c,82}$	0.049661	$X^{12,8}_{c,82}$	0.0089032	$X^{3,2}_{c,85}$	−0.89965	$X^{6,2}_{c,85}$	−0.00032238
$X^{8,2}_{c,85}$	−0.13212	$X^{9,5}_{c,85}$	0.0097766	$X^{10,6}_{c,85}$	0.32319	$X^{11,7}_{c,85}$	0.3429
$X^{12,8}_{c,85}$	−0.073559	$X^{3,2}_{c,86}$	−0.83967	$X^{6,2}_{c,86}$	−0.0049202	$X^{8,2}_{c,86}$	−0.48255
$X^{9,5}_{c,86}$	0.14921	$X^{10,6}_{c,86}$	1.1804	$X^{11,7}_{c,86}$	−0.089869	$X^{12,8}_{c,86}$	−0.04028
$X^{3,2}_{c,88}$	1.2229						

Table 6.2: Magic numbers $X^{k,l}_{c,ij}$ for the evolution from six to four flavours.

The coefficients $C_{7c,\tilde{g}}$ and $C_{8c,\tilde{g}}$ formally have the same expression as $C_{7b,\tilde{g}}$ and $C_{8b,\tilde{g}}$, when the indices $7b$ and $8b$ are replaced by $7c$ and $8c$

$$C^{(0)}_{ic,\tilde{g}}(\mu_H) = \sum_{j=1}^{8}\sum_{k=1}^{16}\sum_{l=1}^{8} X^{k,l}_{c,ij}\alpha_s(\mu_S)^{Y_k}\eta^{Z_l}C^{(0)}_j(\mu_S)\,, \quad i = 7,8 \tag{6.23}$$

and the non vanishing entries in $X^{k,l}_{c,ij}$ are listed in tables (6.2).

Notice that in tables 6.1-6.2 there is no entries with $j = 3, 4$. This is due to the fact that the two operators $O^q_{17,\tilde{g}}$ and $O^q_{18,\tilde{g}}$ do not mix with the remaining ones in eq. (6.16), as it manifest by looking at the corresponding entries of the matrix on the first row of eq. (6.18).

This concludes the list of the formulae that are necessary to consistently provide a leading order resummation of the large log logarithms for the effective Hamiltonian in eq. (6.7). In the next section we turn to the calculation of the Wilson coefficients.

6.4. Wilson coefficients at the μ_S scale

We give here a step-by-step presentation of the LO result for the various Wilson coefficients arising from the virtual exchange of gluinos at the matching scale. Among the diagrams contributing to the operator basis (6.7) it is possible to distinguish three different classes: triangular, box diagrams and penguin topologies. In the case of gluino-mediated processes, these contributions are of the same order, After the reorganization of the perturbative expansion discussed in section 6.2., and therefore must be included in the analysis. Since the strategy to match the full theory into the effective one is different for the abovementionated classes, we will treat them separately, emphasizing the various steps and commenting on each of them.

Magnetic diagrams

The off-shell basis operator basis relevant for this calculation is

$$
\begin{aligned}
Q_{7b,\tilde{g}} &= \frac{e g_s^2}{16\pi^2} m_b \, (\overline{s}\sigma^{\mu\nu} \; P_R b) \, F_{\mu\nu} \; , \\
Q_{7\tilde{g},\tilde{g}} &= \frac{e g_s^2}{16\pi^2} \, (\overline{s}\sigma^{\mu\nu} \; P_R b) \, F_{\mu\nu} \; , \\
Q_{8b,\tilde{g}} &= \frac{g_s^3}{16\pi^2} m_b \, (\overline{s}\sigma^{\mu\nu} \; P_R T^a b) \, G^a_{\mu\nu} \; , \\
Q_{8\tilde{g},\tilde{g}} &= \frac{g_s^3}{16\pi^2} \, (\overline{s}\sigma^{\mu\nu} \; P_R T^a b) \, G^a_{\mu\nu} \; , \\
Q_{9,\tilde{g}} &= \frac{i g_s^2}{16\pi^2} \, (\overline{s} \not{D} \not{D} \not{D} \; P_R b) \; , \\
Q_{10,\tilde{g}} &= \frac{i e g_s^2}{16\pi^2} \overline{s} \, \{\not{D}, \sigma^{\mu\nu} F_{\mu\nu}\} \; P_R b \; , \\
Q_{11,\tilde{g}} &= \frac{e g_s^2}{16\pi^2} \overline{s} \; \gamma_\nu \; P_R b \; D_\mu F^{\mu\nu} \; , \\
Q_{12b,\tilde{g}} &= \frac{g_s^2}{16\pi^2} m_b \, (\overline{s} \not{D} \not{D} \; P_R b) \; , \\
Q_{12\tilde{g},\tilde{g}} &= \frac{g_s^2}{16\pi^2} \, (\overline{s} \not{D} \not{D} \; P_R b) \; , \\
Q_{13,\tilde{g}} &= \frac{i g_s^3}{16\pi^2} \overline{s} \, \{\not{D}, \sigma^{\mu\nu} t^a G^a_{\mu\nu}\} \; P_R b \; , \\
Q_{14,\tilde{g}} &= \frac{g_s^3}{16\pi^2} \overline{s} \; \gamma_\nu \; t^a \; P_R b \; D_\mu G^a_{\mu\nu} \; ,
\end{aligned}
\tag{6.24}
$$

where D_μ is the $SU(3)_c \times U(1)_{\rm em}$ covariant derivative. Notice that i) on-shell $Q_{9,\tilde{g}}, ..., Q_{14,\tilde{g}}$ are no longer independent operators and, by applying the equations of motions, they can be written as linear combinations of the other operators in eq. (6.7). ii) Dimension five

Figure 6.1: Diagrams contributing to the magnetic operators: in the MIA limit the first one contribute to $O_{7b,\tilde{g}}$ through a flavour-violating scalar term, while the second match with $O_{7\tilde{g},\tilde{g}}$ through a flavour and chirality- violating scalar term.

operators in eq. (6.24) do not arise if the only source of flavour violation is the CKM matrix, and are a consequence of the tree-level FCG interactions.

The diagrams arising from a single gluino exchange are represented in fig. 6.1. The strategy adopted for the extraction of the Wilson coefficients it is analogous to that one used for the Neutron EDM. First, we have derived the Feynman rules for the operators in eq. (6.24). The latter can be put in a one-to-one correspondence to the form factors of the general $b \to s\gamma$ and $b \to sg$ vertex [SW90]. Consequently, it is possible to work out the contribution of a given operator as a linear combination of the form factors, calculated following the same strategy of section 4.5. In particular, we have adopted the same kinematical configuration.

The presence of the Z_D matrices, connecting the down squark basis of the mass eigenstates used in our calculation to the flavour diagonal basis (see eq. (2.43)) is removed by performing the MIA limit, as described in detail in appendix A. In particular, the LO magnetic diagrams give rise to a loop function depending on only one squark mass (there is just one squark propagator). Such loop function gets multiplied by one Z_D's and one $Z_D^\dagger$'s. Consequently the MIA limit can be performed by using formula (A.4).

The result obtained must be finally multiplied by an overall factor $(+i)$ to take care of the fact that

$$A_{\text{full}} = \langle i\mathcal{L} \rangle = -\langle i\mathcal{H}_{\text{eff}} \rangle \ . \tag{6.25}$$

After this manipulation our final result read

$$\begin{aligned}
C_{7b,\tilde{g}}(\mu_S) &= 0 \ , \\
C_{7\tilde{g},\tilde{g}}(\mu_S) &= \frac{Q_d}{16\pi^2}\frac{M_{\tilde{g}}}{M_s^2}\frac{4}{3}(\delta_{LR})_{sb}F_4(x) \ , \\
C_{8b,\tilde{g}}(\mu_S) &= 0 \ , \\
C_{8\tilde{g},\tilde{g}}(\mu_S) &= \frac{1}{16\pi^2}\frac{M_{\tilde{g}}}{M_s^2}(\delta_{LR})_{sb}\left[-\frac{1}{6}F_4(x) - \frac{3}{2}F_3(x)\right] \ , \\
C_{9,\tilde{g}}(\mu_S) &= \frac{1}{16\pi^2}\frac{16}{3}(\delta_{LL})_{sb}F_2(x) \ ,
\end{aligned}$$

$$
\begin{aligned}
C_{10,\tilde{g}}(\mu_S) &= -\frac{Q_d}{16\pi^2 M_s^2}\frac{4}{3}(\delta_{LL})_{sb}F_2(x) \ , \\
C_{11,\tilde{g}}(\mu_S) &= \frac{Q_d}{16\pi^2}\frac{4}{3}(\delta_{LL})_{sb}F_5(x) \ , \\
C_{12b,\tilde{g}}(\mu_S) &= 0 \ , \\
C_{12\tilde{g},\tilde{g}}(\mu_S) &= -\frac{1}{16\pi^2}\frac{8}{3}\frac{M_{\tilde{g}}}{M_s^2}(\delta_{LR})_{sb}F_4(x) \ , \\
C_{13,\tilde{g}}(\mu_S) &= -\frac{1}{16\pi^2 M_s^2}(\delta_{LL})_{sb}\left[-\frac{1}{6}F_2(x) - \frac{3}{2}F_1(x)\right] \ , \\
C_{14,\tilde{g}}(\mu_S) &= \frac{1}{16\pi^2 M_s^2}(\delta_{LL})_{sb}\left[-\frac{1}{6}F_5(x) - \frac{3}{2}F_6(x)\right] \ ,
\end{aligned}
\tag{6.26}
$$

where we have defined the dimensionless mass parameter $x = M_{\tilde{g}}^2/M_s^2$ and M_s indicates the average squark mass, introduced in eq. (2.49) as $\overline{M}$. The Wilson coefficients of the corresponding primed operators are obtained through the interchange $L \leftrightarrow R$ in eq. (6.26). The functions $F_i(x)$ which result from the calculation are given in appendix C. Note that there is not explicit dependence of the matching scale μ_S in these functions. However there is an implicit μ_S-dependence via the gluino and squark masses which has to be specified when going beyond the leading calculation presented here.

Then we can derive the on-shell magnetic operators using the EOM

$$
\begin{aligned}
C_{7b,\tilde{g}}^{OS} &= C_{7b,\tilde{g}} + C_{10,\tilde{g}} \ , \\
C_{8b,\tilde{g}}^{OS} &= C_{8b,\tilde{g}} + C_{13,\tilde{g}} \ ,
\end{aligned}
\tag{6.27}
$$

$C_{7b,\tilde{g}}^{OS}$ and $C_{8b,\tilde{g}}^{OS}$ being the coefficients of the on-shell magnetic and chromo-magnetic dipole operators respectively. Given the results in eq. (6.26) we note that it is necessary to use the EOM to project on the physical on-shell basis, since $Q_{7b,\tilde{g}}$ and $Q_{8b,\tilde{g}}$ do not arise in the off-shell effective theory.

We finally observe that the coefficients of the magnetic and chromo-magnetic operators proportional to the c-quark mass, obtained by the mixing of six into five operators discussed in sec. (6.2) vanish at the matching scale at the lowest order in α_s.

Penguin diagrams

Penguin diagram mediated by the virtual exchange of a gluino and a gluon is shown in fig. (6.2) below.

First we note that diagrams (6.2) cannot be calculated with zero momentum external states, because of the gluon propagator in between. So we can suppose the b and s external quark carry a momentum p and r respectively. Then, even without explicit calculation, the effective vertex b-s-g can be written in a form complying with gauge invariance, Lorentz covariance and proper mass dimension as

$$
\Gamma^\mu = F_1(q^2)m_f i\sigma^{\mu\nu}q_\nu + F_2(q^2)(q^2 g^{\mu\nu} - q^\mu q^\nu)\gamma_\nu \ ,
\tag{6.28}
$$

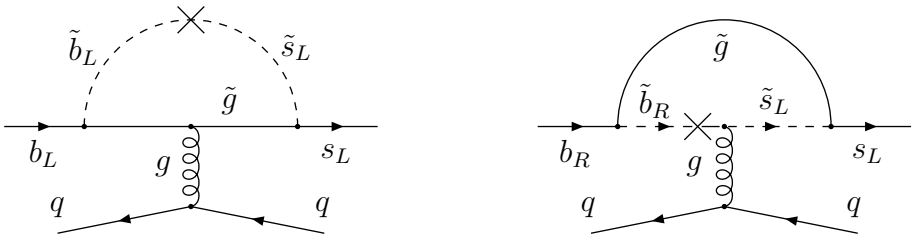

Figure 6.2: Feynman diagrams contributing to the vector operators in eq. (6.10).

where $q = p - r$ is the gluon momentum. The first term, proportional to m_f and signaling an helicity flip in the given fermion line, play a role in the exclusive hadronic decays (for an exhaustive MSSM penguin diagrams analysis see ref. [ACW98]). On the other hand, the second term, when contracted with the gluon propagator and the low quark pair line, give rise to the operators $Q^q_{11,\tilde{g}} - Q^q_{14,\tilde{g}}$ in eq. (6.10) and their corresponding primed counterparts. We obtain in the MIA approximation the following coefficients

$$
\begin{aligned}
C^q_{11,\tilde{g}}(\mu_S) &= \frac{1}{16\pi^2 M_s^2}(\delta_{LL})_{sb}\frac{1}{3}\left[-\frac{1}{6}F_8(x) + \frac{3}{2}F_7(x)\right] \ , \\
C^q_{12,\tilde{g}}(\mu_S) &= -\frac{1}{16\pi^2 M_s^2}(\delta_{LL})_{sb}\left[-\frac{1}{6}F_8(x) + \frac{3}{2}F_7(x)\right] \ , \\
C^q_{13,\tilde{g}}(\mu_S) &= C^q_{11,\tilde{g}}(\mu_S) \ , \\
C^q_{14,\tilde{g}}(\mu_S) &= C^q_{12,\tilde{g}}(\mu_S) \ ,
\end{aligned}
$$

where $x = M^2_{\tilde{g}}/M^2_s$ and the replacement $L \to R$ allows to obtain the primed results.
As dictated by the Ward identities, either the infinities or the finite parts in the limit $q \to 0$ cancel out in the sum of diagrams in fig. 6.2.

Box diagrams

Our amplitude of interest is made up of four box diagrams with exchange of two virtual gluinos

$$
\begin{aligned}
A_{\text{full}} = \quad & A_1 + A_2 \\
& + B_1 + B_2 \ .
\end{aligned}
\tag{6.29}
$$

These diagrams are represented in fig. 6.3. Looking at fig. 6.3, it should be noted that B-type diagrams can be obtained from the corresponding A-type ones by simply inverting the endpoints of the two gluino lines attached to one chosen squark line, without inverting the squark line as well (otherwise one would obviously end up with a topologically equivalent diagram). So it is evident that, while for quark-gluino-quark lines of A-type diagrams one can unambiguously fix a fermion flow as parallel to that of the quark propagators, the same cannot be done for B-type diagrams. In the latter case, in fact, the quark arrows

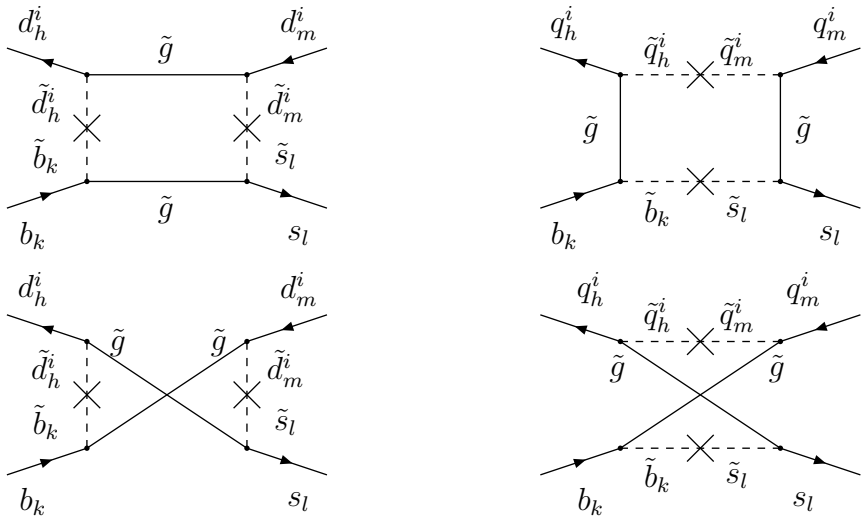

Figure 6.3: Feynman diagrams for A and B type boxes in the first and second row, respectively. A cross indicates a mass insertion and the indices h, k, l, m label the quark and squark chiralities. The index i run over all the quarks for q^i while $d^i = d, s, b$. Moreover d^i is equal to b or s if a single flavour violation is allowed in the squark lines.

in any of the two quark-gluino-quark lines are antiparallel. An unambiguous way to cope with this difficulty, related to interactions involving Majorana fermions, is reported in ref. [DEHK92]. The recipe is as follows

- Fix arbitrarily the fermion flow along any fermion line.
- Suppose such fermion flow encounters a vertex whence a quark line having antiparallel arrow originates. Then use the charge-conjugated vertex, whose quark line has the arrow in the reverse direction.

Before collecting the expressions for all the four inserted amplitudes, some general remarks are in order.

The amplitude of all the diagrams entering our calculation has the structure

$$\text{diagram} \sim \left[\overline{S}_1 \text{ (fermion line 1) } S_2\right] \left[\overline{S}_3 \text{ (fermion line 2) } S_4\right] \tag{6.30}$$

where $S_i, i = 1, ..., 4$ are spinors for the external particles and the sign of proportionality indicates that an overall constant factor was omitted. Henceforth we will indicate as "spinor sequence" the following object

$$\text{spinor sequence} = (\overline{S}_1 S_2)(\overline{S}_3 S_4) \ , \tag{6.31}$$

with reference to the above diagram structure. The quantities to simplify are of course the two fermion lines, via gamma matrix reduction and color contraction; in addition one has to perform the integration in the loop variable. The final form for each diagram will be written in terms of the product (fermion line 1) $\otimes$ (fermion line 2), with the corresponding

spinor sequence indicated as in (6.31).
Now we can write down the 4 LO amplitudes, for A- and B-type diagrams separately. We collect in each diagram a common factor $C_q^{(1)}$ or $C_q^{(2)}$, namely

$$C_l^{(1)} = 4g_s^4 \frac{M_s^2}{(l^2 - M_{\tilde{g}}^2)^2 (l^2 - M_s^2)^3} ,$$
$$C_l^{(2)} = 4g_s^4 \frac{M_s^4}{(l^2 - M_{\tilde{g}}^2)^2 (l^2 - M_s^2)^4} , \tag{6.32}$$

where the superscript (i) indicate the total number of mass insertions in the squark lines, obtained by application of eqs. (A.4) and (A.5), respectively. Moreover, l is the momentum of integration and we have considered external quarks with zero momenta and massless. The factor 4 comes from the corresponding factor $\sqrt{2}$ hidden inside the FCG vertices (see eqs. 2.46-2.47).

A-type diagrams

$$\begin{aligned} A_1 = C_{\text{color,A}_1} \Big\{ & C_l^{d^i} \left((\delta_{LL})_{sd^i} (\delta_{LL})_{d^i b} \not{q}_L \otimes \not{q}_L + (\delta_{RR})_{sd^i} (\delta_{RR})_{d^i b} \not{q}_R \otimes \not{q}_R \right) \\ & + C_l^{(2)} \left((\delta_{LR})_{sd^i} (\delta_{RL})_{d^i b} \not{q}_L \otimes \not{q}_R + (\delta_{RL})_{sd^i} (\delta_{LR})_{d^i b} \not{q}_R \otimes \not{q}_L \right) \\ & + M_{\tilde{g}}^2 \Big[C_l^{(2)} \left((\delta_{RL})_{sd^i} (\delta_{RL})_{d^i b} P_L \otimes P_L + (\delta_{LR})_{sd^i} (\delta_{LR})_{d^i b} P_R \otimes P_R \right) \\ & + C_l^{d^i} \left((\delta_{LL})_{sd^i} (\delta_{RR})_{d^i b} P_R \otimes P_L + (\delta_{RR})_{sd^i} (\delta_{LL})_{d^i b} P_L \otimes P_R \right) \Big] \Big\} , \\ C_{\text{color,A}_1} = & \frac{1}{36} \delta_{c_2 c_3} \, \delta_{c_1 c_4} + \frac{7}{12} \delta_{c_1 c_2} \, \delta_{c_3 c_4} , \\ & \text{spinor sequence :} \quad (\bar{\text{s}}_{\text{c}_1}(\text{k}_1) \; \text{b}_{\text{c}_2}(\text{p}_1)) \; (\bar{\text{d}}^{\text{i}}_{\text{c}_3}(\text{p}_2) \; \text{d}^{\text{i}}_{\text{c}_4}(\text{k}_2)) , \end{aligned} \tag{6.33}$$

and

$$\begin{aligned} A_2 = -C_{\text{color,A}_2} \Big\{ & C_l^{(1)} \left((\delta_{LL})_{sb} \not{q}_L \otimes \not{q}_L + (\delta_{RR})_{sb} \not{q}_R \otimes \not{q}_R \right) \\ & + C_l^{(2)} \left((\delta_{LR})_{sb} (\delta_{RL})_{q^i q^i} \not{q}_L \otimes \not{q}_R + (\delta_{RL})_{sb} (\delta_{LR})_{q^i q^i} \not{q}_R \otimes \not{q}_L \right) \\ & + M_{\tilde{g}}^2 \Big[C_l^{(2)} \left((\delta_{RL})_{sb} (\delta_{RL})_{q^i q^i} P_L \otimes P_L + (\delta_{LR})_{sb} (\delta_{LR})_{q^i q^i} P_R \otimes P_R \right) \\ & + C_l^{(1)} \left((\delta_{LL})_{sb} P_R \otimes P_L + (\delta_{RR})_{sb} P_L \otimes P_R \right) \Big] \Big\} , \\ C_{\text{color,A}_2} = & \frac{7}{12} \delta_{c_2 c_3} \, \delta_{c_1 c_4} + \frac{1}{36} \delta_{c_1 c_2} \, \delta_{c_3 c_4} , \\ & \text{spinor sequence :} \quad (\bar{\text{s}}_{\text{c}_1}(\text{k}_1) \; \text{q}^{\text{i}}_{\text{c}_4}(\text{k}_2)) \; (\bar{\text{q}}^{\text{i}}_{\text{c}_3}(\text{p}_2) \; \text{b}_{\text{c}_2}(\text{p}_1)) . \end{aligned} \tag{6.34}$$

B-type diagrams

$$
\begin{aligned}
B_1 = -C_{\mathrm{color,B_1}} \Big\{ & C_l^{(2)} \left((\delta_{LR})_{sd^i} (\delta_{RL})_{d^i b} \not{q}_L \otimes \not{q}_L + (\delta_{RL})_{sd^i} (\delta_{LR})_{d^i b} \not{q}_R \otimes \not{q}_R \right) \\
& + C_l^{d^i} \left((\delta_{LL})_{sd^i} (\delta_{RR})_{d^i b} \not{q}_L \otimes \not{q}_R + (\delta_{RR})_{sd^i} (\delta_{LL})_{d^i b} \not{q}_R \otimes \not{q}_L \right) \\
& - M_{\tilde{g}}^2 \Big[C_l^{(2)} \left((\delta_{RL})_{sd^i} (\delta_{RL})_{d^i b} P_L \otimes P_L + (\delta_{LR})_{sd^i} (\delta_{LR})_{d^i b} P_R \otimes P_R \right) \\
& + C_l^{d^i} \left((\delta_{LL})_{sd^i} (\delta_{RR})_{d^i b} P_R \otimes P_L + (\delta_{RR})_{sd^i} (\delta_{LL})_{d^i b} P_L \otimes P_R \right) \Big] \Big\} \ , \\
C_{\mathrm{color,B_1}} = & \frac{5}{18} \delta_{c_2 c_3} \ \delta_{c_1 c_4} - \frac{1}{6} \delta_{c_1 c_2} \ \delta_{c_3 c_4} \ , \\
& \text{spinor sequence : } \ (\bar{\mathrm{s}}_{\mathrm{c_1}}(\mathrm{k_1}) \ \mathrm{d}^{\mathsf{ci}}{}_{\mathrm{c_3}}(\mathrm{p_2})) \ (\bar{\mathrm{d}}^{\mathsf{c}}{}^{\mathsf{i}}_{\mathrm{c_4}}(\mathrm{k_2}) \ \mathrm{b}_{\mathrm{c_2}}(\mathrm{p_1})) \ ,
\end{aligned}
\tag{6.35}
$$

and

$$
\begin{aligned}
B_2 = C_{\mathrm{color,B_2}} \Big\{ & C_l^{(1)} \left((\delta_{LL})_{sb} \not{q}_L \otimes \not{q}_L + (\delta_{RR})_{sb} \not{q}_R \otimes \not{q}_R \right) \\
& + C_l^{(2)} \left((\delta_{LR})_{sb} (\delta_{RL})_{q^i q^i} \not{q}_L \otimes \not{q}_R + (\delta_{RL})_{sb} (\delta_{LR})_{q^i q^i} \not{q}_R \otimes \not{q}_L \right) \\
& + M_{\tilde{g}}^2 \Big[C_l^{(2)} \left((\delta_{RL})_{sb} (\delta_{RL})_{q^i q^i} P_L \otimes P_L + (\delta_{LR})_{sb} (\delta_{LR})_{q^i q^i} P_R \otimes P_R \right) \\
& + C_l^{(1)} \left((\delta_{LL})_{sb} P_R \otimes P_L + (\delta_{RR})_{sb} P_L \otimes P_R \right) \Big] \Big\} \\
C_{\mathrm{color,B_2}} = & -\frac{1}{6} \delta_{c_2 c_3} \ \delta_{c_1 c_4} + \frac{5}{18} \delta_{c_1 c_2} \ \delta_{c_3 c_4} \\
& \text{spinor sequence : } \ (\bar{\mathrm{s}}_{\mathrm{c_1}}(\mathrm{k_1}) \ \mathrm{q}^{\mathsf{ci}}{}_{\mathrm{c_3}}(\mathrm{p_2})) \ (\bar{\mathrm{q}}^{\mathsf{c}}{}^{\mathsf{i}}_{\mathrm{c_4}}(\mathrm{k_2}) \ \mathrm{b}_{\mathrm{c_2}}(\mathrm{p_1})) \ .
\end{aligned}
\tag{6.36}
$$

In the above formulae the terms proportional to $C_l^{d^i} = C_l^{(1)} (\delta_{d^i b} + \delta_{d^i s}) + C_l^{(2)} \delta_{d^i d}$ have the obvious condition $(\delta_{LL})_{ss} = (\delta_{LL})_{bb} = 1$, while the superscript c denotes charge conjugation on the corresponding spinor. Going back to formulae (6.33)-(6.36), we notice that color structures are collected separately as variables C_{color}. Such structures are the result of reductions involving matrices $t^{a,}$, which are the objects actually appearing after the substitution of Feynman rules into the diagrams. Their simplification to a form just involving color Kronecker is performed using well known relations among Gell-Mann matrices (see for example appendix A of ref. [Pic95]). Afterwards, color structures can be saturated with external spinors, thus identifying colors between pairs of them. Finally, as anticipated, spinor sequences are collected as the last line of each diagram's formula, and must be understood following the conventions of eqs. (6.30)-(6.31) above. In particular, symbols $p_1,\ p_2$ ($k_1,\ k_2$) are labels for the incoming (outgoing) particles.

We recall at this point that in the matching procedure we need to compare, according to eq. (3.4), the full and the effective theory calculations. For this purpose it is customary to rewrite the full theory amplitude in terms of the matrix elements of the four-fermion operators of basis, taken between the same external states as those considered in the full

theory calculation itself. The relevant formula is the following:

$$\begin{aligned}
\langle \Gamma_A \otimes \Gamma_B \rangle^{c_1 c_2 c_3 c_4} &\equiv \langle \text{out} | (\overline{\psi}_s^{c_1} \Gamma_A \psi_b^{c_2})(\overline{\psi}_{q_i}^{c_3} \Gamma_B \psi_{q_i}^{c_4}) | \text{in} \rangle \\
&\leftrightarrow (\overline{s}^{c_1}(k_1)\ \Gamma_A\ b^{c_2}(p_1))\ (\overline{q_i}^{c_3}(p_2)\ \Gamma_B\ q_i^{c_4}(k_2)) \\
&- (\overline{s}^{c_1}(p_2)\ \Gamma_A\ b^{c_2}(p_1))\ (\overline{s}^{c_3}(k_1)\ \Gamma_B\ s^{c_4}(k_2))\ \delta_{q_i s} \\
&- (\overline{s}^{c_1}(k_1)\ \Gamma_A\ b^{c_2}(k_2))\ (\overline{s}^{c_3}(p_2)\ \Gamma_B\ s^{c_4}(p_1))\ \delta_{q_i b}\ . \qquad (6.37)
\end{aligned}$$

In eq. (6.37) the adoption of the sign "$\leftrightarrow$", instead of the "$=$" deserves a word of explanation. Note that on the left side of the sign there is a four fermion operator, built up with anticommuting fields, whereas on the right side a sum of amplitudes, made up of commuting spinors, appears. So the correspondence between the two sides is only up to an overall $(-)$ sign, which is fixed by convention. In particular, it is fixed by choosing a particular ordering for the creation-destruction operators of the external states (left side). Such convention must be consistent with the one adopted when writing down Feynman diagrams in terms of amplitudes (right side).

Now we sum up (6.33) with (6.34) and (6.35) with (6.36). Our aim is to express the total amplitude in terms of the tree level matrix elements of the operators listed in (6.10-6.11) among the same set of external quark states used in computing the amplitude itself. Such operation is possible, recalling that the operators in eqs. (6.10-6.11) form a complete basis. However, the expressions for the single diagrams will initially present flavour structures beyond those belonging to these operators. Such "redundant" flavour structures can however be rewritten in terms of the "reference" ones through Fierz reshuffling. The relevant Fierz transformations are collected in app. B. On the other hand, in the B-type diagrams, Fierz rearrangements are a useful tool not only to eliminate redundant structures, but also to get rid of the charge conjugation operation in the external spinors. After Fierz rearrangements, introducing the shorthand notation

$$\begin{aligned}
(p_1\ \gamma\ p_2)^{c_1 c_2}_{L,R}(k_1\ \gamma\ k_2)^{c_3 c_4}_{L',R'} &\equiv (\overline{s}_{c_1}(p_1)\ (\gamma^\mu)_{L,R}\ b_{c_2}(p_2))\ (\overline{q}^i_{c_3}(k_1)\ (\gamma_\mu)_{L',R'}\ q^i_{c_4}(k_2))\ , \\
(p_1\ \sigma\ p_2)^{c_1 c_2}_{L,R}(k_1\ \sigma\ k_2)^{c_3 c_4}_{L',R'} &\equiv (\overline{s}_{c_1}(p_1)\ (\sigma^{\mu\nu})_{L,R}\ b_{c_2}(p_2))\ (\overline{q}^i_{c_3}(k_1)\ (\sigma_{\mu\nu})_{L',R'}\ q^i_{c_4}(k_2))\ , \\
(p_1\ p_2)^{c_1 c_2}_{L,R}(k_1\ k_2)^{c_3 c_4}_{L',R'} &\equiv (\overline{s}_{c_1}(p_1)\ P_{L,R}\ b_{c_2}(p_2))\ (\overline{q}^i_{c_3}(k_1)\ P_{L',R'}\ q^i_{c_4}(k_2))\ , \qquad (6.38)
\end{aligned}$$

we write the sum $A_1 + A_2$ as

$$\begin{aligned}
A_1 + A_2 = \frac{l^2}{4} \Bigg\{ & C_l^{(1)} (\delta_{LL})_{sb} \left[\frac{1}{36} (k_1 \gamma p_1)^{\alpha\alpha}_L (p_2 \gamma k_2)^{\beta\beta}_L + \frac{7}{12} (k_1 \gamma p_1)^{\alpha\beta}_L (p_2 \gamma k_2)^{\beta\alpha}_L \right] \\
& + C_l^{(2)} (\delta_{LL})_{sd} (\delta_{LL})_{db} \delta_{q^i d} \left[\frac{7}{12} (k_1 \gamma p_1)^{\alpha\alpha}_L (p_2 \gamma k_2)^{\beta\beta}_L + \frac{1}{36} (k_1 \gamma p_1)^{\alpha\beta}_L (p_2 \gamma k_2)^{\beta\alpha}_L \right] \\
& - C_l^{(1)} \left[(\delta_{LL})_{sb} \delta_{q^i s} \left(\frac{1}{36} (p_2 \gamma p_1)^{\alpha\alpha}_L (k_1 \gamma k_2)^{\beta\beta}_L + \frac{7}{12} (p_2 \gamma p_1)^{\alpha\beta}_L (k_1 \gamma k_2)^{\beta\alpha}_L \right) \right.
\end{aligned}$$

$$
\begin{aligned}
&+\delta_{q^ib}\left(\frac{1}{36}(k_1\gamma k_2)_L^{\alpha\alpha}(p_2\gamma p_1)_L^{\beta\beta}\frac{7}{12}(k_1\gamma k_2)_L^{\alpha\beta}(p_2\gamma p_1)_L^{\beta\alpha}\right)\Bigg]\\
&+C_l^{(2)}\Bigg[(\delta_{LR})_{sb}(\delta_{RL})_{q^iq^i}\left(-\frac{1}{18}(k_1p_1)_R^{\alpha\alpha}(p_2k_2)_L^{\beta\beta}-\frac{7}{6}(k_1p_1)_R^{\alpha\beta}(p_2k_2)_L^{\beta\alpha}\right)\\
&+(\delta_{LR})_{sd}(\delta_{RL})_{db}\delta_{q^id}\left(\frac{7}{12}(k_1\gamma p_1)_L^{\alpha\alpha}(p_2\gamma k_2)_R^{\beta\beta}+\frac{1}{36}(k_1\gamma p_1)_L^{\alpha\beta}(p_2\gamma k_2)_R^{\beta\alpha}\right)\\
&+(\delta_{LR})_{ss}(\delta_{RL})_{sb}\delta_{q^is}\left(\frac{1}{18}(p_2p_1)_L^{\alpha\alpha}(k_1k_2)_L^{\beta\beta}+\frac{7}{6}(p_2p_1)_L^{\alpha\beta}(k_1k_2)_L^{\beta\alpha}\right)\\
&+\ (\delta_{LR})_{sb}(\delta_{RL})_{bb}\delta_{q^ib}\left(\frac{1}{18}(k_1k_2)_R^{\alpha\alpha}(p_2p_1)_L^{\beta\beta}+\frac{7}{6}(k_1k_2)_R^{\alpha\beta}(p_2p_1)_L^{\beta\alpha}\right)\Bigg]\Bigg\}\\
&+M_{\tilde g}^2\Bigg\{C_l^{(2)}\Bigg[(\delta_{LR})_{sb}(\delta_{LR})_{q_iq_i}\left(-\frac{1}{72}(k_1p_1)_R^{\alpha\alpha}(p_2k_2)_R^{\beta\beta}-\frac{7}{24}(k_1p_1)_R^{\alpha\beta}(p_2k_2)_R^{\beta\alpha}\right.\\
&\qquad\left.-\frac{1}{288}(k_1\sigma p_1)_R^{\alpha\alpha}(p_2\sigma k_2)_R^{\beta\beta}-\frac{7}{96}(k_1\sigma p_1)_R^{\alpha\beta}(p_2\sigma k_2)_R^{\beta\alpha}\right)\\
&+(\delta_{LR})_{sd}(\delta_{LR})_{db}\delta_{q^id}\left(\frac{7}{12}(k_1p_1)_R^{\alpha\alpha}(p_2k_2)_R^{\beta\beta}+\frac{1}{36}(k_1p_1)_R^{\alpha\beta}(p_2k_2)_R^{\beta\alpha}\right)\\
&+(\delta_{LR})_{ss}(\delta_{LR})_{sb}\delta_{q^is}\left(\frac{1}{72}(p_1p_2)_R^{\alpha\alpha}(k_1k_2)_R^{\beta\beta}+\frac{7}{24}(p_1p_2)_R^{\alpha\beta}(k_1k_2)_R^{\beta\alpha}\right.\\
&\qquad\left.+\frac{1}{288}(p_1\sigma p_2)_R^{\alpha\alpha}(k_1\sigma k_2)_R^{\beta\beta}+\frac{7}{96}(p_1\sigma p_2)_R^{\alpha\beta}(k_2\sigma k_1)_R^{\beta\alpha}\right)\\
&+(\delta_{LR})_{sb}(\delta_{LR})_{bb}\delta_{q^ib}\left(\frac{1}{72}(k_1k_2)_R^{\alpha\alpha}(p_2p_1)_R^{\beta\beta}+\frac{7}{24}(k_1k_2)_R^{\alpha\beta}(p_2p_1)_R^{\beta\alpha}\right.\\
&\qquad\left.+\frac{1}{288}(k_1\sigma k_2)_R^{\alpha\alpha}(p_2\sigma p_1)_R^{\beta\beta}+\frac{7}{96}(k_1\sigma k_2)_R^{\alpha\beta}(p_2\sigma p_1)_R^{\beta\alpha}\right)\Bigg]\\
&+C_l^{(1)}(\delta_{LL})_{sb}\left[-\frac{1}{72}(k_1\gamma p_1)_L^{\alpha\alpha}(p_2\gamma k_2)_R^{\beta\beta}-\frac{7}{24}(k_1\gamma p_1)_L^{\alpha\beta}(p_2\gamma k_2)_R^{\beta\alpha}\right]\\
&+C_l^{(2)}(\delta_{LL})_{sd}(\delta_{RR})_{db}\delta_{q^id}\left[\frac{7}{12}(k_1p_1)_R^{\alpha\alpha}(p_2k_2)_L^{\beta\beta}+\frac{1}{36}(k_1p_1)_R^{\alpha\beta}(p_2k_2)_L^{\beta\alpha}\right]\\
&+C_l^{(1)}(\delta_{LL})_{sb}\left[\delta_{q^is}\left(\frac{1}{72}(p_2\gamma p_1)_L^{\alpha\alpha}(k_1\gamma k_2)_R^{\beta\beta}+\frac{7}{24}(p_2\gamma p_1)_L^{\alpha\beta}(k_1\gamma k_2)_R^{\beta\alpha}\right)\right.\\
&\left.+\ \delta_{q^ib}\left(\frac{1}{72}(k_1\gamma k_2)_L^{\alpha\alpha}(p_2\gamma p_1)_R^{\beta\beta}+\frac{7}{24}(k_1\gamma k_2)_L^{\alpha\beta}(p_2\gamma p_1)_R^{\beta\alpha}\right)\right]\Bigg\}\\
&+L\leftrightarrow R\ .
\end{aligned}
\tag{6.39}
$$

For $B_1 + B_2$ we instead obtains

$$
\begin{aligned}
B_1 + B_2 = \frac{l^2}{4} \Bigg\{ & C_l^{(1)} (\delta_{LL})_{sb} \left(-\frac{5}{18} (k_1 \gamma p_1)_L^{\alpha\alpha} (p_2 \gamma k_2)_R^{\beta\beta} + \frac{1}{6} (k_1 \gamma p_1)_L^{\alpha\beta} (p_2 \gamma k_2)_R^{\beta\alpha} \right) \\
& + C_l^{(2)} (\delta_{LL})_{sd} (\delta_{RR})_{db} \delta_{q^i d} \left(-\frac{1}{3} (k_1 p_1)_R^{\alpha\alpha} (p_2 k_2)_L^{\beta\beta} + \frac{5}{9} (k_1 p_1)_R^{\alpha\beta} (p_2 k_2)_L^{\beta\alpha} \right) \\
& + C_l^{(1)} (\delta_{LL})_{sb} \Bigg[\delta_{q^i b} \left(\frac{5}{18} (k_1 \gamma k_2)_L^{\alpha\alpha} (p_2 \gamma p_1)_R^{\beta\beta} - \frac{1}{6} (k_1 \gamma k_2)_L^{\alpha\beta} (p_2 \gamma p_1)_R^{\beta\alpha} \right) \\
& + \delta_{q^i s} \left(\frac{5}{18} (p_2 \gamma p_1)_L^{\alpha\alpha} (k_1 \gamma k_2)_R^{\beta\beta} - \frac{1}{6} (p_2 p_1)_L^{\alpha\beta} (k_1 k_2)_R^{\beta\alpha} \right) \Bigg] \\
& + C_l^{(2)} \Bigg[(\delta_{LR})_{sb} (\delta_{RL})_{q^i q^i} \left(-\frac{5}{9} (k_1 p_1)_R^{\alpha\alpha} (p_2 k_2)_L^{\beta\beta} + \frac{1}{3} (k_1 p_1)_R^{\alpha\beta} (p_2 k_2)_L^{\beta\alpha} \right) \\
& + (\delta_{LR})_{sd} (\delta_{RL})_{db} \delta_{q^i d} \left(-\frac{1}{6} (k_1 \gamma p_1)_L^{\alpha\alpha} (p_2 \gamma k_2)_R^{\beta\beta} + \frac{5}{18} (k_1 \gamma p_1)_L^{\alpha\beta} (p_2 \gamma k_2)_R^{\beta\alpha} \right) \\
& + (\delta_{LR})_{sb} (\delta_{RL})_{bb} \delta_{q^i b} \left(\frac{5}{9} (k_1 k_2)_R^{\alpha\alpha} (p_2 p_1)_L^{\beta\beta} - \frac{1}{3} (k_1 k_2)_R^{\alpha\beta} (p_2 p_1)_L^{\beta\alpha} \right) \\
& + (\delta_{LR})_{sb} (\delta_{RL})_{ss} \delta_{q^i s} \left(\frac{5}{9} (p_2 p_1)_R^{\alpha\alpha} (k_1 k_2)_L^{\beta\beta} - \frac{1}{3} (p_2 p_1)_R^{\alpha\beta} (k_1 k_2)_L^{\beta\alpha} \right) \Bigg] \\
+ M_{\tilde{g}}^2 \Bigg\{ & C_l^{(2)} \Bigg[(\delta_{LR})_{sb} (\delta_{LR})_{q^i q^i} \left(-\frac{5}{36} (k_1 p_1)_R^{\alpha\alpha} (p_2 k_2)_R^{\beta\beta} + \frac{1}{12} (k_1 p_1)_R^{\alpha\beta} (p_2 k_2)_R^{\beta\alpha} \right. \\
& \left. + \frac{5}{144} (k_1 \sigma p_1)_R^{\alpha\alpha} (p_2 \sigma k_2)_R^{\alpha\alpha} - \frac{1}{48} (k_1 \sigma p_1)_R^{\alpha\beta} (p_2 \sigma k_2)_R^{\beta\alpha} \right) \\
& + (\delta_{LR})_{sd} (\delta_{LR})_{db} \delta_{q^i d} \left(\frac{1}{12} (k_1 p_1)_R^{\alpha\alpha} (p_2 k_2)_R^{\beta\beta} - \frac{5}{36} (k_1 p_1)_L^{\alpha\beta} (p_2 k_2)_R^{\beta\alpha} \right. \\
& \left. - \frac{1}{48} (k_1 \sigma p_1)_R^{\alpha\alpha} (p_2 \sigma k_2)_R^{\beta\beta} + \frac{5}{144} (k_1 \sigma p_1)_L^{\alpha\beta} (p_2 \sigma k_2)_R^{\beta\alpha} \right) \\
& + (\delta_{LR})_{sb} (\delta_{LR})_{bb} \delta_{q^i b} \left(\frac{5}{36} (k_1 k_2)_R^{\alpha\alpha} (p_2 p_1)_R^{\beta\beta} - \frac{1}{12} (k_1 k_2)_R^{\alpha\beta} (p_2 p_1)_R^{\beta\alpha} \right. \\
& \left. - \frac{5}{144} (k_1 \sigma k_2)_R^{\alpha\alpha} (p_2 \sigma p_1)_R^{\beta\beta} + \frac{1}{48} (k_1 \sigma k_2)_R^{\alpha\beta} (p_2 \sigma p_1)_R^{\beta\alpha} \right) \\
& + (\delta_{LR})_{sb} (\delta_{LR})_{ss} \delta_{q^i s} \left(\frac{5}{36} (p_2 p_1)_R^{\alpha\alpha} (k_1 k_2)_R^{\beta\beta} - \frac{1}{12} (p_2 p_1)_R^{\alpha\beta} (k_1 k_2)_R^{\beta\alpha} \right. \\
& \left. - \frac{5}{144} (p_2 \sigma p_1)_R^{\alpha\alpha} (k_1 \sigma k_2)_R^{\beta\beta} + \frac{1}{48} (p_2 \sigma p_1)_R^{\alpha\beta} (k_1 \sigma k_2)_R^{\beta\alpha} \right) \Bigg] \\
& + C_l^{(1)} (\delta_{LL})_{sb} \left(\frac{5}{36} (k_1 \gamma p_1)_L^{\alpha\alpha} (p_2 \gamma k_2)_L^{\beta\beta} - \frac{1}{12} (k_1 \gamma p_1)_L^{\alpha\beta} (p_2 \gamma k_2)_L^{\beta\alpha} \right) \\
& + C_l^{(2)} (\delta_{LL})_{sd} (\delta_{LL})_{db} \delta_{q^i d} \left(-\frac{1}{12} (k_1 \gamma p_1)_L^{\alpha\alpha} (p_2 \gamma k_2)_L^{\beta\beta} + \frac{5}{36} (k_1 \gamma p_1)_L^{\alpha\beta} (p_2 \gamma k_2)_L^{\beta\alpha} \right)
\end{aligned}
$$

$$
\begin{aligned}
&+C_l^{(1)}(\delta_{LL})_{sb}\left[\delta_{q^i b}\left(-\frac{5}{36}(k_1\gamma k_2)_L^{\alpha\alpha}(p_2\gamma p_1)_L^{\beta\beta}+\frac{1}{12}(k_1\gamma k_2)_L^{\alpha\beta}(p_2\gamma p_1)_L^{\beta\alpha}\right)\right.\\
&\left.+\ \delta_{q^i s}\left(-\frac{5}{36}(p_2\gamma p_1)_L^{\alpha\alpha}(k_1\gamma k_2)_L^{\beta\beta}+\frac{1}{12}(p_2\gamma p_1)_L^{\alpha\beta}(k_1\gamma k_2)_L^{\beta\alpha}\right)\right]\Bigg\}\\
&+L\leftrightarrow R
\end{aligned}
\tag{6.40}
$$

Now, grouping amplitudes in (6.39) according to (6.37), we end up with

$$
\begin{aligned}
(A_1+A_2)_{\text{phys}} = \frac{l^2}{4}\Bigg\{&C_l^{(1)}(\delta_{LL})_{sb}\left(\frac{1}{36}\langle Q_{11,\tilde g}^{q^i}\rangle^{(0)}+\frac{7}{12}\langle Q_{12,\tilde g}^{q^i}\rangle^{(0)}\right)\\
&+C_l^{(2)}(\delta_{LL})_{sd}(\delta_{LL})_{db}\left(\frac{7}{12}\langle Q_{11,\tilde g}^{d}\rangle^{(0)}\frac{1}{36}\langle Q_{12,\tilde g}^{d}\rangle^{(0)}\right)\\
&+C_l^{(2)}\left[(\delta_{LR})_{sb}(\delta_{RL})_{q^iq^i}\left(-\frac{1}{18}\langle Q_{17,\tilde g}^{q^i}\rangle^{(0)}-\frac{7}{6}\langle Q_{18,\tilde g}^{q^i}\rangle^{(0)}\right)\right.\\
&\left.+\ (\delta_{LR})_{sd}(\delta_{RL})_{db}\left(\frac{7}{12}\langle Q_{13,\tilde g}^{d}\rangle^{(0)}+\frac{1}{36}\langle Q_{14,\tilde g}^{d}\rangle^{(0)}\right)\right]\Bigg\}\\
&+M_{\tilde g}^2\Bigg\{C_l^{(2)}\left[(\delta_{LR})_{sb}(\delta_{LR})_{q^iq^i}\left(-\frac{1}{72}\langle Q_{15,\tilde g}^{q^i}\rangle^{(0)}-\frac{7}{24}\langle Q_{16,\tilde g}^{q^i}\rangle^{(0)}-\frac{1}{288}\langle Q_{19,\tilde g}^{q^i}\rangle^{(0)}\right.\right.\\
&\left.\left.-\frac{7}{96}\langle Q_{20,\tilde g}^{q^i}\rangle^{(0)}\right)+(\delta_{LR})_{sd}(\delta_{LR})_{db}\left(\frac{7}{12}\langle Q_{15,\tilde g}^{d}\rangle^{(0)}+\frac{1}{36}\langle Q_{16,\tilde g}^{d}\rangle^{(0)}\right)\right]\\
&+C_l^{(1)}(\delta_{LL})_{sb}\left(-\frac{1}{72}\langle Q_{13,\tilde g}^{q^i}\rangle^{(0)}-\frac{7}{24}\langle Q_{14,\tilde g}^{q^i}\rangle^{(0)}\right)\\
&+C_l^{(2)}(\delta_{LL})_{sd}(\delta_{RR})_{db}\left(\frac{7}{12}\langle Q_{17,\tilde g}^{d}\rangle^{(0)}+\frac{1}{36}\langle Q_{18,\tilde g}^{d}\rangle^{(0)}\right)\Bigg\}\\
&+Q_{i,\tilde g}^{q^i}\leftrightarrow\tilde Q_{i,\tilde g}^{q^i}\,,
\end{aligned}
\tag{6.41}
$$

whereas the same operation performed on the sum (6.40) gives

$$
\begin{aligned}
(B_1+B_2)_{\text{phys}} = \frac{l^2}{4}\Bigg\{&C_l^{(1)}(\delta_{LL})_{sb}\left(-\frac{5}{18}\langle Q_{13,\tilde g}^{q^i}\rangle^{(0)}+\frac{1}{6}\langle Q_{14,\tilde g}^{q^i}\rangle^{(0)}\right)\\
&+C_l^{(2)}\left[(\delta_{LL})_{sd}(\delta_{RR})_{db}\left(-\frac{1}{3}\langle Q_{17,\tilde g}^{d}\rangle^{(0)}+\frac{5}{9}\langle Q_{18,\tilde g}^{d}\rangle^{(0)}\right)\right.\\
&+(\delta_{LR})_{sb}(\delta_{RL})_{q^iq^i}\left(-\frac{5}{9}\langle Q_{17,\tilde g}^{q^i}\rangle^{(0)}+\frac{1}{3}\langle Q_{18,\tilde g}^{q^i}\rangle^{(0)}\right)\\
&\left.+\ (\delta_{LR})_{sd}(\delta_{RL})_{db}\left(-\frac{1}{6}\langle Q_{13,\tilde g}^{d}\rangle^{(0)}+\frac{5}{18}\langle Q_{14,\tilde g}^{d}\rangle^{(0)}\right)\right]
\end{aligned}
$$

$$
\begin{aligned}
&+M_{\tilde{g}}^2 \Bigg\{ C_l^{(2)} \Bigg[(\delta_{LR})_{sb}(\delta_{LR})_{q^i q^i} \left(-\frac{5}{36}\langle Q^{q^i}_{15,\tilde{g}}\rangle^{(0)} + \frac{1}{12}\langle Q^{q^i}_{16,\tilde{g}}\rangle^{(0)} + \frac{5}{144}\langle Q^{q^i}_{19,\tilde{g}}\rangle^{(0)} \right. \\
&\left. -\frac{1}{48}\langle Q^{q^i}_{20,\tilde{g}}\rangle^{(0)} \right) + (\delta_{LR})_{sd}(\delta_{LR})_{db} \left(\frac{1}{12}\langle Q^{d}_{15,\tilde{g}}\rangle^{(0)} - \frac{5}{36}\langle Q^{d}_{16,\tilde{g}}\rangle^{(0)} - \frac{1}{48}\langle Q^{d}_{19,\tilde{g}}\rangle^{(0)} \right. \\
&\left. +\frac{5}{144}\langle Q^{d}_{20,\tilde{g}}\rangle^{(0)} \right) + (\delta_{LL})_{sd}(\delta_{LL})_{db} \left(-\frac{1}{12}\langle Q^{d}_{11,\tilde{g}}\rangle^{(0)} + \frac{5}{36}\langle Q^{d}_{12,\tilde{g}}\rangle^{(0)} \right) \Bigg] \\
&+ C_l^{(1)}(\delta_{LL})_{sd} \left(\frac{5}{36}\langle Q^{d}_{11,\tilde{g}}\rangle^{(0)} - \frac{1}{12}\langle Q^{d}_{12,\tilde{g}}\rangle^{(0)} \right) \Bigg\} \\
&+Q^{q^i}_{i,\tilde{g}} \leftrightarrow \tilde{Q}^{q^i}_{i,\tilde{g}}
\end{aligned}
\tag{6.42}
$$

In eqs. (6.41) and (6.42) the subscript "phys" is there to remind us that such amplitudes come from the contributions of physical operators. Contributions related to evanescent operators are not reported here, since they are relevant only at the NLO level.

As a closing remarks, we stress that the feature of the full theory amplitude to be expressible (at any order in perturbation theory) in terms of tree level matrix elements of the effective operators is in general true for amplitude *as a whole*, namely summing all the diagrams belonging to it. Notably, it is not true for the single diagrams. Nonetheless, we have just seen that $A_1 + A_2$ and separately $B_1 + B_2$ can actually be expressed in terms of the abovementioned matrix elements.

In eqs. (6.41-6.42) we still have to perform the understood loop integration. Recalling the expression for $C_l^{(1)}$ and $C_l^{(2)}$, we see that the only integrals appearing in the LO calculation are those generated by a single mass insertion

$$
\begin{aligned}
I_m^{(1)} &= M_{\tilde{g}}^2 \int \frac{d^4l}{(2\pi)^4} \frac{1}{(l^2 - M_{\tilde{g}}^2)^2 (l^2 - M_s^2)^3} \ , \\
I_l^{(1)} &= \int \frac{d^4l}{(2\pi)^4} \frac{l^2}{(l^2 - M_{\tilde{g}}^2)^2 (l^2 - M_s^2)^3} \ ,
\end{aligned}
\tag{6.43}
$$

or a double mass insertion

$$
\begin{aligned}
I_m^{(2)} &= M_{\tilde{g}}^2 \int \frac{d^4l}{(2\pi)^4} \frac{1}{(l^2 - M_{\tilde{g}}^2)^2 (l^2 - M_s^2)^4} \ , \\
I_l^{(2)} &= \int \frac{d^4l}{(2\pi)^4} \frac{l^2}{(l^2 - M_{\tilde{g}}^2)^2 (l^2 - M_s^2)^4} \ .
\end{aligned}
\tag{6.44}
$$

Both of them are finite and can be written in terms of $x = M_{\tilde{g}}^2/M_s^2$. The corresponding loop functions $B_1, B_2, f_6, \tilde{f}_6$ are explicitely reported in appendix C.

In particular, we can now plug in formulae (C.7) into (6.41) and (6.42). The result obtained is all what is needed in a LO calculation. In fact the one loop full amplitude must be matched in this case with just the tree level effective one, and we have done it when rewriting our results in terms of the $\langle Q_{i,\tilde{g}}\rangle^{(0)}$, according to formula (6.37). So the Wilson coefficients of the LO effective Hamiltonian are just the sum of (6.41) and (6.42), once multiplied by an overall $(+i)$ to take care of eq. (6.25).

After this manipulation we can list out results for the various Dirac structures. We obtain for the Wilson coefficients of the vector operators

$$C^q_{11,\tilde{g}}(\mu_S) = -\frac{1}{16\pi^2 M^2_{\tilde{g}}}\left\{(\delta_{LL})_{sb}\ \left(\frac{1}{36}B_1(x)+\frac{5}{9}B_2(x)\right)+\delta_{qd}\ (\delta_{LL})_{sq}\ (\delta_{LL})_{qb}\left(\frac{7}{12}\tilde{f}_6(x)-\frac{1}{3}f_6(x)\right)\right\}\ ,$$

$$C^q_{12,\tilde{g}}(\mu_S) = -\frac{1}{16\pi^2 M^2_{\tilde{g}}}\left\{(\delta_{LL})_{sb}\ \left(\frac{7}{12}B_1(x)-\frac{1}{3}B_2(x)\right)+\delta_{qd}\ (\delta_{LL})_{sq}\ (\delta_{LL})_{qb}\left(\frac{1}{36}\tilde{f}_6(x)+\frac{5}{9}f_6(x)\right)\right\}\ ,$$

$$C^q_{13,\tilde{g}}(\mu_S) = -\frac{1}{16\pi^2 M^2_{\tilde{g}}}\left\{(\delta_{LL})_{sb}\ \left(-\frac{5}{18}B_1(x)-\frac{1}{18}B_2(x)\right)+\delta_{qd}\ (\delta_{LR})_{sd}\ (\delta_{RL})_{db}\left(\frac{5}{12}\tilde{f}_6(x)\right)\right\}\ ,$$

$$C^q_{14,\tilde{g}}(\mu_S) = -\frac{1}{16\pi^2 M^2_{\tilde{g}}}\left\{(\delta_{LL})_{sb}\ \left(\frac{1}{6}B_1(x)-\frac{7}{6}B_2(x)\right)+\delta_{qd}\ (\delta_{LR})_{sd}\ (\delta_{RL})_{db}\left(\frac{11}{36}\tilde{f}_6(x)\right)\right\}\ , \qquad (6.45)$$

while those concerning the scalar/tensor ones the result is

$$C^q_{15,\tilde{g}}(\mu_S) = -\frac{1}{16\pi^2 M^2_{\tilde{g}}}\left\{(\delta_{LR})_{sb}\ (\delta_{LR})_{qq}\left(-\frac{11}{18}f_6(x)\right)+\delta_{qd}\ (\delta_{LR})_{sq}\ (\delta_{LR})_{qb}\left(\frac{8}{3}f_6(x)\right)\right\}\ ,$$

$$C^q_{16,\tilde{g}}(\mu_S) = -\frac{1}{16\pi^2 M^2_{\tilde{g}}}\left\{(\delta_{LR})_{sb}\ (\delta_{LR})_{qq}\left(-\frac{5}{6}f_6(x)\right)+\delta_{qd}\ (\delta_{LR})_{sq}\ (\delta_{LR})_{qb}\left(-\frac{4}{9}f_6(x)\right)\right\}\ ,$$

$$C^q_{17,\tilde{g}}(\mu_S) = -\frac{1}{16\pi^2 M^2_{\tilde{g}}}\left\{(\delta_{LR})_{sb}\ (\delta_{RL})_{qq}\left(-\frac{11}{18}\tilde{f}_6(x)\right)+\delta_{qd}\ (\delta_{LL})_{sq}\ (\delta_{RR})_{qb}\left(-\frac{1}{3}\tilde{f}_6(x)+\frac{7}{3}f_6(x)\right)\right\}\ ,$$

$$C^q_{18,\tilde{g}}(\mu_S) = -\frac{1}{16\pi^2 M^2_{\tilde{g}}}\left\{(\delta_{LR})_{sb}\ (\delta_{RL})_{qq}\left(-\frac{5}{6}\tilde{f}_6(x)\right)+\delta_{qd}\ (\delta_{LL})_{sq}\ (\delta_{RR})_{qb}\left(\frac{5}{9}\tilde{f}_6(x)+\frac{1}{9}f_6(x)\right)\right\}\ ,$$

$$C^q_{19,\tilde{g}}(\mu_S) = -\frac{1}{16\pi^2 M^2_{\tilde{g}}}\left\{(\delta_{LR})_{sb}\ (\delta_{LR})_{qq}\left(\frac{1}{8}f_6(x)\right)+\delta_{qd}\ (\delta_{LR})_{sq}\ (\delta_{LR})_{qb}\left(-\frac{1}{12}f_6(x)\right)\right\}\ ,$$

$$C^q_{20,\tilde{g}}(\mu_S) = -\frac{1}{16\pi^2 M^2_{\tilde{g}}}\left\{(\delta_{LR})_{sb}\ (\delta_{LR})_{qq}\left(-\frac{3}{8}f_6(x)\right)+\delta_{qd}\ (\delta_{LR})_{sq}\ (\delta_{LR})_{qb}\left(\frac{5}{36}f_6(x)\right)\right\}\ , \qquad (6.46)$$

where again the primed coefficients can be obtained from the $C^q_{i,\tilde{g}}$ just by the exchange $L \leftrightarrow R$.

We finally recall that, under renormalization, the operators corresponding to the coefficients (6.46) mix with the magnetic and chromomagnetic operators by undergoing a chirality flip proportional to m_q. Therefore, only $q = b, c$ can contribute to the decay $b \to s\gamma$ via eqs. (6.20-6.23) in the approximation $m_u = m_d = m_s = 0$ made here.

Comparison with ref. [BGHW00]

A comment about the differences of this results from that of ref. [BGHW00] on the same subject is in order now. The authors of ref. [BGHW00] give the results in the mass-eigenstate basis, while we have used the Mass Insertion Approximation, applying the formulae given in appendix A. We have verified that, if we translate their formulae (29-33) in our approximation using eqs. (A.4-A.5) we find complete agreement with our Wilson coefficients in eqs. (6.45-6.46).

6.5. BR(B → X$_s$γ) at Leading Order

We turn now to discuss the formulae useful to evaluate the branching ratio.

Since here we are discussing the LO approximation, several general considerations can be made.

(i) The inclusive meson decays $B \to X_s\gamma$ is given in the spectator model by the corresponding quark decay $b \to X_s\gamma$. The spectator model has been shown to correspond to the leading approximation in the $1/m_b$ expansion, whose corrections can be obtained with the method of the Heavy Quark Effective Theory [BIR98].

(ii) At the LO accuracy there is no difference between the running masses and the pole ones. Initially, when the heavy particles are integrated out, it is convenient to work out the matching conditions in terms of the running masses.

(iii) The branching ratio is obtained as

$$BR(B \to X_s\gamma) = \frac{\Gamma(B \to X_s\gamma)}{\Gamma(B \to X_c e\overline{\nu}_e)}\ BR(B \to X_c e\overline{\nu}_e)\ , \tag{6.47}$$

where $BR(B \to X_c e\overline{\nu}_e)$ is the measured semileptonic branching ratio. The normalization to the semileptonic rate is usually introduced in order to cancel the uncertainties due to the CKM matrix elements and factors of m_b in the right side of eq. (6.47). The latter are present both in the semileptonic decay width given by

$$\Gamma(b \to ce\overline{\nu}_e) = \frac{m_b^5\ G_F^2\ |V_{cb}|^2}{192\pi^3}\ f(z)\ , \tag{6.48}$$

where the phase-space $f(z) = 1 - 8z + 8z^3 - z^4 - 12z^2 \ln z$ is a function of $z = m_c^2/m_b^2$, and in the $b \to s\gamma$ rate. The latter turns out to be [BGHW00]

$$\Gamma(b \to s\gamma) = \frac{m_b^5\ G_F^2\ |V_{tb}V_{ts}^*|^2\alpha_{em}}{32\pi^4}\ \left\{|\hat{C}_7^{(0)}(\mu_b)|^2 + |\hat{C}_7^{(0)'}(\mu_b)|^2\right\}\ , \tag{6.49}$$

where unprimed and primed coefficients refer respectively to right-handed b and s external quarks and can be expressed in terms of the SM and gluino induced functions by means of

$$\begin{aligned}
\hat{C}_7^{(0)}(\mu_b) &= C_7^{(0)eff}(\mu_b) - \frac{16\sqrt{2}\pi^3\alpha_s(\mu_b)}{G_F V_{tb}V_{ts}^*}\left[C_{7b.\tilde{g}}^{(0)}(\mu_b) + \frac{1}{m_b}C_{7\tilde{g},\tilde{g}}^{(0)}(\mu_b) + \frac{m_c}{m_b}C_{7c,\tilde{g}}^{(0)}(\mu_b)\right]\ , \\
\hat{C}_7^{\prime(0)}(\mu_b) &= \frac{16\sqrt{2}\pi^3\alpha_s(\mu_b)}{G_F V_{tb}V_{ts}^*}\left[C_{7b.\tilde{g}}^{\prime(0)}(\mu_b) + \frac{1}{m_b}C_{7\tilde{g},\tilde{g}}^{\prime(0)}(\mu_b) + \frac{m_c}{m_b}C_{7c,\tilde{g}}^{\prime(0)}(\mu_b)\right]\ .
\end{aligned} \tag{6.50}$$

To conclude, we have derived all the analytic and numerical formulae to extract from $\Gamma(B \to X_s\gamma)$ possible constraints on the flavour-violating sources in the squark sector, generated by the FCG interactions. We have expressed the additional CKM-type mixings arising from the MSSM sector as a function of the $(\delta_{AB})_{ij}$ parameters, with indices i, j indicating the external quarks flavours and $A, B = L, R$ referring to their helicity.

We point put that the SM contribution already successfully saturates the experimental result for this branching ratio. Furthermore, the $B \to X_s\gamma$ rate could be enhanced significantly also without gluino contributions or any other source of flavour violation in addition to the CKM matrix elements. The charged Higgs contribution always enhance the rate, while chargino diagrams can reduce it if the μ parameter in the superpotential is positive. These two types of contributions are related in MFV models [CDGG98].

A possible method to analyze the FCG contribution is the direct comparison of eq. (6.49) with the measured value in eq. (1.5). The theoretical expectation is the sum of the SM contribution, which is a function of quark masses and CKM parameters, and the SUSY contribution, function of squark and gluino masses and $(\delta_{AB})_{ij}$ parameters.

The bounds on the mass insertions can be obtained fixing a pair of values for $(M_{\tilde{g}}, M_s)$ and setting to zero in the Wilson coefficients all the $(\delta_{AB})_{ij}$ except for one. With this procedure, the amplitude (6.49) to be compared with the experimental number depends on a single mass insertion for each case considered.

The $\Delta B = 1$ constraint of $B \to X_s\gamma$, with respect to those considering in the $\Delta F = 2$ systems, has the following features:
(i) Only $(\delta_{LL})_{sb}$ and $(\delta_{LR})_{sb}$ generate amplitudes that interference with the SM contribution. Therefore the constraint from $B \to X_s\gamma$ for $(\delta_{RL})_{sb}$ and $(\delta_{RR})_{sb}$ are symmetric around zero, while the interference with the SM produce a circular shape for $(\delta_{RL})_{sb}$ and $(\delta_{LR})_{sb}$. We point out that in $\Delta F = 2$ FCNC processes all the constraints are symmetric around zero.
(ii) The operator $Q_{7b,\tilde{g}}$ is suppressed by a factor $m_b/M_{\tilde{g}}$ at the μ_b scale, where the branching ratio is evaluated, with respect to $Q_{7\tilde{g},\tilde{g}}$. In fact, the latter is generated by an helicity flip mediated by the gluino mass, proportional to $(\delta_{LR})_{sb}$ and $(\delta_{RL})_{sb}$. Therefore the $B \to X_s\gamma$ constraint is much more effective on these insertions.
(iii) Among the four-quark operators, only the scalar/tensor ones contribute at LO, but they are naively supposed to have a small impact since they are generated by $(\delta_{LR})_{sb}$ or $(\delta_{RL})_{sb}$ but contribute to the numerically less important operator $O_{7b,\tilde{g}}$.

Our formulae for the Wilson coefficients are obtained using a common value for the up- and down- type average squark mass $\overline{M}$. One should actually check if this assumption is not a oversimplification, affecting the generality of the numerical results. As already remarked in sec. 2.3, this simplified approach is reliable only in absence of interference effects between the various $(\delta_{AB})_{ij}$. This is the main condition under which such a model independent analysis are performed. In addition, the latter can be applied to particular directions of the supersymmetric parameter space, in which charged Higgs, chargino and neutralino contributions can be safely neglected with respect to the gluino and SM contributions.

Summary of the results and outlook

In the present Ph.D. Thesis we have investigated two main arguments:

1. The EDM of the Neutron in supersymmetric extensions of the Standard Model where contributions from new physics originate from extra heavy particles.

2. The rare inclusive $B \to X_s\gamma$ decay in presence of supersymmetric FCG interactions.

We now briefly summarize the main results achieved and presented in this work.

EDM of the Neutron

In chapters 4 and 5 we have presented the calculation of the perturbative strong corrections to the EDM of the Neutron. The most important feature of the present study, with respect to most of the results presented in the literature, is the use of a correct LO ADM, the inclusion of the mixing between the electric and chromoelectric operators and the study of the Wilson coefficients including NLO corrections.

The main results are collected in chapter 4 and 5, with the corresponding analytic formulae presented in appendix C. For a detailed discussion on the results of the phenomenological analysis performed in the framework of mSUGRA models., the reader is referred to sec. 4.6. One interesting novelty in our analysis is the numerical irrelevance of the neutralino contribution, as a consequence of our correct inclusion of the mixing. The main result achieved by the inclusion of the NLO corrections for the gluino contribution, discussed in chapter 5, is a neat improvement on the scale dependence with respect to LO, from $15 - 20\%$ to few percent, as summarized in fig. 5.8.

Finally, we point out that possible sources of improvement of our analysis of the EDM of the Neutron concerning both the perturbative and non-perturbative aspects of the observable are

1. The inclusion of the QCD NLO corrections for the supersymmetric chargino and neutralino exchange.

2. A lattice determination of the matrix elements for the relevant dipole and Weinberg operators, including an estimate of the θ-parameter.

The last point, in particular, is essential in view of any study of the supersymmetric CP violation, since actually there are too many unknown parameters for a reliable analysis of that kind.

$\mathbf{B \to X_s \gamma}$

In the sixth chapter we have turned to a less restrictive scenario for the MSSM space parameter at the Electroweak scale, respect to that dictated by the mSUGRA models. As discussed in sec. 2.3, we have considered the presence of tree level FCG interactions. The latter have a phenomenological impact on many observables in the B_s, B_d, K and D mesons systems.

We have analyzed the FCG contribution to the branching ratio $\Gamma(B \to X_s\gamma)$ at LO and confirmed all the previous studies about this issue, in particular those collected in [BGHW00]. Given the theoretical prediction, a general analysis is complicated even at LO. The main reason is that the FCG interaction translate in a very large number of new flavour violating parameter with respect to the Standard Model. Therefore, we have adopted the Mass Insertion Approximation, as a very useful method to permit the direct comparison of our results with the experimental bounds in a physically transparent fashion.

We have provided all the numerical factors to study the effects of the new supersymmetric sources of flavour violation in the MSSM as a function of the $(\delta_{AB})_{ij}$ parameter defined in the MIA.

A. The Mass Insertion Approximation

A.1. MIA expansions

When adopting the MIA, things get considerably simplified for loop functions. Since we use propagators and vertices involving the mass‘ eigenstates basis U, D, such loop functions will depend on $(\mathcal{M}^2_{U(D)})_k$.

Let us consider, as a starting point, a function f depending just on one mass $\mathcal{M}^2_k$ (for ease of notation we suppress from now on the subscript $_{U(D)}$). We can Taylor expand it as

$$f(\mathcal{M}^2_k) = \sum_{n=0}^{\infty} \frac{\partial^n f(x)}{\partial x^n}|_{x=0} \frac{(\mathcal{M}^2_k)^n}{n!} \ . \tag{A.1}$$

Substituting the definition of the MIA expansion parameter Δ defined in the first line of eq. (2.49), one finds

$$\begin{aligned} \left(Z^\dagger\right)_{ik} f(\mathcal{M}^2_k) \left(Z\right)_{kj} &= \sum_{n=0}^{\infty} \frac{d^n f(x)}{dx^n}|_{x=0} \frac{\left(M_i^2 \delta_{ij} + \Delta_{ij}\right)^n}{n!} \\ &\simeq f(M_i^2)\ \hat{1}_{ij} + \sum_{n=0}^{\infty} \frac{d^n f(x)}{dx^n}|_{x=0} \frac{(M_i^2)^n - (M_j^2)^n}{n!(M_i^2 - M_j^2)} \Delta_{ij} \\ &= f(M_i^2)\ \hat{1}_{ij} + \frac{f(M_i^2) - f(M_j^2)}{M_i^2 - M_j^2}\ \Delta_{ij} \ , \end{aligned} \tag{A.2}$$

where we have expanded as follows

$$\left(M_i^2 \delta_{ij} + \Delta_{ij}\right)^n \sim (M_i^2)^n\ \delta_{ij} + \left[(M_i^2)^{n-1} + (M_i^2)^{n-2} M_j^2 + ... + (M_j^2)^{n-1}\right] \Delta_{ij} \ . \tag{A.3}$$

Eq. (A.2) is a consequence of the MIA assumption for the smallness of the off-diagonal entries Δ_{ij} with respect to the diagonal ones. If we also apply the other MIA condition in eq. (2.49) for the approximate degeneracy of the diagonal entries of M, eq. (A.2) turns to

$$\left(Z^\dagger\right)_{ik} f(\mathcal{M}^2_k) \left(Z\right)_{kj} = f(\overline{M}^2)\ \hat{1}_{ij} + f'(\overline{M}^2)\ \Delta_{ij} \ . \tag{A.4}$$

One can note that, if $f(\mathcal{M}^2_k)$ is the propagator of a squark with mass $\mathcal{M}_k$, eq. (A.4) tells us that its expression in the basis of the flavour eigenstates can be approximated as

a propagator of a scalar with an average mass $\overline{M}$ plus a double propagator (f') of the same kind with a flavour $\times$ chirality changing mass insertion. Hence the name of the approximation.

The case with two masses - and in general with an arbitrary number of masses - is just a generalization of eq. (A.4). We explicitly write it down as our last example

$$\begin{aligned}
&\left(Z^\dagger\right)_{ir}\left(Z^\dagger\right)_{ks} f(\mathcal{M}_r^2,\mathcal{M}_s^2)\,(Z)_{rj}\,(Z)_{sl} = \\
&\quad f(\overline{M}^2,\overline{M}^2)\hat{1}_{ij}\hat{1}_{kl} + \partial_1 f(\overline{M}^2,\overline{M}^2)\Delta_{ij}\hat{1}_{kl} + \partial_2 f(\overline{M}^2,\overline{M}^2)\hat{1}_{ij}\Delta_{kl} \\
&\quad + \frac{1}{2}\partial_1^2 f(\overline{M}^2,\overline{M}^2)(\Delta^2)_{ij}\hat{1}_{kl} + \frac{1}{2}\partial_2^2 f(\overline{M}^2,\overline{M}^2)\hat{1}_{ij}(\Delta^2)_{kl} \\
&\quad + \partial_1\partial_2 f(\overline{M}^2,\overline{M}^2)\Delta_{ij}\Delta_{kl} + O(\Delta^3)\ ,
\end{aligned} \tag{A.5}$$

where for the derivatives with respect to the first or second argument of the function f we adopted the shorthand notation $\partial_{1,2} = \partial_{M_r^2,M_s^2}$.

B. Fierz transformations

Fierz transformations are a needful tool for expressing all the structures appearing in the calculations of chapter 6 in terms of a set of "reference" ones, those corresponding to the operator basis in eqs. (6.10) and (6.11). For B-type diagrams (see chapter 6, or below), recalling that they involve external spinors subject to the charge conjugation operator C, a second benefit adds up. One is able to eliminate C from the spinors again using suitable Fierz reshuffling, of course together with the properties of C.

B.1. Fierz identities for Dirac Algebra

Let us consider the generic fermionic quadrilinear

$$(\overline{\psi}_1\ \Gamma^A\ \psi_2)\ \otimes\ (\overline{\psi}_3\ \Gamma^B\ \psi_4)\ . \tag{B.1}$$

The Fierz transformation allows to change the position of the external spinor, giving rise to $4!/2 - 1 = 11$ equivalent combination to the initial one. For definiteness, by Fierz transformations we mean the following algebraic identities [1]

$$(\Gamma^A)_{\alpha\delta}\ \otimes\ (\Gamma^A)_{\gamma\beta} = \sum_B C_B^A\ (\Gamma^A)_{\alpha\beta}\ \otimes\ (\Gamma^A)_{\gamma\delta}\ , \tag{B.2}$$

namely the interchanging $\psi_2 \leftrightarrow \psi_4$. In eq. (B.2), C_B^A are numbers, $\alpha, ..., \delta$ are Dirac indices and i, j run over the Dirac basis of 16 matrices defined as

$$\Gamma^A \equiv \left\{\hat{1}, \gamma^\mu, \sigma^{\mu\nu}, i\gamma^\mu\gamma_5, \gamma_5\right\}\ ,\ \mu > \nu \tag{B.3}$$

where $\sigma^{\mu\nu} = \frac{i}{2}[\gamma^\mu, \gamma^\nu]$. To obtain the C_B^A it is easy to derive the following relation [NP04]

$$C_B^A = \frac{1}{4} f_{AB}, \tag{B.4}$$

where the matrix f is determined by $\Gamma^{A\mu}\ \Gamma^{B\nu}\ \Gamma^A_\mu = f_{AB}\ \Gamma^B_\nu$ and his explicit form is the following

$$f = \begin{pmatrix} 1 & 1 & 1 & 1 & 1 \\ 4 & -2 & 0 & 2 & -4 \\ 6 & 0 & -2 & 0 & 6 \\ 4 & 2 & 0 & -2 & -4 \\ 1 & 1 & 1 & -1 & 1 \end{pmatrix}\ . \tag{B.5}$$

[1] We recall that the overall $(-)$ sign coming from the anticommutation of the four spinor fields saturating these structures is not included.

Combining relations (B.2-B.5) one can find Fierz relations for Dirac bilinears with definite chiralities, obtained by applying the chirality projectors $P_{R,L} = (1 \pm \gamma_5)/2$. Here we collect only those which are useful for the present work.

$$\begin{aligned}
\{P_L \otimes P_L\}_F &= \frac{1}{2} P_L \otimes P_L + \frac{1}{8} \sigma^{\mu\nu} \otimes \sigma_{\mu\nu} \ , \\
\{P_L \otimes P_R\}_F &= \frac{1}{2} \gamma_R^\mu \otimes \gamma_{\mu L} \ , \\
\{\gamma_L^\mu \otimes \gamma_{\mu L}\}_F &= -\gamma_L^\mu \otimes \gamma_{\mu L} \ , \\
\{\gamma_L^\mu \otimes \gamma_{\mu R}\}_F &= 2 P_R \otimes P_L \ ,
\end{aligned} \tag{B.6}$$

plus those obtained by exchanging $L \leftrightarrow R$.

B.2. Relations involving charge conjugates of spinors

We collect here some relations between Dirac bilinears involving charge conjugates of spinors. They will be important for deriving Fierz relations necessary in the treatment of B-type diagrams and collected in section B.3. We first recall the following basic definitions (see appendix A of [DeA])

$$\psi^c \equiv C(\overline{\psi})^T \Leftrightarrow (\overline{\psi^c}) \equiv -\psi^T C^{-1} \ , \tag{B.7}$$

where ψ is a spinor [2]. Then one can write

$$\begin{aligned}
(\overline{\psi_1})_\alpha \Gamma_{\alpha\beta} (\psi_2)_\beta &= (\psi_2^{cT})_\beta (\Gamma^T)_{\beta\alpha} (\overline{\psi_1^c}^T)_\alpha \\
&= \left(\psi_2^{cT} C^{-1}\right)_\beta \left(C \Gamma^T C^{-1}\right)_{\beta\alpha} \left(C \overline{\psi_1^c}^T\right)_\alpha \\
&= -\overline{\psi_{2\beta}} \left(C \Gamma^T C^{-1}\right)_{\beta\alpha} \psi_{1\alpha} \ .
\end{aligned} \tag{B.8}$$

Choosing for the C matrix the standard representation, $C = i\gamma^2\gamma^0$, one can exploit the first and the last member in the chain of equalities (B.8) to get the following relations between Dirac bilinears

$$\begin{aligned}
\overline{\psi_1^c} \gamma_L^\mu \psi_2^c &= \overline{\psi_2} \gamma_R^\mu \psi_1 \ , \\
\overline{\psi_1^c} P_L \psi_2^c &= -\overline{\psi_2} P_L \psi_1 \ , \\
\overline{\psi_1^c} \sigma^{\mu\nu} \psi_2^c &= \overline{\psi_2} \sigma^{\mu\nu} \psi_1 \ , \\
\overline{\psi_1^c} \sigma^{\mu\nu} \gamma_5 \psi_2^c &= \overline{\psi_2} \sigma^{\mu\nu} \gamma_5 \psi_1 \ ,
\end{aligned} \tag{B.9}$$

plus those obtained interchanging $L \leftrightarrow R$.

[2] We recall that spinor are commuting objects.

B.3. Fierz relations for A- and B-type diagrams

In this section we collect all the Fierz relations needed in the treatment of the full theory diagrams.

In order to saturate the Dirac indices and give rise to amplitudes, appearing in practical calculations of Feynman diagrams, we will introduce four spinors (see footnote 1) for the separate cases of A-type and B-type diagrams. In particular

$$\begin{aligned} &(\overline{a}_\alpha\ b_\beta),\ (\overline{c}_\gamma\ d_\delta) \qquad \mathrm{A-type\ diagrams} \\ &(\overline{a}^c_\alpha\ b_\beta),\ (\overline{c}_\gamma\ d^c_\delta) \qquad \mathrm{B-type\ diagrams.} \end{aligned} \tag{B.10}$$

In practice the two spinor sequences (B.10) can be assumed as a definition of A- and B-type diagrams respectively.

A-type diagrams

$$(\overline{a}\ \gamma^{\mu L}\ b)\ (\overline{c}\ \gamma^\mu_L\ d) = -(\overline{a}\ \gamma^{\mu L}\ d)\ (\overline{c}\ \gamma^\mu_L\ b) \tag{B.11}$$

$$(\overline{a}\ \gamma^{\mu L}\ b)\ (\overline{c}\ \gamma^\mu_R\ d) = +2(\overline{a}\ P_R\ d)\ (\overline{c}\ P_L\ b) \tag{B.12}$$

$$(\overline{a}\ P_L\ b)\ (\overline{c}\ P_L\ d) = \frac{1}{2}(\overline{a}\ P_L\ d)\ (\overline{c}\ P_L\ b) + \frac{1}{8}(\overline{a}\ \sigma^{\mu\nu}_L\ d)\ (\overline{c}\ \sigma_{\mu\nu L}\ b) \tag{B.13}$$

B-type diagrams

Recalling the spinor sequences (B.10), we see that in the case of B-type diagrams it is useful to use together Fierz relations and transformations involving the charge conjugation operator C, in order to get rid of C in spinors. Relations for Dirac bilinears saturated with charge-conjugates of spinors were obtained in section B.2, eqs. (B.9). Below they are used together with the results of B.1 to derive all the Fierz transformations needed in the treatment of B-type diagrams.

$$(\overline{a}\ \gamma^{\mu L}\ b^c)\ (\overline{c}^c\ \gamma^\mu_L\ d) = -(\overline{a}\ \gamma^{\mu L}\ d)\ (\overline{b}\ \gamma^\mu_R\ c) = -2(\overline{a}\ P_R\ c)\ (\overline{b}\ P_L\ d) \tag{B.14}$$

$$(\overline{a}\ \gamma^{\mu L}\ b^c)\ (\overline{c}^c\ \gamma^\mu_R\ d) = -2(\overline{a}\ P_R\ d)\ (\overline{b}\ P_L\ c) \tag{B.15}$$

$$(\overline{a}\ P_L\ b^c)\ (\overline{c}^c\ P_L\ d) = -\frac{1}{2}(\overline{a}\ P_L\ d)\ (\overline{b}\ P_L\ c) + \frac{1}{8}(\overline{a}\ \sigma^{\mu\nu}_L\ d)\ (\overline{b}\ \sigma_{\mu\nu L}\ c) \tag{B.16}$$

$$= \frac{1}{2}(\overline{a}\ P_L\ c)\ (\overline{b}\ P_L\ d) - \frac{1}{8}(\overline{a}\ \sigma^{\mu\nu}_L\ c)\ (\overline{b}\ \sigma_{\mu\nu L}\ d) \tag{B.17}$$

$$= -(\overline{a}\ P_L\ d)\ (\overline{b}\ P_L\ c) + (\overline{a}\ P_L\ c)\ (\overline{b}\ P_L\ d) \tag{B.18}$$

$$(\overline{a}\ P_L\ b^c)\ (\overline{c}^c\ P_R\ d) = \frac{1}{2}(\overline{a}\ \gamma^{\mu R}\ d)\ (\overline{b}\ \gamma^\mu{}_R\ c) \tag{B.19}$$

Eqs.(B.11)-(B.13) and (B.14)-(B.19) represent the full set of Fierz relations we need to handle Dirac structures in the full theory.

C. Loop functions for the Wilson coefficients

In this appendix we give the explicit expressions of the one- and two- loop functions that appear in the Wilson coefficients.
Before listing the functions, we recall the basic notation used.

$$x_i = m_{\tilde{g}}^2/m_{\tilde{q}_i}^2 \quad , \quad x_t = m_t^2/m_{\tilde{q}}^2$$

$$Li_2[z] = \int_z^0 dt \frac{\ln[1-t]}{t} = \text{PolyLog[2, z] as defined in Mathematica} \ .$$

C.1. EDM of the Neutron

$$\begin{aligned}
\tilde{A}(x_1,x_2) &= -\frac{x_1x_2(x_1x_2+x_1+x_2-3)}{2(x_1-1)^2(x_2-1)^2} - \frac{x_1x_2}{(x_1-x_2)}\left[\frac{x_1\ln x_1}{(x_1-1)^3} - \frac{x_2\ln x_2}{(x_2-1)^3}\right] \\
\tilde{B}(x_1,x_2) &= \frac{x_1x_2(3x_1x_2-x_1-x_2-1)}{2(x_1-1)^2(x_2-1)^2} + \frac{x_1x_2}{(x_1-x_2)}\left[\frac{x_1^2\ln x_1}{(x_1-1)^3} - \frac{x_2^2\ln x_2}{(x_2-1)^3}\right] \\
\tilde{C}(x_1,x_2) &= \frac{x_1x_2(3x_1x_2+5x_1+5x_2-13)}{3(x_1-1)^2(x_2-1)^2} \\
&\quad -\frac{x_1x_2}{3(x_1-x_2)}\left[\frac{x_1(x_1-9)\ln x_1}{(x_1-1)^3} - \frac{x_2(x_2-9)\ln x_2}{(x_2-1)^3}\right] \\
A(x) &= \frac{x(x-3)}{2(x-1)^2} + \frac{x\ln x}{(x-1)^3} \\
B(x) &= \frac{x(x+1)}{2(x-1)^2} - \frac{x^2\ln x}{(x-1)^3} \ .
\end{aligned} \tag{C.1}$$

In the case of equal masses the functions $\tilde{A}$, $\tilde{B}$, $\tilde{C}$ reduce to

$$\begin{aligned}
\tilde{A}(x) &= -\frac{x^2(x+5)}{2(x-1)^3} + \frac{x^2(2x+1)\ln x}{(x-1)^4} \\
\tilde{B}(x) &= \frac{x^2(5x+1)}{2(x-1)^3} - \frac{x^3(x+2)\ln x}{(x-1)^4} \\
\tilde{C}(x) &= \frac{2x^2(x+11)}{3(x-1)^3} + \frac{x^2(x^2-16x-9)\ln x}{3(x-1)^4} \ .
\end{aligned} \tag{C.2}$$

We list now the two-loop functions that appear in eqs. (5.13-5.14). To simplify the expressions, we perform an expansion in the top mass reporting only the first term in x_t. In particular, recalling eq. (5.15), we write

$$\begin{aligned}
F_2\left(x_{\tilde{g}}, x_t\right) &= G_2\left(x_{\tilde{g}}, x_t\right) + \Delta_2\left(x_{\tilde{g}}\right) \ln \frac{\mu_S^2}{m_{\tilde{q}}^2} \\
&\simeq G_2\left(x_{\tilde{g}}\right) + x_t\, G_2^t\left(x_{\tilde{g}}\right) + \Delta_2\left(x_{\tilde{g}}\right) \ln \frac{\mu_S^2}{m_{\tilde{q}}^2} \\
F_4\left(x_{\tilde{g}}, x_t\right) &= G_4\left(x_{\tilde{g}}, x_t\right) + \Delta_4\left(x_{\tilde{g}}\right) \ln \frac{\mu_S^2}{m_{\tilde{q}}^2} \\
&\simeq G_4\left(x_{\tilde{g}}\right) + x_t\, G_4^t\left(x_{\tilde{g}}\right) + x_t \ln x_t\, S_4\left(x_{\tilde{g}}\right) + \Delta_4\left(x_{\tilde{g}}\right) \ln \frac{\mu_S^2}{m_{\tilde{q}}^2} \\
N_i\left(x_{\tilde{g}}, x_t\right) &\simeq \sqrt{x_t}\, N_i^t\left(x_{\tilde{g}}\right) + \sqrt{x_t} \ln x_t\, R_i^t\left(x_{\tilde{g}}\right) \ . \qquad \text{(C.3)}
\end{aligned}$$

We find

$$\begin{aligned}
G_1(x) &= \frac{8x^2\left(51x^3+413x^2-1473x-251\right)}{27\left(x-1\right)^4} - \frac{16\left(8x^2+293x-13\right)}{27\left(x-1\right)^4}\mathrm{Li}_2\left(1-x\right) \\
&+\frac{8x^2\left(127x^4-1075x^3+480x^2+405x+27\right)\ln^2 x}{27\left(x-1\right)^6} \\
&-\frac{8x^2\left(48x^4+228x^3-1105x^2-548x+81\right)\ln x}{27\left(x-1\right)^5} \\
G_2(x) &= \frac{64x^2\left(x^2+4x-2\right)}{3\left(x-1\right)^4} - \frac{16x^2\left(x+5\right)}{3\left(x-1\right)^3}\mathrm{Li}_2\left(1-x\right) - \frac{16x^3\left(x^2+4x-1\right)\ln x}{\left(x-1\right)^5} \\
G_3(x) &= -\frac{x^2\left(129x^3-2903x^2+1083x+21851\right)}{54\left(x-1\right)^4} - \frac{4\left(113x^2+281x+110\right)}{27\left(x-1\right)^4}\mathrm{Li}_2\left(1-x\right) \\
&+\frac{x^2\left(539x^4-2282x^3-6744x^2+7578x+621\right)\ln^2 x}{27\left(x-1\right)^6} \\
&+\frac{x^2\left(96x^4-5019x^3+13357x^2+10583x+1719\right)\ln x}{54\left(x-1\right)^5} \\
G_4(x) &= -\frac{x^2\left(17x^2-310x+101\right)}{3\left(x-1\right)^4} + \frac{2x^2\left(x-40\right)}{3\left(x-1\right)^3}\mathrm{Li}_2\left(1-x\right) + \frac{x^2\left(2x^3-67x^2+4x-3\right)\ln x}{\left(x-1\right)^5} \\
G_2^t(x) &= \frac{8x^2\left(x^2+76x+175\right)}{9\left(x-1\right)^4} + \frac{32x^2\left(x+3\right)}{\left(x-1\right)^5}\mathrm{Li}_2\left(1-x\right) - \frac{32x^3\left(2x+7\right)\ln x}{3\left(x-1\right)^5} \\
G_4^t(x) &= -\frac{x^2\left(17x^2+230x-4387\right)}{18\left(x-1\right)^4} + \frac{2x^2\left(3x^2-8x+81\right)}{\left(x-1\right)^5}\mathrm{Li}_2\left(1-x\right) \\
&+\frac{x^2\left(53x^2-305x+18\right)\ln x}{3\left(x-1\right)^5}\ln x
\end{aligned}$$

$$
\begin{aligned}
S_4(x) &= -\frac{x^2(x^2+10x+1)}{(x-1)^4} + \frac{6x^3(x+1)\ln x}{(x-1)^5} \\
N_1^t(x) &= -\frac{4x^{\frac{5}{2}}(x^3+8x^2+173x+34)}{9(x-1)^4} - \frac{32x^{\frac{7}{2}}(x+2)\ln x}{3(x-1)^5} \\
&\quad -\frac{16x^{\frac{5}{2}}(5x^2+17x+2)}{3(x-1)^5}\mathrm{Li}_2(1-x) \\
N_2^t(x) &= -\frac{4x^{\frac{5}{2}}(x^2+x+34)}{9(x-1)^3} - \frac{16x^{\frac{5}{2}}(x+2)}{3(x-1)^4}\mathrm{Li}_2(1-x) \\
N_3^t(x) &= -\frac{x^{\frac{5}{2}}(11x^3-158x^2+1225x+542)}{18(x-1)^4} + \frac{2x^{\frac{5}{2}}(2x^2-86x-9)\ln x}{3(x-1)^5} \\
&\quad +\frac{2x^{\frac{5}{2}}(5x^2-181x-52)}{3(x-1)^5}\mathrm{Li}_2(1-x) \\
N_4^t(x) &= -\frac{x^{\frac{5}{2}}(11x^3-114x^2+753x-758)}{18(x-1)^4} - \frac{6x^{\frac{5}{2}}(6x-1)\ln x}{(x-1)^5} \\
&\quad +\frac{2x^{\frac{5}{2}}(x^2-89x+52)}{3(x-1)^5}\mathrm{Li}_2(1-x) \\
R_3^t(x) &= -\frac{x^{\frac{7}{2}}(x^2-8x-17)}{2(x-1)^4} - \frac{3x^{\frac{7}{2}}(3x+1)\ln x}{(x-1)^5} \\
R_4^t(x) &= -\frac{x^{\frac{7}{2}}(x^2-8x-17)}{2(x-1)^4} - \frac{3x^{\frac{7}{2}}(3x+1)\ln x}{(x-1)^5} \\
\Delta_1(x) &= \frac{16x^2(8x^3+13x^2-176x-37)}{9(x-1)^4} - \frac{16x^2(29x^3-97x^2-115x-9)\ln x}{9(x-1)^5} \\
\Delta_2(x) &= \frac{8x^2(7x^2+16x+1)}{3(x-1)^4} - \frac{16x^3(x^2+7x+4)\ln x}{3(x-1)^5} \\
\Delta_3(x) &= -\frac{8x^2(2x^3-83x^2+268x+197)}{9(x-1)^4} - \frac{4x^2(59x^3-67x^2-643x-117)\ln x}{9(x-1)^5} \\
\Delta_4(x) &= \frac{2x^2(x^2+64x+31)}{3(x-1)^4} + \frac{2x^2(x^3-29x^2-59x-9)\ln x}{3(x-1)^5}
\end{aligned}
\tag{C.4}
$$

Finally, the function H entering in the Weinberg operator (see eq. (5.16)) is given by

$$
\begin{aligned}
H(x_{\tilde{g}}, x_t) &\simeq H(x_{\tilde{g}}) + x_t H_1^t(x_{\tilde{g}}) + x_t \ln x_t H_2^t(x_{\tilde{g}}) \\
H(x) &= \frac{x^2(x+11)}{3(x-1)^3} + \frac{x^2(x^2-16x-9)\ln x}{6(x-1)^4}
\end{aligned}
$$

$$H_1^t(x) = \frac{x\,(5x^3+265x^2+455x+27)}{6\,(x-1)^5} + \frac{2x^2\,(4x^3-93x^2-258x-81)\ln x}{3\,(x-1)^6} + \frac{2x^2\,(x^3-12x^2-51x-18)}{(x-1)^6}\mathrm{Li}_2\,(1-x)$$

$$H_2^t(x) = -\frac{x\,(11x^3-223x^2-259x-9)}{6\,(x-1)^5} + \frac{x^2\,(x^3-12x^2-51x-18)\ln x}{(x-1)^6} \quad . \quad \text{(C.5)}$$

C.2. $B \to X_s\gamma$

Listed below are the loop functions appearing in the eqs. (6.26)-(6.29)

$$F_1(x) = \frac{1+9x-9x^2-x^3+6x(1+x)\ln x}{6(x-1)^5} \ ,$$

$$F_2(x) = \frac{1-9x-9x^2+17x^3-6x^2(x+3)\ln x}{12(x-1)^5} \ ,$$

$$F_3(x) = \frac{5-4x-x^2+2(1+2x)\ln x}{2(x-1)^4} \ ,$$

$$F_4(x) = \frac{-1-4x+5x^2-2x(2+x)\ln x}{2(x-1)^4} \ ,$$

$$F_5(x) = \frac{-1+6x-18x^2+10x^3+3x^4-12x^3\ln x}{9(x-1)^5} \ ,$$

$$F_6(x) = \frac{-14+36x-14x^2-4x^3-(6-18x^2)\ln x}{9(x-1)^5} \ ,$$

$$F_7(x) = \frac{-9+31x-18x^2-4x^3+(-1+15x+18x^2)\ln x}{(x-1)^5} \ ,$$

$$F_8(x) = \frac{1-6x+18x^2-10x^3-3x^4+12x^3\ln x}{(x-1)^5} \ . \quad \text{(C.6)}$$

while for the box-diagram functions in eqs. (6.45)-(6.46) we follow the notation of refs. [HKT94, GGMS96]

$$I_m^{(1)} = \frac{i}{16\pi^2 M_{\tilde{g}}^2} B_2(x) \ , \quad \text{with} \quad B_2(x) = \frac{x^2(5-4x-x^2+2\ln x+4x\ln x}{2(x-1)^4} \ ,$$

$$I_q^{(1)} = \frac{i}{16\pi^2 M_{\tilde{g}}^2} B_1(x) \ , \quad \text{with} \quad B_1(x) = \frac{x(1+4x-5x^2+4x\ln x+2x^2\ln x}{2(x-1)^4} \ ,$$

$$I_m^{(2)} = \frac{i}{16\pi^2 M_{\tilde{g}}^2} f_6(x) \ , \quad \text{with} \quad f_6(x) = \frac{x^2(17-9x-9x^2+x^3+6(1+3x))\ln x}{6(x-1)^5} \ ,$$

$$I_q^{(2)} = \frac{i}{16\pi^2 M_{\tilde{g}}^2} \tilde{f}_6(x) \ , \quad \text{with} \quad \tilde{f}_6(x) = \frac{x(1+9x-9x^2-x^3+6x(1+x)\ln x)}{3(x-1)^5} \ . \quad \text{(C.7)}$$

References

[A+02] B. C. Allanach et al. *"The Snowmass points and slopes: Benchmarks for SUSY searches"*. Eur. Phys. J., **C25**:113–123, (2002). [arXiv:hep-ph/0202233].

[ABC98] G. Altarelli, R. Barbieri, and F. Caravaglios. *"Electroweak precision tests: A concise review"*. Int. J. Mod. Phys., **A13**:1031–1058, (1998). [arXiv:hep-ph/9712368].

[ACW98] S. A. Abel, W. N. Cottingham, and I. B. Whittingham. *"Gluon and gluino penguins and the charmless decays of the b quark"*. Phys. Rev., **D58**:073006, (1998). [arXiv:hep-ph/9803401].

[AI94] G. Altarelli and G. Isidori. *"Lower limit on the Higgs mass in the standard model: An Update"*. Phys. Lett., **B337**:141–144, (1994).

[AKP03] B. C. Allanach, S. Kraml, and W. Porod. *"Theoretical uncertainties in sparticle mass predictions from computational tools"*. JHEP, **03**:016, (2003). [arXiv:hep-ph/0302102].

[ALN90] R. Arnowitt, Jorge L. Lopez, and D. V. Nanopoulos. *"Keeping the demon of SUSY at bay"*. Phys. Rev., **D42**:2423–2426, (1990).

[Alt] G. Altarelli. *"Concluding talk: Status of the standard model and beyond"*. CERN-PH-TH-2005-051.

[B+06] E. Barberio et al. *"Averages of b-hadron properties at the end of 2005"*, (2006). [arXiv:hep-ex/0603003].

[Bal79] V. Baluni. *"CP violating effects in QCD"*. Phys. Rev., **D19**:2227–2230, (1979).

[BBL96] G. Buchalla, A. J. Buras, and M. E. Lautenbacher. *"Weak Decays Beyond Leading Logarithms"*. Rev. Mod. Phys., **68**:1125–1144, (1996).

[BFNS82] R. Barbieri, S. Ferrara, D. V. Nanopoulos, and K. S. Stelle. *"Supergravity, R Invariance and spontaneous supersymmetry breaking"*. Phys. Lett., **B113**:219, (1982).

[BGHW00] F. Borzumati, C. Greub, T. Hurth, and D. Wyler. *"Gluino contribution to radiative B decays: Organization of QCD corrections and leading order results"*. Phys. Rev., **D62**:075005, (2000). [arXiv:hep-ph/9911245].

[BGTW90] G. Boyd, A. K. Gupta, S. P. Trivedi, and M. B. Wise. *"Effective Hamiltonian for the Electric Dipole Moment of the Neutron"*. Phys. Lett., **B241**:584, (1990).

[BIR98] G. Buchalla, G. Isidori, and S. J. Rey. *"Corrections of order Λ^2_{QCD}/m^2_c to inclusive rare B decays"*. Nucl. Phys., **B511**:594–610, (1998). [arXiv:hep-ph/9705253].

[BJLW92] A. J. Buras, M. Jamin, M. E. Lautenbacher, and P. H. Weisz. *"Effective Hamiltonians for $\Delta S = 1$ and $\Delta B = 1$ nonleptonic decays beyond the leading logarithmic approximation"*. Nucl. Phys., **B370**:69–104, (1992).

[BLY90a] E. Braaten, Chong-Sheng Li, and Tzu-Chiang Yuan. *"The evolution of Weinberg's gluonic CP violation operator"*. Phys. Rev. Lett., **64**:1709, (1990).

[BLY90b] Eric Braaten, Chong-Sheng Li, and Tzu-Chiang Yuan. *"The evolution of Weinberg's gluonic CP violation operator"*. Phys. Rev. Lett., **64**:1709, (1990).

[BMMP94] A. J. Buras, M. Misiak, M. Munz, and S. Pokorski. *"Theoretical uncertainties and phenomenological aspects of $B \to X_s\gamma$ decay"*. Nucl. Phys., **B424**:374–398, (1994). [hep-ph/9311345].

[BMU00] A. J. Buras, M. Misiak, and J. Urban. *"Two-loop QCD anomalous dimensions of flavour-changing four- quark operators within and beyond the standard model"*. Nucl. Phys., **B586**:397–426, (2000). [arXiv:hep-ph/0005183].

[BP57] N. N. Bogoliubov and O. S. Parasiuk. *"On the Multiplication of the causal function in the quantum theory of fields"*. Acta Math., **97**:227–266, (1957).

[BS00] R. Barbieri and A. Strumia. *"The 'LEP paradox'"*. (2000). [arXiv:hep-ph/0007265].

[Bur98] A. J. Buras. *"Weak Hamiltonian, CP violation and rare decays"*, (1998). [arXiv:hep-ph/9806471].

[C$^+$98] M. Ciuchini et al. *"Next-to-leading order QCD corrections to $\Delta F = 2$ effective Hamiltonians*. Nucl. Phys., **B523**:501–525, (1998). [arXiv:hep-ph/9711402].

[CDGG97] M. Ciuchini, G. Degrassi, P. Gambino, and G. F. Giudice. *"Next-to-leading QCD corrections to $B \to X_s\gamma$: Standard model and two-Higgs doublet model"*. Nucl. Phys., **B527**:21–43, (1997). [arXiv:hep-ph/9710335].

[CDGG98] M. Ciuchini, G. Degrassi, P. Gambino, and G. F. Giudice. *"Next-to-leading QCD corrections to $B \to X_s\gamma$ in supersymmetry"*. Nucl. Phys., **B534**:3–20, (1998). [arXiv:hep-ph/9806308].

[CFM+93] M. Ciuchini, E. Franco, G. Martinelli, L. Reina, and L. Silvestrini. *"Scheme independence of the effective Hamiltonian for $b \to s\gamma$ and $b \to sg$ decays"*. Phys. Lett., **B316**:127–136, (1993). [arXiv:hep-ph/9307364].

[Che] Hai-Yang Cheng. *"Weak and strong CP violation"*. Lecture given at Int. Spring School on Medium and High Energy Nuclear Physics, Taipei, Taiwan, May 16-21, 1988.

[CJvN80] D. M. Capper, D. R. T. Jones, and P. van Nieuwenhuizen. *"Regularization by dimensional reduction of supersymmetric and nonsupersymmetric gauge theories"*. Nucl. Phys., **B167**:479, (1980).

[CM67] S. R. Coleman and J. Mandula. *"All Possible Symmetries Of The S Matrix"*. Phys. Rev., **159**:1251–1256, (1967).

[CM94] P. L. Cho and M. Misiak. *"$b \to s\gamma$ decay in $SU(2)$-$L \times SU(2)$-$r \times U(1)$ extensions of the Standard Model"*. Phys. Rev., **D49**:5894–5903, (1994). [arXiv:hep-ph/9310332].

[CMM98] K. G. Chetyrkin, M. Misiak, and M. Munz. *"$|\Delta F| = 1$ nonleptonic effective Hamiltonian in a simpler scheme"*. Nucl. Phys., **B520**:279–297, (1998). [arXiv:hep-ph/9711280].

[CMPP79] N. Cabibbo, L. Maiani, G. Parisi, and R. Petronzio. *"Bounds on the fermions and Higgs boson masses in grand unified theories"*. Nucl. Phys., **B158**:295, (1979).

[Col] J. C. Collins. *"Renormalization. An introduction to renormalization, the renormalization group, and the operator product expansion"*. Cambridge, Uk: Univ. Pr. (1984) 380p.

[COPW94] M. Carena, M. Olechowski, S. Pokorski, and C. E. M. Wagner. *"Electroweak symmetry breaking and bottom - top Yukawa unification"*. Nucl. Phys., **B426**:269–300, (1994). [arXiv:hep-ph/9402253].

[Dar00] S. Dar. *"The neutron EDM in the SM: A review"*. (2000). [arXiv:hep-ph/0008248].

[DDL+90] J. Dai, H. Dykstra, R. G. Leigh, S. Paban, and D. Dicus. *"CP violation from three gluon operators in the supersymmetric standard model"*. Phys. Lett., **B237**:216, (1990).

[DeA] An exhaustive collection of the conventions and basic identities concerning spinor algebra in four-and two- component notation can be found in [Der], appendices A and B, respectively.

[DEHK92] A. Denner, H. Eck, O. Hahn, and J. Kublbeck. *"Feynman rules for fermion number violating interactions"*. Nucl. Phys., **B387**:467–484, (1992).

[Der] J.-P. Derendinger. *"Lectures notes on globally supersymmetric theories in four dimensions and two dimensions"*. Prepared for 3rd Hellenic School on Elementary Particle Physics, Corfu, Greece, 13-23 Sep 1989.

[DF90] M. Dine and W. Fischler. *"Constraints on new physics from Weinberg's analysis of the neutron electric dipole moment"*. Phys. Lett., **B242**:239–244, (1990).

[DFMS05] G. Degrassi, E. Franco, S. Marchetti, and L. Silvestrini. *"QCD corrections to the electric dipole moment of the neutron in the MSSM"*. JHEP, **11**, 2005. [arXiv:hep-ph/0510137].

[DGIS02] G. D'Ambrosio, G. F. Giudice, G. Isidori, and A. Strumia. *"Minimal flavour violation: An effective field theory approach"*. Nucl. Phys., **B645**:155–187, (2002). [arXiv:hep-ph/0207036].

[DGS06] G. Degrassi, P. Gambino, and P. Slavich. *"QCD corrections to radiative B decays in the MSSM with minimal flavor violation"*. Phys. Lett., **B635**:335–342, (2006). [arXiv:hep-ph/0601135].

[DLO$^+$04] D. A. Demir, O. Lebedev, K. A. Olive, M. Pospelov, and A. Ritz. *"Electric dipole moments in the MSSM at large tan β"*. Nucl. Phys., **B680**:339–374, (2004). [arXiv:hep-ph/0311314].

[DS95] S. Dimopoulos and D. W. Sutter. *"The Supersymmetric flavor problem"*. Nucl. Phys., **B452**:496–512, (1995). [arXiv:hep-ph/9504415].

[DT93] A. I. Davydychev and J. B. Tausk. *"Two loop selfenergy diagrams with different masses and the momentum expansion"*. Nucl. Phys., **B397**:123–142, (1993).

[EGN76] J. R. Ellis, M. K. Gaillard, and D. V. Nanopoulos. *"Lefthanded currents and CP violation"*. Nucl. Phys., **B109**:213, (1976).

[EKN91] J. R. Ellis, S. Kelley, and D. V. Nanopoulos. *"Probing the desert using gauge coupling unification"*. Phys. Lett., **B260**:131–137, (1991).

[FNA] See website of the Collaborations.
CDF:http://www-cdf.fnal.gov/;
DO:http://www-d0.fnal.gov/;
NuTeV:http://www-e815.fnal.gov/.

[Gam06] P. Gambino. *"Semileptonic and radiative B decays circa 2005"*. Nucl. Phys. Proc. Suppl., **156**:169–173, (2006). [arXiv:hep-ph/0510085].

[GGMS96] F. Gabbiani, E. Gabrielli, A. Masiero, and L. Silvestrini. *"A complete analysis of FCNC and CP constraints in general SUSY extensions of the standard model"*. Nucl. Phys., **B477**:321–352, (1996). [arXiv:hep-ph/9604387].

[GM84] H. Georgi and A. Manohar. *"Chiral quarks and the nonrelativistic quark model"*. Nucl. Phys., **B234**:189, (1984).

[Hah01] T. Hahn. *"Generating Feynman diagrams and amplitudes with FeynArts 3"*. Comput. Phys. Commun., **140**:418–431, (2001). [arXiv:hep-ph/0012260].

[Har99] P. G. et al. Harris. *"New experimental limit on the electric dipole moment of the neutron"*. Phys. Rev. Lett., **82**:904–907, (1999).

[Hep66] K. Hepp. *"Proof of the Bogolyubov-Parasiuk theorem on renormalization"*. Commun. Math. Phys., **2**:301–326, (1966).

[HKR86] L. J. Hall, V. A. Kostelecky, and S. Raby. *"New Flavor Violations In Supergravity Models"*. Nucl. Phys., **B267**:415, (1986).

[HKT94] J. S. Hagelin, S. Kelley, and T. Tanaka. *"Supersymmetric flavor changing neutral currents: exact amplitudes and phenomenological analysis"*. Nucl. Phys., **B415**:293–331, (1994).

[HLS75] R. Haag, J. T. Lopuszanski, and M. Sohnius. *"All Possible Generators Of Supersymmetries Of The S Matrix"*. Nucl. Phys., **B88**:257, (1975).

[HR90] L. J. Hall and L. Randall. *"Weak scale effective supersymmetry"*. Phys. Rev. Lett., **65**:2939–2942, (1990).

[IL81] T. Inami and C. S. Lim. *"Effects of superheavy quarks and leptons in low-energy weak processes $K_L \to \mu\overline{\mu}$, $K^+ \to \pi^+\nu\overline{\nu}$ and $K_0 \leftrightarrow \overline{K_0}$"*. Prog. Theor. Phys., **65**:297, (1981).

[IN98] T. Ibrahim and P. Nath. *"The neutron and the lepton EDMs in MSSM, large CP violating phases, and the cancellation mechanism"*. Phys. Rev., **D58**:111301, (1998). [arXiv:hep-ph/9807501].

[IRS01] G. Isidori, G. Ridolfi, and A. Strumia. *"On the metastability of the standard model vacuum"*. Nucl. Phys., **B609**:387–409, (2001). [arXiv:hep-ph/0104016].

[Isi] See lectures 2 and 3 of G. Isidori at the 2004 "Seminario Nazionale di Fisica Teorica", Parma Sep. 2004.
Website: http://pr.infn.it/snft/2004/snft-2004.html.

[Jar] (Ed.) Jarlskog, C. *"CP Violation"*. Singapore, Singapore: World scientific (1989) 723 P. (Advanced series on directions in high energy physics, 3).

[LEP] See website of the LEP EW Working Group:
http://lepewwg.web.cern.ch/LEPEWWG/.

[LP02] Oleg Lebedev and Maxim Pospelov. *"Electric dipole moments in the limit of heavy superpartners"*. Phys. Rev. Lett., **89**:101801, (2002). [arXiv:hep-ph/0204359].

[LSZ55] H. Lehmann, K. Symanzik, and W. Zimmermann. *"On the formulation of quantized field theories"*. Nuovo Cim., **1**:205–225, (1955).

[M+06] M. Misiak et al. *"The first estimate of BR(B → $X_s\gamma$) at $O(\alpha_s^2)$"*. (2006). [arXiv:hep-ph/0609232].

[Mar97] S. P. Martin. *"A supersymmetry primer"*. (1997). [arXiv:hep-ph/9709356].

[Mis93] M. Misiak. *"The $b \to se^+e^-$ and $b \to s\gamma$ decays with next- to-leading logarithmic QCD corrections"*. Nucl. Phys., **B393**:23–45, (1993).

[MM95] M. Misiak and M. Munz. *"Two loop mixing of dimension five flavor changing operators"*. Phys. Lett., **B344**:308–318, (1995). [arXiv:hep-ph/9409454].

[MPR98] M. Misiak, S. Pokorski, and J. Rosiek. *"Supersymmetry and FCNC effects"*. Adv. Ser. Direct. High Energy Phys., **15**:795–828, (1998). [arXiv:hep-ph/9703442].

[Mu] See H. Murayama, concluding talk at Lepton Photon 2003 at Fermilab, Aug. 11-16, 2003,
website: http://conferences.fnal.gov/lp2003/program/index.html.

[MV93] S. P. Martin and M. T. Vaughn. *"Regularization dependence of running couplings in softly broken supersymmetry"*. Phys. Lett., **B318**:331–337, (1993). [arXiv:hep-ph/9308222].

[MV94] S. P. Martin and M. T. Vaughn. *"Two loop renormalization group equations for soft supersymmetry breaking couplings"*. Phys. Rev., **D50**:2282, (1994). [hep-ph/9311340].

[Nil82] H. P. Nilles. *"Dynamically broken supergravity and the hierarchy problem"*. *Phys. Lett.*, B115:193, 1982.

[NP04] J. F. Nieves and P. B. Pal. *"Generalized Fierz identities"*. Am. J. Phys., **72**:1100–1108, (2004). [arXiv:hep-ph/0306087].

[O'R75] L. O'Raifeartaigh. *"Spontaneous symmetry breaking for chirals scalar superfields"*. Nucl. Phys., **B96**:331–352, (1975).

[PdR91] A. Pich and E. de Rafael. *"Strong CP violation in an effective chiral Lagrangian approach"*. Nucl. Phys., **B367**:313–333, (1991).

[Pic95] A. Pich. *"Quantum chromodynamics"*, (1995). [arXiv:hep-ph/9505231].

[PQ77] R. D. Peccei and H. R. Quinn. *"CP conservation in the presence of instantons"*. Phys. Rev. Lett., **38**:1440–1443, (1977).

[PR01] M. Pospelov and A. Ritz. *"Neutron EDM from electric and chromoelectric dipole moments of quarks"*. Phys. Rev., **D63**:073015, (2001). [arXiv:hep-ph/0010037].

[PRS00] S. Pokorski, J. Rosiek, and C. A. Savoy. *"Constraints on phases of supersymmetric flavour conserving couplings"*. Nucl. Phys., **B570**:81–116, (2000). [arXiv:hep-ph/9906206].

[Ros90] J. Rosiek. *"Complete set of Feynman rules for the MSSM"*, (1990). Erratum [arXiv:hep-ph/9511250].

[S+05] E. Shintani et al. *"Neutron electric dipole moment from lattice QCD"*. Phys. Rev., **D72**:014504, (2005). [arXiv:hep-lat/0505022].

[Sak85] J. J. Sakurai. *"Modern Quantum Mechanics"*. Addison-Wesley Publishing Company Inc., (1985).

[Sha80] E. P. Shabalin. *"The electric dipole moments of baryons in the Kobayashi-Maskawa CP noninvariant theory"*. Sov. J. Nucl. Phys., **32**:228, (1980).

[Sie79] W. Siegel. *"Supersymmetric dimensional regularization via dimensional reduction"*. Phys. Lett., **B84**:193, (1979).

[Sim94] H. Simma. *"Equations of motion for effective Lagrangians and penguins in rare B decays"*. Z. Phys., **C61**:67–82, (1994). [arXiv:hep-ph/9307274].

[SLC] See website of the SLD Collaboration: http://www-sld.slac.stanford.edu/sldwww/sld.html.

[Smi95] V. A. Smirnov. *"Asymptotic expansions in momenta and masses and calculation of Feynman diagrams"*. Mod. Phys. Lett., **A10**:1485–1500, (1995). [arXiv:hep-th/9412063].

[SS75] A. Salam and J. A. Strathdee. *"On superfields and Fermi-Bose symmetry"*. Phys. Rev., **D11**:1521–1535, (1975).

[St] See lectures by A. Strumia at the "2005 Seminario Nazionale di Fisica Teorica", Parma Sep. 2005, website: http://pr.infn.it/snft/2005/snft-2005.html.

[SW90] H. Simma and D. Wyler. *"Hadronic rare B decays: the case $b \to sgg$"*. Nucl. Phys., **B344**:283–316, (1990).

[Sym70] K. Symanzik. *"Small distance behavior in field theory and power counting"*. Commun. Math. Phys., **18**:227–246, (1970).

[tHV72] G. 't Hooft and M. J. G. Veltman. *"Regularization and renormalization of gauge fields"*. *Nucl. Phys.*, **B44**:189–213, (1972).

[Wei79] Steven Weinberg. *Phenomenological Lagrangians.* Physica, **A96**:327, (1979).

[Wei89] Steven Weinberg. *"Larger Higgs exchange terms in the Neutron Electric Dipole Moment".* Phys. Rev. Lett., **63**:2333, (1989).

[Wol88] S. Wolfram. *Mathematica: A System for Doing Mathematics by Computer".* Addison-Wesley Publishing Company Inc., 1988.

[WZ72] K. G. Wilson and W. Zimmermann. *"Operator product expansions and composite field operators in the general framework of quantum field theory".* Commun. Math. Phys., 24:87–106, 1972.

[Zim69] W. Zimmermann. *"Convergence of Bogolyubov's method of renormalization in momentum space".* Commun. Math. Phys., **15**:208–234, (1969).